

## Substructural randomness in complex bodies

P. M. MARIANO

*Dipartimento di Ingegneria Strutturale e Geotecnica  
Università di Roma “La Sapienza”  
via Eudossiana 18, I-00184 Roma, Italy  
Università del Molise, Campobasso, Italy  
paolo.mariano@uniroma1.it*

Complex bodies are characterized by a (prominent) influence of the material texture (substructure) on the gross mechanical behavior. In real materials the shape and/or the distribution of substructures may have random nature from place to place and/or in time. When required from physical circumstances, such randomness needs to be accounted for in modeling and simulations. In the present lectures, attention is paid both to the general mechanical description of complex bodies (the abstract setting of multifield theories) and to special cases where possible substructural randomness may have a prominent role. Elastic bodies with random distributions of microcracks, quasicrystals and fullerene-based composites are thus analyzed with a certain detail. Research themes are also suggested.

### Introduction

Bodies are called complex when their material texture (substructure) from nano- to meso-level has a prominent influence on their gross behavior. Liquid crystals, polymeric fluids, ferroelectric and microcracked bodies, fullerene based composites (including forests of nanotubes) are prominent examples. For them and other cases, special models have been formulated challenging some basic axioms of standard continuum mechanics up to a certain extent. Such models compose rich classes but a unifying framework seems to be available. In fact, the geometry and the mechanics of maps between manifolds constitute on one hand a unifying setting for common models of condensed matter physics, while on the other hand they are tools to build up new models.

For a complex body, the material element is a sort of a ‘system’ and, to describe it, one needs the introduction of an appropriate morphological de-

scriptor  $\nu$  (order parameter) in addition to its place in space. In the unifying framework, it is required only that  $\nu$  be an element of an abstract manifold (in general not coinciding with a linear space). Each special choice of it characterizes each special model.

Moreover, the order parameter represents the substructure of a material element only at a gross level. In certain sense it is a coarse grained representation of substructural events. For them, appropriate statistical analyses (or better statistical mechanics) may be necessary. In addition, geometric characteristic features attributed to the material element may vary from place to place as random fields over the body. Then in some cases, higher order moments of the fields involved need to be used to furnish a satisfactory representation of the special physical phenomenon under examination. Some aspects of substructural randomness in complex bodies are treated in the three lectures below.

Lecture I deals with the special case of elastic bodies endowed with a random distribution of microcracks smeared throughout the volume. In this case the order parameter field is a vector field. It coincides with the kinematic perturbation induced by the deformation of microcracks over the macroscopic displacement field. Strain localization phenomena occur already within the setting of linear constitutive equations. Such phenomena are indicators toward the irreversible growth and coalescence of microcracks. Monte Carlo simulations underline also the existence of pattern formation for the stochastic moments of the displacements. The lecture allows us to explain in a rather simple special case the nature of some general ideas.

Lecture II deals with the geometrical nature of substructural interactions in the general unifying framework. They are induced by the variation of the energetic landscape at substructural level, accrue within each material element, also between it and the neighboring ones, and are quantities power conjugated with the rate of the order parameter. So that they are elements of the cotangent bundle of the manifold in which the order parameter field takes values. Time dependent states are also discussed. They may be generated by dissipative effects and may be also associated with martingale processes in appropriate special cases.

Lecture III deals with the suggestion of research themes. Three topics are discussed explaining in detail the mechanical model:

1. interaction between a macrocrack and a population of microcracks;
2. phason effects around the tip of a macrocrack in icosahedral quasicrystals;
3. linear elastic fullerene based composites.

In all three cases, the manner to investigate stochastic features are suggested to the audience leaving it the necessary developments by indicating the way for them.

**Level and background.** Lecture notes are written imagining that the readers are familiar with a rather solid background in standard continuum mechanics (Cauchy's model) from linear to non-linear setting. I imagine also that the readers have basic notions of differential geometry and elementary knowledge of some concepts of statistical mechanics and probability theory. Notwithstanding these presumptions, some concepts are recalled when necessary to render accessible the material to an audience as large as possible.

**Notations.** Standard notations are used throughout almost all lectures. Occasionally, a few non standard notations are introduced and their meaning explained at their first appearance. Strict distinction is made between abstract tensors, indicated with boldface type, and their components. When component representations are involved, Einstein's summation convention over repeated indices is assumed unless otherwise stated. Analogous distinction is made between elements of an abstract manifold and their coordinates. If  $\mathbf{A}$  and  $\mathbf{B}$  are tensors of the same order,  $\mathbf{A} \cdot \mathbf{B}$  denotes their scalar product, while  $\mathbf{AB}$  is the internal product giving as a result a tensor of the same order of  $\mathbf{A}$  and  $\mathbf{B}$ . If  $\mathbf{c}$  is of tensor order lesser than the one of  $\mathbf{A}$ , the product  $\mathbf{Ac}$  (or  $\mathbf{cA}$ ) saturates the indices of  $\mathbf{A}$  up to the order of  $\mathbf{c}$ . For example, if  $\mathbf{A}$  is a covariant second order tensor of components  $A_{ij}$  and  $\mathbf{c}$  is a vector of components  $c^j$ , we get  $(\mathbf{Ac})_i = A_{ij}c^j$  (or  $(\mathbf{cA})_j = c^i A_{ij}$ ). We will encounter two types of regions in the Euclidean point space  $\mathcal{E}^n$  (considered in general of dimension 3 and with associated translation vector-space  $Vec$ ). They are denoted with  $\mathcal{B}_0$  and  $\mathcal{B}$  and their meaning is explained later. Here we underline only that capital latin indices, say  $A, B \dots$ , denote coordinates in  $\mathcal{B}_0$  where a typical point of it is indicated with  $\mathbf{X}$ ; indices like  $i, j, \dots$  are related with coordinates in  $\mathcal{B}$ , where  $\mathbf{x}$  indicates a typical point there. When an abstract manifold  $\mathcal{M}$  is introduced, Greek indices  $\alpha, \beta, \dots$  indicate relevant coordinates. Standard notations are also used for differential operators. More precisely,  $\nabla$  and  $\text{Div}$  denote gradient and divergence with respect to  $\mathbf{X}$ ,  $\text{grad}$  and  $\text{div}$  the same operators calculated with respect to  $\mathbf{x}$  and  $\partial_y$  partial derivative with respect to the entry  $y$ .

**Bibliographic remark.** All models involving order parameters as observable quantities, interactions power conjugated with them and appropriately balanced are called *multifield theories*. The first formulation of their abstract

framework is due to Capriz (1985, 1989). In addition to special cases describing prominent physical circumstances in different classes of complex bodies (the bibliography about them is rather vast), the general framework has been further developed in (Capriz and Virga, 1990; Segev, 1994; Capriz, 2000; Mariano, 2000, 2001, 2003; Capriz and Mariano, 2003, 2004).

## Lecture I

### A special case: randomly microcracked elastic bodies

Microcracks can be considered as sharp defects (planar regions in a three-dimensional body not interpenetrated by interatomic bonds) or elliptic voids with one dimension smaller with respect to the other two. The observation of a body endowed with diffused microcracks reveals that they are in general distributed randomly throughout the volume. Their influence on the macroscopic mechanical behavior is as sensible as the matter composing the body is softer and softer. Cooperation of microcrack families may generate strain localization effects already in the regime of linear constitutive equations. Stress increments are naturally associated with strain localization and may generate damage growth or even loss of serviceability of devices and structures.

Here, for the sake of simplicity, just with the aim to investigate the influence of substructural randomness of the microcrack distribution on the macroscopic behavior, *we analyze only elastic microcracked bodies without considering irreversible phenomena*. Hence, *from now on, for us microcracks may deform but do not grow*.

Common models of microcracked bodies are based on homogenization techniques developed in general in the linear elastic range. Their aim is to obtain a standard continuum free of microcracks, but with a stiffness 'weakened' with respect to the one of the virgin material composing the body. The resulting continuum is 'equivalent' in some energetic sense to the original microcracked body.

Three classes of techniques may be recalled:

1. *self-consistent method*,
2. *differential scheme*,
3. *Mori-Tanaka method*.

Microcracks are assumed to be sufficiently random distributed and uncorrelated so that the body can be considered homogeneous and uncorrelated in the large. Ergodicity is also used in the definition of the homogenized stiffness and implies that stress and strain are statistically independent.

In the self-consistent method, one calculates first the energetic loss due to a single microcrack in an infinite body with stiffness equal to the one of

the target homogenized continuum. In this manner, interactions between microcracks are accounted for in a way stronger than differential scheme and Mori–Tanaka method. However, when one uses the self-consistent method, one gets an unphysical result: the stiffness vanishes when the microcrack density attains a value lesser than 1. Such an inconsistency may be eliminated. The way is the reduction of the weight (or better the role) attributed in the procedure to interactions between neighboring microcracks. In fact, in homogenization techniques, microcrack interactions are considered only indirectly or even neglected. However, when the microcrack density becomes larger and larger and the matter softer and softer they may have prominent effects.

We present here a continuum multifield model of microcracked bodies in which possible interactions between neighboring microcracks are accounted for directly. Our point of view differs from the ones in (i)-(iii) in its basic foundations. For us the description of macroscopic effects due to the presence of microcracks enters the model already at the geometric level of kinematics. Then, after constructing the appropriate multifield continuum model, we identify constitutive equations from lattice schemes and analyze macroscopic effects of microcrack randomness.

## 1. Multifield continuum modeling of microcracked bodies

### 1.1. Kinematics

$\mathcal{B}_0$  denotes the regular region of the Euclidean space  $\mathcal{E}^3$  that contains the body in its reference place. Here the word ‘regular’ means that  $\mathcal{B}_0$  is an open set coinciding with the interior of its closure. It is also endowed with a surface like boundary  $\partial\mathcal{B}_0$  where the outward unit normal  $\mathbf{n}$  is defined to within a finite number of corners and edges.

Each material element is pictured as a ‘patch’ of matter endowed with a family of microcracks and collapsed at its reference place  $\mathbf{X} \in \mathcal{B}_0$ . Let us consider first the microcracks frozen in the material element during a change of place of the body. In this case a deformation is represented by a sufficiently smooth orientation preserving map  $\hat{\mathbf{x}}$  such that

$$\mathcal{B}_0 \ni \mathbf{X} \xrightarrow{\hat{\mathbf{x}}} \mathbf{x} = \hat{\mathbf{x}}(\mathbf{X}) \in \mathcal{E}^3. \quad (1.1)$$

The point  $\mathbf{x}$  is the current place of the material element resting at  $\mathbf{X}$  in  $\mathcal{B}_0$ . The image of the whole  $\mathcal{B}_0$  is indicated with  $\mathcal{B}$ . It has the same regularity properties as  $\mathcal{B}_0$ .  $\mathbf{F}$  represents the gradient  $\nabla\hat{\mathbf{x}}(\mathbf{X})$ . At each  $\mathbf{X}$  it maps tangent vectors of  $\mathcal{B}_0$  into tangent vectors of  $\mathcal{B}$  at  $\mathbf{x}$ . As usual we require that  $\hat{\mathbf{x}}$  is orientation preserving, that is  $\det \mathbf{F} > 0$  at each  $\mathbf{X}$ .

If we imagine the microcracks free to deform without growing further, in principle a generic material element will be displaced from its current place  $\mathbf{x}$  as a consequence of the kinematic ‘perturbation’ induced by the deformation of the microcracks and will occupy a new place  $\mathbf{x}'$ . We indicate with  $\mathcal{B}'$  the minimal regular region containing the collection of  $\mathbf{x}'$  and assume that it can be reached from  $\mathcal{B}$  by means of a sufficiently smooth orientation preserving embedding  $\xi$ , namely

$$\mathcal{B} \ni \mathbf{x} \xrightarrow{\xi} \mathbf{x}' = \xi(\mathbf{x}) \in \mathcal{E}^3 \quad \text{s. t.} \quad \xi(\mathcal{B}) = \mathcal{B}'. \quad (1.2)$$

Let us define  $\hat{\mathbf{x}}' = \xi \circ \hat{\mathbf{x}}$ , then  $\mathbf{x}' = \hat{\mathbf{x}}'(\mathbf{X}) = (\xi \circ \hat{\mathbf{x}})(\mathbf{X})$  and indicate with  $\mathbf{F}_{\text{tot}}$  the gradient  $\nabla \hat{\mathbf{x}}'(\mathbf{X})$ . By using the notation  $\mathbf{F}^m$  for  $\text{grad } \xi(\mathbf{x})$ , by chain rule we obtain the *multiplicative decomposition*

$$\mathbf{F}_{\text{tot}} = \nabla \mathbf{x}' = (\text{grad } \xi(\mathbf{x})) \nabla \mathbf{x} = \mathbf{F}^m \mathbf{F}. \quad (1.3)$$

where  $\mathbf{F}^m$  is the gradient of deformation from  $\mathcal{B}$  to  $\mathcal{B}'$ : at each  $\mathbf{x}$  it maps linearly tangent vectors of  $\mathcal{B}$  at  $\mathbf{x}$  into tangent vectors of  $\mathcal{B}'$  at  $\mathbf{x}'$ .  $\mathbf{F}_{\text{tot}}$  behaves in the same way from  $\mathcal{B}$  to  $\mathcal{B}'$ .

The vector field

$$\begin{aligned} \mathcal{B}_0 \ni \mathbf{X} \xrightarrow{\hat{\mathbf{d}}} \mathbf{d} = \hat{\mathbf{d}}(\mathbf{X}) &= \hat{\mathbf{x}}'(\mathbf{X}) - \hat{\mathbf{x}}(\mathbf{X}) = \\ &= (\xi \circ \hat{\mathbf{x}})(\mathbf{X}) - \hat{\mathbf{x}}(\mathbf{X}) \in \text{Vec} \end{aligned} \quad (1.4)$$

is the displacement from  $\mathcal{B}$  to  $\mathcal{B}'$ , seen as a field over  $\mathcal{B}_0$ . It is the Lagrangian description of the Euclidean field  $\mathcal{B} \ni \mathbf{x} \mapsto \xi(\mathbf{x}) - \mathbf{x}$ , that is the displacement from  $\mathcal{B}$  to  $\mathcal{B}'$  defined over  $\mathcal{B}$ . The change of representation from the natural definition  $\xi(\mathbf{x}) - \mathbf{x}$  on  $\mathcal{B}$  to  $\hat{\mathbf{d}}(\mathbf{X})$  on  $\mathcal{B}_0$  is possible because  $\hat{\mathbf{x}}$  is one-to-one.

We call  $\mathbf{d}$  *microdisplacement*, reminding in this way its origin due to microcrack deformation. Since by chain rule  $\nabla \mathbf{d} = (\text{grad } \mathbf{d}) \mathbf{F}$ , and also  $\text{grad } \xi = \mathbf{I} - \text{grad } \mathbf{d}$ , with  $\mathbf{I}$  second order unit tensor, we obtain from (1.3) the *additive decomposition*

$$\mathbf{F}_{\text{tot}} = \mathbf{F} + \nabla \mathbf{d}. \quad (1.5)$$

At each  $\mathbf{X}$ ,  $\mathbf{d}$  can be considered an *order parameter* representing the contribution, in terms of displacement, of the presence of microcracks to the overall deformation. It is a coarse grained descriptor of the influence of microcracks on the gross mechanical behavior of the body.

In summary, when microcracks are considered ‘frozen’, the relative change of placement between neighboring elements patches is measured through the standard displacement field

$$\mathcal{B}_0 \ni \mathbf{X} \xrightarrow{\hat{\mathbf{u}}} \mathbf{u} = \hat{\mathbf{u}}(\mathbf{X}) = \hat{\mathbf{x}}(\mathbf{X}) - \mathbf{X} \in \text{Vec} \quad (1.6)$$

from  $\mathcal{B}_0$  to  $\mathcal{B}$ . When the microcracks deform, they induce an additional displacement  $\mathbf{d}$  that ‘perturbs’  $\mathbf{u}$  and the total displacement  $\mathbf{u}_{\text{tot}}$  is given by the sum  $\mathbf{u}_{\text{tot}} = \mathbf{u} + \mathbf{d}$ , a decomposition associated with (1.5).

Motions are time parametrized families (sufficiently smooth in time) of places  $\mathbf{x}$  and microdisplacements  $\mathbf{d}$ , and we write  $\mathbf{x} = \hat{\mathbf{x}}(\mathbf{X}, t)$  and  $\mathbf{d} = \hat{\mathbf{d}}(\mathbf{X}, t)$  for the current placement and the order parameter at time  $t \in [0, \bar{t}]$  of a material element resting at  $\mathbf{X}$  when  $t = 0$ . The rates in the material (Lagrangian) representation (i.e. as fields over  $\mathcal{B}_0$ ) are indicated with  $\dot{\mathbf{x}}$  and  $\dot{\mathbf{d}}$  at  $\mathbf{X}$  and  $t$ .

In using  $\mathbf{d}$  as a morphological descriptor, we forget the real existence of microcracks as defects in the body and account only indirectly for their existence.

### 1.2. Changes of observers

The descriptors of the morphology of the body are then placement and microdisplacement fields  $\hat{\mathbf{x}}$  and  $\hat{\mathbf{d}}$  respectively. They take values in  $\mathcal{E}^3$  and  $Vec$ , the geometrical environments that we use to describe the body together with the time interval  $[0, \bar{t}]$  along which motion develops.

Here an observer is a *representation* of all these three environments.

The standard definition of the observer is extended to include  $Vec$ . This point of view is a special case of the definition of observers adopted in the general setting of multifield theories.

Let  $\mathcal{O}$  and  $\mathcal{O}^\#$  be two distinct observers agreeing about the measure of time. We assume that they are related by a time-parametrized family of isometric transformations (rigid body motions), ruled by the special orthogonal group  $SO(3)$ . For a given material element,  $\mathcal{O}^\#$  and  $\mathcal{O}$  ‘evaluate’ two different contemporary places,  $\mathbf{x}^\#$  and  $\mathbf{x}$  respectively, related by the isometry

$$\mathbf{x}^\# = \mathbf{x}_0^\# + \mathbf{Q}(t)(\mathbf{x} - \mathbf{x}_0) \tag{1.7}$$

where  $\mathbf{x}_0^\#$  is the value at  $t$  of an arbitrary point valued function  $[0, \bar{t}] \ni t \mapsto \mathbf{x}_0^\# = \hat{\mathbf{x}}_0^\#(t) \in \mathcal{E}^3$  of time and  $\mathbf{x}_0$  an arbitrary fixed point in space. At each  $t$ ,  $\mathbf{Q}(t)$  is an element of the special orthogonal group  $SO(3)$ , thus it is represented by an orthogonal  $3 \times 3$  matrix with positive unitary determinant.

If a time parametrized family of elements of  $SO(3)$  act over  $Vec$ , we get

$$\mathbf{d}^\# = \mathbf{Q}(t)\mathbf{d}, \tag{1.8}$$

so that  $\mathbf{d}$  is an *objective* vector with respect to isometric changes of observers.

The rates evaluated by the observer  $\mathcal{O}^\#$  can be obtained simply by deriving (1.7) and (1.8) with respect to time:

$$\dot{\mathbf{x}}^\# = \dot{\mathbf{x}}_0^\# + \mathbf{Q}\dot{\mathbf{x}}(t) + \dot{\mathbf{Q}}(\mathbf{x} - \mathbf{x}_0), \tag{1.9}$$

$$\dot{\mathbf{d}}^\# = \mathbf{Q}\dot{\mathbf{d}} + \dot{\mathbf{Q}}\mathbf{d}. \quad (1.10)$$

The images of these rates in the frame of the observer  $\mathcal{O}$  are a result of the application of the inverse mapping  $[0, \bar{t}] \ni t \mapsto \mathbf{Q}^T(t) \in SO(3)$ . By denoting  $\mathbf{Q}^T\dot{\mathbf{x}}^\#$ ,  $\mathbf{Q}^T\dot{\mathbf{x}}_0^\#$  and  $\mathbf{Q}^T\dot{\mathbf{d}}^\#$ , with  $\dot{\mathbf{x}}^*$ ,  $\mathbf{c}$ ,  $\dot{\mathbf{d}}^*$  respectively, we obtain, at each  $t \in [0, \bar{t}]$ ,

$$\dot{\mathbf{x}}^* = \dot{\mathbf{x}} + \mathbf{c} + \dot{\mathbf{q}} \times (\mathbf{x} - \mathbf{x}_0), \quad (1.11)$$

$$\dot{\mathbf{d}}^* = \dot{\mathbf{d}} + \dot{\mathbf{q}} \times \mathbf{d}, \quad (1.12)$$

where  $\dot{\mathbf{q}}$  is the axial vector of the skew-symmetric tensor  $\dot{\mathbf{Q}}^T\dot{\mathbf{Q}}$ .

Notice that  $\mathbf{d}$  is not affected by the counterpart of the translational velocity  $\mathbf{c}$  because it is a 'relative' displacement between two current places, namely  $\mathbf{d} = \mathbf{x}' - \mathbf{x}$ .

### 1.3. Interactions and balance equations

We call *part* of  $\mathcal{B}_0$  any subset  $b$  of it with non-null volume measure and the same regularity properties as  $\mathcal{B}_0$ . Any  $b$  exchange interactions with the rest body and the environment. They are power conjugated with the kinematical mechanisms involved. Standard interactions (stresses and bulk forces) are associated with the rate of change of place of each material element, thus with  $\dot{\mathbf{x}}$ . Non-standard interactions are associated with the rate of change of microdisplacement  $\dot{\mathbf{d}}$ , i.e. with the rate of change of substructural morphology within each material element and its spatial variations from element to element. For this reason they are called *substructural* and measure the extra power due to the deformation of microcracks.

In the referential (Lagrangian) representation, for any arbitrary part  $b$ , we write the external power  $\mathcal{P}_b^{\text{ext}}(\dot{\mathbf{x}}, \dot{\mathbf{d}})$  of all interactions acting on  $b$  as a consequence of the different kinematical mechanisms involved in the form

$$\mathcal{P}_b^{\text{ext}}(\dot{\mathbf{x}}, \dot{\mathbf{d}}) = \int_b (\mathbf{b} \cdot \dot{\mathbf{x}}) d(\text{vol}) + \int_{\partial b} (\mathbf{P}\mathbf{n} \cdot \dot{\mathbf{x}} + \mathcal{S}\mathbf{n} \cdot \dot{\mathbf{d}}) d(\text{area}). \quad (1.13)$$

Here  $\mathbf{n}$  is the outward unit normal at the boundary  $\partial b$ ,  $\mathbf{b}$  the vector of body forces,  $\mathbf{P}$  the first Piola–Kirchhoff stress tensor and  $\mathcal{S}$  the so-called microstress tensor, a measure of the substructural interactions.

The terms  $\mathbf{b} \cdot \dot{\mathbf{x}}$  and  $\mathbf{P}\mathbf{n} \cdot \dot{\mathbf{x}}$  measure at each  $\mathbf{X}$  the power developed in the rate of change of placement of the material elements (considering the microcracks frozen).  $\mathcal{S}\mathbf{n} \cdot \dot{\mathbf{d}}$  is the density of extra power due to the interactions induced by the deformation of microcracks between neighboring material elements.

No external bulk interactions on the microcracks are considered. In other words, terms of the type  $\int_b (\beta \cdot \dot{\mathbf{d}}) d(vol)$  do not appear in the expression of the power because microcracks are not composed of matter, rather they are determined by the surrounding matter. In this sense microcracks are a sort of ‘virtual’ substructures.

As basic **axiom** we assume that the *external power is invariant under Galilean (translational) and rotational changes of observer*. In other words we impose that

$$\mathcal{P}_b^{\text{ext}}(\dot{\mathbf{x}}^*, \dot{\mathbf{d}}^*) = \mathcal{P}_b^{\text{ext}}(\dot{\mathbf{x}}, \dot{\mathbf{d}}), \tag{1.14}$$

for any choice of translational  $\mathbf{c}(t)$  and rotational  $\dot{\mathbf{q}}(t)$  velocities and  $b$ .

By substituting (1.11) and (1.12) in (1.13) and taking into account the arbitrariness of  $\mathbf{c}, \dot{\mathbf{q}}$ , from (1.14) the integral balances of forces and torques follow:

$$\int_b \mathbf{b} d(vol) + \int_{\partial b} \mathbf{P} \mathbf{n} d(area) = 0, \tag{1.15}$$

$$\int_b ((\mathbf{x} - \mathbf{x}_0) \times \mathbf{b}) d(vol) + \int_{\partial b} ((\mathbf{x} - \mathbf{x}_0) \times \mathbf{P} \mathbf{n} + \mathbf{d} \times \mathcal{S} \mathbf{n}) d(area) = 0. \tag{1.16}$$

The arbitrariness of  $b$  and Gauss theorem imply from (1.15) the standard Cauchy’s balance of forces

$$\mathbf{b} + \text{Div } \mathbf{P} = 0 \quad \text{in } \mathcal{B}_0, \tag{1.17}$$

From (1.16) we then obtain with the use of (1.17) the pointwise balance

$$\mathbf{d} \times \text{Div } \mathcal{S} = -\mathbf{e} (\mathbf{P} \mathbf{F}^T) + \mathbf{e} \left( (\nabla \mathbf{d})^T \mathcal{S} \right) \quad \text{in } \mathcal{B}_0, \tag{1.18}$$

where  $\mathbf{e}$  is Ricci’s alternating index<sup>1)</sup>.

This last relation states (i) that its right-hand side term is a vector obtained by the vector product of  $\mathbf{d}$  with another vector, say  $\mathbf{z}$ , namely

$$\mathbf{d} \times \mathbf{z} = -\mathbf{e} (\mathbf{P} \mathbf{F}^T) + \mathbf{e} \left( (\nabla \mathbf{d})^T \mathcal{S} \right), \tag{1.19}$$

and (ii) that this vector  $\mathbf{z}$  has just the structure of  $\text{Div } \mathcal{S}$ . The balance (1.19) then reduces to

$$\text{Div } \mathcal{S} - \mathbf{z} = 0. \tag{1.20}$$

---

<sup>1)</sup> The componentwise representation of  $\mathbf{e}$  is  $\mathbf{e}_{ijk}$ . In particular it is equal to 1 if  $ijk$  are an even permutation of 123 while it equals  $-1$  for odd permutations. When at least two indices reach the same value (say e.g. 122), the relevant component of  $\mathbf{e}$  is equal to zero. Remind that if  $\mathbf{A}$  is a second order tensor, one gets  $\mathbf{e} \mathbf{e} \mathbf{A} = 2 \text{skw } \mathbf{A}$ , i.e.  $\mathbf{e}_{ijk} \mathbf{e}_{klm} \mathbf{A}_{lm} = \mathbf{A}_{ij} - \mathbf{A}_{ji}$ .

Equation (1.20) is the balance of substructural interactions. It states that a *self-force*  $\mathbf{z}$  within the material element is needed to render balanced the actions induced by the surrounding material elements and measured by  $\mathcal{S}$ .

By pre-multiplication by  $\mathbf{e}$ , equation (1.19) can be rewritten as

$$\text{skw} (\mathbf{P}\mathbf{F}^T + \mathbf{z} \otimes \mathbf{d} + \mathcal{S}^T (\nabla \mathbf{d})) = 0. \quad (1.21)$$

where  $\text{skew}(\cdot)$  extract the skew-symmetric part of its entry. Cauchy's stress tensor  $(\det \mathbf{F}) \mathbf{P}\mathbf{F}^{-T}$  is then not symmetric when substructural interactions due to microcracks are taken into account.

The Gauss theorem and balance equations imply

$$\mathcal{P}_b^{\text{ext}} (\dot{\mathbf{x}}, \dot{\mathbf{d}}) = \int_b (\mathbf{P} \cdot \dot{\mathbf{F}} + \mathbf{z} \cdot \dot{\mathbf{d}} + \mathcal{S} \cdot \nabla \dot{\mathbf{d}}) d(\text{vol}) \equiv \mathcal{P}_b^{\text{int}}. \quad (1.22)$$

$\mathcal{P}_b^{\text{int}}$  is the internal power developed within the part  $b$ .

To obtain balance equations one could adopt (1.22) as basic axiom of virtual power requiring its validity for any choice of velocity fields and any  $b$ . In standard continuum mechanics (Cauchy's model) the axiom of invariance of the external power under the action of  $SO(3)$  and the principle of virtual power (involving the internal power) are completely equivalent. Here (as in the whole general setting of multifield theories), in the former case one assumes only the existence of a microstress and 'deduce' the need of a self-force  $\mathbf{z}$  while in the latter  $\mathbf{z}$  is postulated a priori.

#### 1.4. Constitutive equations: general restrictions and identifications from lattices

As anticipated in the first Sections of this lecture, the attention is here focused on the elastic behavior: microcracks may deform but do not grow. In the conservative setting considered here, we indicate with  $e$  the elastic energy density. It is such that its rate equals the density of power at each point, namely

$$\frac{d}{dt} \int_b (e) d(\text{vol}) - \mathcal{P}_b^{\text{ext}} (\dot{\mathbf{x}}, \dot{\mathbf{d}}) = 0, \quad (1.23)$$

for any part  $b$  and any choice of the rates involved in  $\mathcal{P}_b^{\text{ext}}$ .

Since our treatment deals with the elastic behavior, for the measures of interactions we presume constitutive structures of the form

$$\mathbf{P} = \hat{\mathbf{P}} (\mathbf{F}, \mathbf{d}, \nabla \mathbf{d}), \quad \mathbf{z} = \hat{\mathbf{z}} (\mathbf{F}, \mathbf{d}, \nabla \mathbf{d}), \quad \mathcal{S} = \tilde{\mathcal{S}} (\mathbf{F}, \mathbf{d}, \nabla \mathbf{d}), \quad (1.24)$$

and assume also that

$$e = \hat{e}(\mathbf{F}, \mathbf{d}, \nabla \mathbf{d}). \quad (1.25)$$

Then, by developing the time derivative in (1.23), the arbitrariness of  $b$  and (1.22) imply

$$(\partial_{\mathbf{F}} e - \mathbf{P}) \cdot \dot{\mathbf{F}} + (\partial_{\mathbf{d}} e - \mathbf{z}) \cdot \dot{\mathbf{d}} + (\partial_{\nabla \mathbf{d}} e - \mathcal{S}) \cdot \nabla \dot{\mathbf{d}} = 0. \quad (1.26)$$

Since equation (1.26) must be valid for any possible choice of the rates, which can be chosen arbitrarily from any given state  $(\mathbf{F}, \mathbf{d}, \nabla \mathbf{d})$ , the following constitutive restrictions hold:

$$\mathbf{P} = \partial_{\mathbf{F}} e, \quad \mathbf{z} = \partial_{\mathbf{d}} e, \quad \mathcal{S} = \partial_{\nabla \mathbf{d}} e. \quad (1.27)$$

Note that, if we substitute (1.27) in (1.21), we realize that (1.21) is just the condition assuring the ‘objectivity’ of the elastic energy density (i.e. the condition for which  $e$  is invariant under changes of observers ruled by  $SO(3)$ ). Then, when we choose an observer-independent expression of  $e$ , equation (1.21) is automatically satisfied.

To develop calculations, an explicit constitutive expression of the energy is necessary. One may obtain it by using either imagination addressed by general theoretical constraints as objectivity or experimental results. However, in absence of experimental results, a considerable help is given by lattice models. From them, constitutive equations can be obtained by using procedures based on energetic equivalence and Born rule, or extensions of it. In the present case, constitutive equations are deduced from a complex lattice, by using an integral procedure based on the equivalence of internal energy per unit volume in the continuum model with the internal energy of the characteristic cell in the discrete model of microcracked bodies.

The discrete model of a microcracked body discussed here is periodic. We indicate with  $V_{RVE}$  the volume of the smallest convex region containing the generic representative volume element (RVE), i.e. the generic cell. The discrete model is made of two superposed lattices, the former (*macrolattice*) represents the virgin material at the molecular level and is made of material points (spheres) connected by rods; the latter (*mesolattice*) is a mesoscale representation of the microcrack system and is made of empty shells linked each other by rods. Elastic shells represent microcracks and the rods among them the interactions between neighboring microcracks. Interactions between virgin material and microcracks are represented through the links connecting the two lattices. Figure 1 displays a two dimensional point of view of a possible geometry of the lattice.

Points of the macrolattice occupied by the rigid spheres are labelled by  $\mathbf{a}$ ,  $\mathbf{b}$ ,  $\dots$ , while points occupied by centers of mass of shells of the mesolattice are

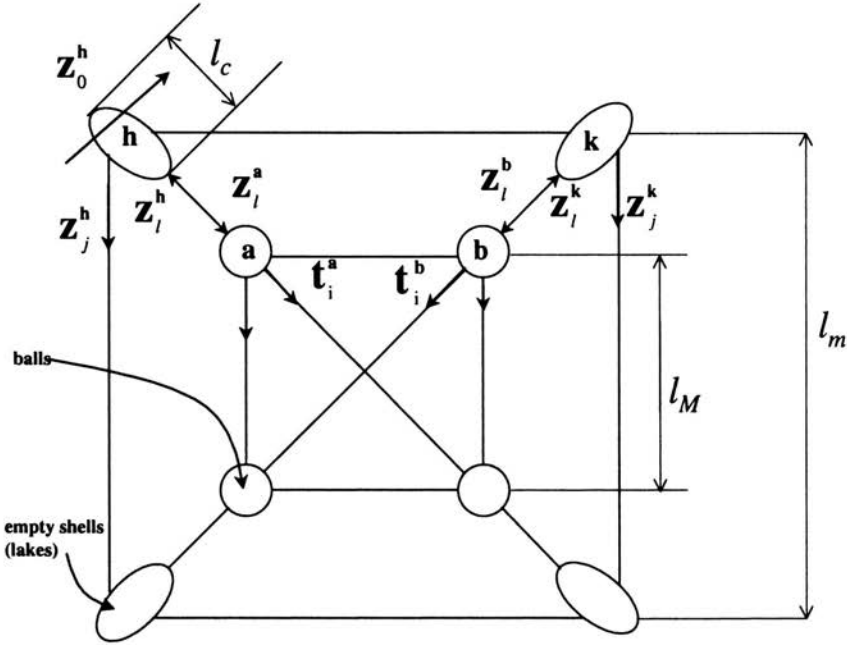


FIGURE 1. Schematic two-dimensional view of a possible lattice scheme for a microcracked body.

labelled by  $\mathbf{h}, \mathbf{k}, \dots$ . The relative displacement  $\mathbf{d}^h$  of the margin of the shell placed at  $\mathbf{h}$  along its major axis, the relative displacement  $\mathbf{d}^h - \mathbf{d}^k$  between two adjacent microcracks, the relative displacement  $\mathbf{u}^a - \mathbf{d}^h$  between a shell and the rigid spheres connected to it and the deformation  $\mathbf{u}^a - \mathbf{u}^b$  of a generic rod between two rigid spheres (where  $\mathbf{u}^a$  is the displacement at the point  $\mathbf{a}$ ) are measures of deformation in the lattice if *rigid components of the displacement in the lattice are avoided* as we assume here. Related interactions are represented by the following vectors:

- $\mathbf{t}_i$  (the force along the  $i$ -th link of the macrolattice);
- $\mathbf{z}_0^h$  (the force induced by the relative displacement  $\mathbf{d}^h$  in a shell);
- $\mathbf{z}_j$  (the force in the  $j$ -th link of the mesolattice);
- $\mathbf{z}_l$  (the force in the  $l$ -th interlattice link).

*The identification procedure from discrete to continuum model is strictly developed in the range of infinitesimal deformations.*

The steps of the procedure are as follows: first we write the power  $\pi_{RVE}$  developed by the interactions in a generic cell, then we equalize it to the density of the power in the continuum, namely we impose

$$\pi_{RVE} = (\mathbf{P} \cdot \nabla \mathbf{u} + \mathbf{z} \cdot \mathbf{d} + \mathbf{S} \cdot \nabla \mathbf{d}) V_{RVE}. \tag{1.28}$$

Here, since we are in the range of infinitesimal deformations, we may approximate the rates of the displacement fields (macro- and micro-) with the fields themselves. In this case, the right hand side term of (1.28) is then the density of internal power in the continuum.

With the identification procedure we assign all mechanical and geometrical properties of the RVE to each point of the continuum. In other words, we collapse the RVE into a point, the geometrical features of the RVE become then internal lengths of the continuum. Such a procedure allows us to express the measures of interaction in the continuum (namely  $\mathbf{P}$ ,  $\mathbf{z}$ , and  $\mathcal{S}$ , approximating in the infinitesimal deformation regime their actual counterparts) in terms of the ones of the discrete model and the geometry of it. Preliminarily, it is necessary to link the measures of deformation in the lattice with the ones in the continuum. To this end we assume that the macrolattice undergoes a homogeneous deformation, and that each shell deforms also homogeneously but differently from the neighboring one. In this way, we may find a point  $\bar{\mathbf{x}}$  in the RVE such that

$$\mathbf{d}^h = \mathbf{d}(\bar{\mathbf{x}}) + \nabla \mathbf{d}(\bar{\mathbf{x}})(\mathbf{h} - \bar{\mathbf{x}}), \tag{1.29}$$

$$\mathbf{u}^a - \mathbf{u}^b = \nabla \mathbf{u}(\bar{\mathbf{x}})(\mathbf{a} - \mathbf{b}), \tag{1.30}$$

$$\mathbf{d}^h - \mathbf{d}^k = \nabla \mathbf{d}(\bar{\mathbf{x}})(\mathbf{h} - \mathbf{k}), \tag{1.31}$$

$$\mathbf{u}^a - \mathbf{d}^h = \nabla \mathbf{u}(\bar{\mathbf{x}})(\mathbf{a} - \bar{\mathbf{x}}) - \nabla \mathbf{d}(\bar{\mathbf{x}})(\mathbf{h} - \bar{\mathbf{x}}). \tag{1.32}$$

Such an assumption is not restrictive because the RVE, as a model of material element, is collapsed into a point.

By inserting previous relations in (1.28), we obtain

$$\mathbf{P} = \frac{1}{V_{RVE}} \left( \sum_{i=1}^L \mathbf{t}_i \otimes (\mathbf{a} - \mathbf{b}) + \sum_{l=1}^{L_N} \mathbf{z}_l \otimes (\mathbf{a} - \bar{\mathbf{x}}) \right), \tag{1.33}$$

$$\mathbf{z} = \frac{1}{V_{RVE}} \sum_{h=1}^M \mathbf{z}_0^h, \tag{1.34}$$

$$\mathcal{S} = \frac{1}{V_{RVE}} \left( \sum_{h=1}^M \mathbf{z}_0^h \otimes (\mathbf{h} - \bar{\mathbf{x}}) + \sum_{j=1}^{L_M} \mathbf{z}_j \otimes (\mathbf{h} - \mathbf{k}) - \sum_{l=1}^{L_N} \mathbf{z}_l \otimes (\mathbf{h} - \mathbf{k}) \right), \tag{1.35}$$

where  $L$  is the number of rods among rigid spheres in the macrolattice,  $L_N$  the number of rods between macro- and micro-lattices,  $M$  the number of shells in the microlattice and  $L_M$  the number of rods between elastic shells.

We assign linear constitutive equations to the rods and the shells in the lattice, obtaining after a subsequent linearization the following simple form of the general constitutive equations (1.33)-(1.35):

$$\mathbf{P} = \mathbb{A}\nabla\mathbf{u}-\mathbb{A}'\nabla d, \tag{1.36}$$

$$\mathbf{z} = \mathbb{C}d, \tag{1.37}$$

$$\mathbf{S} = \mathbb{G}'\nabla\mathbf{u}-\mathbb{G}\nabla d. \tag{1.38}$$

With reference to the special geometry adopted in Fig. 1, the constitutive tensors  $\mathbb{A}$ ,  $\mathbb{A}'$ ,  $\mathbb{C}$ ,  $\mathbb{G}'$  and  $\mathbb{G}$  have the following explicit structure:

$$\mathbb{A} = \frac{EA}{l_M} \begin{bmatrix} 2 + \frac{1}{\sqrt{2}} & 0 & 0 & \frac{1}{\sqrt{2}} \\ 0 & \frac{1}{\sqrt{2}} & \frac{1}{\sqrt{2}} & 0 \\ 0 & \frac{1}{\sqrt{2}} & \frac{1}{\sqrt{2}} & 0 \\ \frac{1}{\sqrt{2}} & 0 & 0 & 2 + \frac{1}{\sqrt{2}} \end{bmatrix} + \frac{\frac{1}{2}l_M^2 \frac{2E^*A}{\sqrt{2}(l_m-l_M)}}{|l_M^2 - l_m^2|} \begin{bmatrix} 1 & 0 & 0 & 1 \\ 0 & 1 & 1 & 0 \\ 0 & 1 & 1 & 0 \\ 1 & 0 & 0 & 1 \end{bmatrix}, \tag{1.39}$$

$$\mathbb{A}' = \mathbb{G}' = \frac{\frac{1}{2}l_m l_M \frac{2E^*A}{\sqrt{2}(l_m-l_M)}}{|l_M^2 - l_m^2|} \begin{bmatrix} 1 & 0 & 0 & 1 \\ 0 & 1 & 1 & 0 \\ 0 & 1 & 1 & 0 \\ 1 & 0 & 0 & 1 \end{bmatrix}, \tag{1.40}$$

$$\mathbb{C} = \frac{2E\hat{A}}{l_m^2} \begin{bmatrix} 1 & 0 \\ 0 & 1 \end{bmatrix}, \tag{1.41}$$

$$\mathbb{G} = \frac{1}{2} \frac{EA}{\pi l_c} \begin{bmatrix} 1 & 0 & 0 & 1 \\ 0 & 1 & 1 & 0 \\ 0 & 1 & 1 & 0 \\ 1 & 0 & 0 & 1 \end{bmatrix} + \frac{\frac{1}{2}l_m^2 \frac{2E^*A}{\sqrt{2}(l_m-l_M)}}{|l_M^2 - l_m^2|} \begin{bmatrix} 1 & 0 & 0 & 1 \\ 0 & 1 & 1 & 0 \\ 0 & 1 & 1 & 0 \\ 1 & 0 & 0 & 1 \end{bmatrix}, \tag{1.42}$$

where  $E$  is the Young modulus of the rods between spheres,  $E^*$  the Young modulus of the rods between elastic shells and rigid spheres (it is a parameter that allows us to describe the interactions between each microcrack and the surrounding matter),  $A$  the area of the cross section of the rods among rigid spheres and between rigid spheres and elastic shells (another parameter useful to describe interactions),  $l_m$  and  $l_M$  are characteristic lengths,  $l_c$  the characteristic length of the shells in the lattice,  $\hat{A}$  the cross section of rods between adjacent microcracks (this parameter is used to model interactions between microcracks).

The matrices (1.39)-(1.42) have been written taking into account the Voigt notation by which

$$\bullet \nabla\mathbf{u} = \{u_{x/x}; u_{y/y}; u_{x/y}; u_{y/x}\}^T,$$

- $\nabla d = \{d_{x/x}; d_{y/y}; d_{x/y}; d_{y/x}\}^T$ , and
- $d = \{d_x; d_y\}^T$ .

The choice of appropriate values for the material and geometrical quantities characterizing the discrete model is delicate matter of modeling. When one imagines to eliminate the mesolattice, then its contribution, the final results must be the constitutive equation of the real material free of microcracks, so  $E$ ,  $A$ , and  $l_M$  must be selected accordingly. The length  $l_c$  is the averaged maximal dimension of the microcracks, the average being calculated over the population of microcracks. For fixed symmetry properties of the microcrack distribution, the density of microcracks increases as  $l_m$  decreases. In principle both  $l_c$  and  $l_m$  can be evaluated by means of X-ray techniques. The remaining coefficients may be obtained by means of an appropriate inverse analysis. For example, let us consider a strip of microcracked material and load it with two opposite tensile forces of unitary modulus. We may evaluate the total displacement  $u_{tot}$  between the points in which the two forces are applied, remaining strictly in the linear setting. We may also calculate the analogous displacement with the strip made of virgin material. The difference of the two values is the perturbation induced by the microcracks; call it  $\bar{d}$ . Then, once for the special material under examination  $E$ ,  $A$ ,  $l_M$ ,  $l_c$  and  $l_m$  have been selected with the criteria described above, we should choose  $E^*$  and  $\hat{A}$  in order to fit the value  $\bar{d}$  in the special case of the strip. The set of values of the parameters giving rise to  $\bar{d}$  is not unique. However, at the end, when experimental analysis suggests that the microcrack distribution can be considered with cubic symmetry, the various choices of the above listed parameters should lead to unique values of the fractions in (1.39)-(1.42).

Actually, the discrete model chosen here is only a simple device useful to simulate the mechanical behavior of the material element. The selection of the values of the geometric and constitutive quantities of the lattice is guided by the possibility to fit experimental data about the real material.

## 2. Stochastic nature of the microcrack distribution

The constitutive relations obtained in previous section contain elastic moduli of the links in the lattice and the characteristic lengths of the RVE.

With reference to Fig.1, in fact,  $l_M$  is the microscopic scale, i.e. the molecular scale, while  $l_m$  is the mesoscopic scale, i.e. the characteristic distance between microcracks. Their ratio is crucial in the linear constitutive equations.

Experiments based on imaging or scattering techniques show that real distributions of microcracks can be considered stochastic throughout the body.

Thus, the interactions between neighboring microcracks and interactions between each microcrack and the surrounding material may be considered random.

To describe such a randomness, we may follow different strategies involving the geometry of the lattice (in particular of the mesolattice) and/or the elastic constants. In the former case we can assume that the scale of the mesolattice is stochastic, whereas in the latter we consider random only the values at a mesolevel scale.

We assume as deterministic all material and geometrical parameters of the RVE except the length  $l_m$  of the mesoscale. Thus we consider (in a certain sense indirectly) random the density of microcracks.

The length  $l_m$  of the mesoscale is then a random field

$$\mathcal{B}_0 \ni \mathbf{X} \mapsto l_m(\mathbf{X}) \quad (2.1)$$

over the body.

In principle, we cannot consider  $l_m$  as a Gaussian field because such a choice would imply negative values for  $l_m$ , thus an unphysical circumstance. We adopt for  $l_m$  a shifted lognormal model with a lower cut-off at  $l_M$  and construct it by making use of a Gaussian field.

Let  $\mathbf{X} \mapsto Y(\mathbf{X}) \in \mathbb{R}$  be a real valued Gaussian field (function of the points  $\mathbf{X}$  in space) with mean 0, variance 1, covariance  $C_{YY}$  such that

$$\mathbb{R}^3 \ni \mathbf{Z} \mapsto C_{YY}(\mathbf{Z}) = \mathbb{E}[Y(\mathbf{X})Y(\mathbf{X} + \mathbf{Z})], \quad (2.2)$$

and marginal standard distribution  $\mathbb{R} \ni s \mapsto \phi_Y(s)$  given by the standard Gaussian distribution. For any arbitrary distribution  $s \mapsto F_A(s)$ , we may derive a memoryless non-linear transformation given by

$$\mathbf{X} \mapsto A(\mathbf{X}) = (F_A^{-1} \circ \Phi_Y)(Y(\mathbf{X})) = \tilde{g}(Y(\mathbf{X})), \quad (2.3)$$

that is the so called translation field, characterized by the distribution  $F_A(\cdot)$  and the covariance  $C_{AA}$ . In a two-dimensional setting, the covariance function of the scaled non-Gaussian process

$$\hat{A}(\mathbf{X}) = \frac{A(\mathbf{X}) - \mu_A}{\sigma_A} \quad (2.4)$$

and the covariance  $C_{YY}$  are related by

$$\mathbb{R}^3 \ni \mathbf{Z} \mapsto C_{\hat{A}\hat{A}}(\mathbf{Z}) = \int_{\mathbb{R}^2} \tilde{g}(y_1) \tilde{g}(y_2) \bar{\phi}(y_1, y_2; C_{YY}(\mathbf{Z})) dy_1 dy_2, \quad (2.5)$$

where  $\bar{\phi}$  is the joint density of the dependent standard Gaussian variables  $Y(\mathbf{X})$  and  $Y(\mathbf{X} + \mathbf{Z})$  with covariance coefficient  $C_{YY}$ . The covariance function  $C_{\hat{A}\hat{A}}$  takes values in the range  $[C_{\hat{A}\hat{A}}^*, 1]$ , where  $C_{\hat{A}\hat{A}}^*$  is the value of  $C_{\hat{A}\hat{A}}$  corresponding to  $C_{YY} = -1$ .

Since our treatment deals with bounded bodies, we should restrict previous definitions to fields with support in  $\mathcal{B}_0$ . Out of  $\mathcal{B}_0$  the stochastic fields under examination are deterministic and vanish uniformly.

As anticipated earlier, we assume that the characteristic length  $l_m$  of the mesoscopic scale is a special translation field, the shifted lognormal field:

$$\mathcal{B} \ni \mathbf{X} \mapsto l_m(\mathbf{X}) = A(\mathbf{X}) = r + \exp[\mu_Y + \sigma_Y Y(\mathbf{X})], \quad (2.6)$$

where  $r$ ,  $\mu_Y$  and  $\sigma_Y$  are parameters that need to be selected in order to give the target values  $\mu_A$  and  $\sigma_A$  of  $l_m(\mathbf{X})$  and to match the physical condition  $l_m > l_M$  at each  $\mathbf{X}$ .

We consider three cases of correlation for  $l_m$ :

- H – perfect random correlation, i.e.  $l_m(\mathbf{X}) = \bar{l}_m$  for any  $\mathbf{X} \in \mathcal{B}_0$ ;
- U – absence of correlation, i.e.  $\mathbf{X} \mapsto l_m(\mathbf{X})$  is an uncorrelated field;
- C – intermediate case between U and H.

The assumption of case H is too strong, and physically not plausible, because one assumes that the value of  $l_m$  at a certain  $\mathbf{X}$  depends on all the other values of  $l_m$  over the whole body, independently of its size. However, the discussion of the limit cases H and U helps us to evaluate the influence of the stochastic non-local correlation on the localization of the characteristic moments of the distributions (namely coefficient of variation, skewness and kurtosis). They indicate respectively upper and lower bounds of the stochastic behavior.

We develop numerical calculations in a two-dimensional setting: the plane  $0X_1X_2$ . There case C is ruled by the correlation function

$$R(X_1, X_2) = s^2 \exp[-(cX_1)^2 - (cX_2)^2], \quad (2.7)$$

in which  $s^2$  is the standard deviation of  $l_m$  and  $c$  a constant.

Note that the assumption of some type of random correlation implies a non-local constitutive behavior of the body, while the absence of random correlation corresponds to a completely local behavior.

### 3. Pattern formation

Numerical solutions put in evidence some unusual characteristic features of the behavior of microcracked elastic bodies as the formation of strain localization zones already in the linear elastic range (a phenomenon that cannot

be recognized in standard linear elasticity). To obtain numerical results, we need to combine finite element techniques with Monte Carlo simulations. We develop simulations in the linear elastic range and build up first a finite element scheme in a two-dimensional setting because the sample case developed deals with the boundary value problem sketched in Fig. 2.

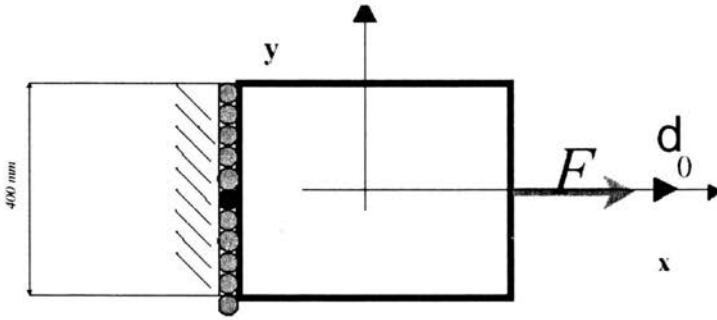


FIGURE 2. Square microcracked membrane.

Let  $\{b^e\}$  a tessellation of  $\mathcal{B}_0$ . Two generic elements  $b_1^e$  and  $b_2^e$  of  $\{b^e\}$  are disjoint regular subsets of  $\mathcal{B}_0$  and  $\bigcup_e b^e = \mathcal{B}_0$ , where  $\bigcup_e$  indicates the union of all  $b^e$ .

We assume that both the compatibility and constitutive equations are valid and impose equilibrium.

In a two-dimensional setting, each node of each  $b^e$  has *four degrees of freedom*, two for  $\mathbf{u}$  and two for  $\mathbf{d}$ .

We indicate with  $\hat{\mathbf{u}}^e$  and  $\hat{\mathbf{d}}^e$  nodal displacements, so that the approximate expressions of the element displacements are given by

$$\mathbf{u}^e = \Phi_{\mathbf{u}}^e \hat{\mathbf{u}}^e, \quad \mathbf{d}^e = \Phi_{\mathbf{d}}^e \hat{\mathbf{d}}^e \tag{3.1}$$

in which  $\Phi_{\mathbf{u}}^e$  and  $\Phi_{\mathbf{d}}^e$  are the matrices of the relevant *shape functions*.

Numerical simulations below are developed within the infinitesimal deformation regime in which the first Piola–Kirchhoff stress  $\mathbf{P}$  and the microstress  $\mathcal{S}$  can be approximated by their actual counterparts, namely the Cauchy stress  $\sigma$  and the actual microstress  $\mathcal{S}_a$ . Moreover, if we introduce variations  $\delta \mathbf{u}$  and  $\delta \mathbf{d}$  of the displacement fields, we may approximate the power with the virtual work, namely

$$\mathcal{P}_{b^e}^{\text{int}} \approx \delta W_{b^e}^{\text{int}} = \int_{b^e} (\mathbf{P} \cdot \delta(\nabla \mathbf{u}) + \mathbf{z} \cdot \delta \mathbf{d} + \mathcal{S} \cdot \delta(\nabla \mathbf{d})), \tag{3.2}$$

$$\mathcal{P}_{b^e}^{\text{ext}} \approx \delta W_{b^e}^{\text{ext}} = \int_{b^e} \mathbf{b} \cdot \delta \mathbf{u} + \int_{\partial b^e} (\mathbf{t} \cdot \delta \mathbf{u} + \tau \cdot \delta \mathbf{d}), \tag{3.3}$$

where  $\mathbf{t}$  and  $\tau$  indicate values at the boundary of  $b^e$  of  $\mathbf{Pn}$  and  $\mathbf{Sn}$  respectively.

As a consequence of (1.22), at the equilibrium we have

$$\delta W_{b^e}^{\text{ext}} - \delta W_{b^e}^{\text{int}} = 0. \tag{3.4}$$

By substituting the linear constitutive prescriptions (1.36)-(1.38) we get

$$\begin{aligned} \int_{b^e} (\delta (\nabla \mathbf{u}) \cdot (\mathbb{A} \nabla \mathbf{u} + \mathbb{A}' \nabla \mathbf{d}) + \delta \mathbf{d} \cdot \mathbb{C} \mathbf{d} + \delta (\nabla \mathbf{d}) \cdot (\mathbb{G} \nabla \mathbf{d} + \mathbb{G}' \nabla \mathbf{u})) \\ = \int_{b^e} (\delta \mathbf{u} \cdot \mathbf{b}) + \int_{\partial b^e} (\delta \mathbf{u} \cdot \mathbf{t} + \delta \mathbf{d} \cdot \tau) \end{aligned} \tag{3.5}$$

which, after some algebra, becomes

$$\begin{aligned} \delta \hat{\mathbf{u}} \cdot \left( \int_{b^e} (\nabla \Phi_{\mathbf{u}}^e)^T \mathbb{A} \nabla \Phi_{\mathbf{u}}^e \hat{\mathbf{u}}^e + (\nabla \Phi_{\mathbf{u}}^e)^T \mathbb{A}' \nabla \Phi_{\mathbf{d}}^e \hat{\mathbf{d}}^e \right) \\ + \delta \hat{\mathbf{d}}^e \cdot \left( \int_{b^e} \Phi_{\mathbf{d}}^T \mathbb{C} \Phi_{\mathbf{d}}^e \hat{\mathbf{d}}^e + (\nabla \Phi_{\mathbf{d}}^e)^T \mathbb{G} \nabla \Phi_{\mathbf{d}}^e \hat{\mathbf{d}}^e + \nabla \Phi_{\mathbf{d}}^{eT} \mathbb{G}' \nabla \Phi_{\mathbf{u}}^e \hat{\mathbf{u}}^e \right) \\ = \delta \hat{\mathbf{u}}^e \cdot \left( \int_{b^e} \Phi_{\mathbf{u}}^{eT} \mathbf{b} + \int_{\partial b^e} \Phi_{\mathbf{u}}^{eT} \mathbf{t} \right) + \delta \hat{\mathbf{d}}^e \cdot \left( \int_{\partial b^e} \Phi_{\mathbf{d}}^{eT} \tau \right). \end{aligned} \tag{3.6}$$

Equation (3.6) must be valid for every  $\delta \hat{\mathbf{u}}^e$  and  $\delta \hat{\mathbf{d}}^e$ . This condition implies that

$$\mathbf{K} \begin{Bmatrix} \hat{\mathbf{u}}^e \\ \hat{\mathbf{d}}^e \end{Bmatrix} - \begin{Bmatrix} \mathbf{r}_{\mathbf{u}}^e \\ \mathbf{r}_{\mathbf{d}}^e \end{Bmatrix} = 0 \tag{3.7}$$

where the stiffness matrix  $\mathbf{K}$  is given by

$$\mathbf{K} = \begin{bmatrix} \int_{b^e} (\nabla \Phi_{\mathbf{u}}^e)^T \mathbb{A} \nabla \Phi_{\mathbf{u}}^e & \int_{b^e} \nabla \Phi_{\mathbf{u}}^{eT} \mathbb{G}' \nabla \Phi_{\mathbf{d}}^e \\ \int_{b^e} \nabla \Phi_{\mathbf{d}}^{eT} \mathbb{G}' \nabla \Phi_{\mathbf{u}}^e & \int_{b^e} \Phi_{\mathbf{d}}^{eT} \mathbb{C} \Phi_{\mathbf{d}}^e + (\nabla \Phi_{\mathbf{d}}^e)^T \mathbb{G} \nabla \Phi_{\mathbf{d}}^e \end{bmatrix}, \tag{3.8}$$

and the vector of the residuals is given by

$$\begin{Bmatrix} \mathbf{r}_{\mathbf{u}}^e \\ \mathbf{r}_{\mathbf{d}}^e \end{Bmatrix} = \begin{Bmatrix} \int_{b^e} \Phi_{\mathbf{u}}^{eT} \mathbf{b} + \int_{\partial b^e} \Phi_{\mathbf{u}}^{eT} \mathbf{t} \\ \int_{\partial b^e} \Phi_{\mathbf{d}}^{eT} \tau \end{Bmatrix}. \tag{3.9}$$

As sample case, we analyze the square membrane in Fig. 2.

On the left side, only vertical displacements are allowed, except at a fixed point. A mixed boundary value problem is considered on the right side: in the middle a tensile force  $F$  is applied assuming that it is sustained by the standard stress, and a value  $d_0$  is assigned at the same point in which  $F$  is applied.

Note that, in principle, we might not assign any condition on  $\mathbf{d}$  on the right-hand-side of the membrane and consider only an initial boundary value problem and we could consider a boundary condition of the type  $\mathcal{S}\mathbf{n} = 0$ , with  $\mathbf{n}$  the outward unit normal at the boundary. The possible assumption that the microtractions  $\mathcal{S}\mathbf{n}$  vanish at the boundary is the only one which is physically reasonable about microtractions because at the external boundary of the body microcracks are absent since each of them is determined by the surrounding matter and do not exist per se.

The numerical values chosen for constitutive constants and the properties of the random field used in the sample case are summarized in Table 1.

TABLE 1. Summary of the numerical values used in the two dimensional examples.

$l_m$	200 mm (mean value)
$l_M$	10 mm
$d_0$	0.1 mm
$E$	$10^5$ N/mm <sup>2</sup>
$A$	1 mm <sup>2</sup>
$\hat{A}$	0.314 mm <sup>2</sup>
$l_c$	1 mm
$\delta$	0.1
$c$	0.00278

The mesh is made of 1600 square finite elements and the shape function used for the macrodisplacement and the microdisplacement are linear.

A total of 10000 sample values of  $l_m$  is generated by using a Monte-Carlo technique. It makes use of (i) calibration of the marginal distribution  $\bar{F}_W$  and the covariance function  $C_{WW}$  to obtain the target stochastic properties of  $l_m$ , (ii) generation of samples of the Gaussian field  $Y$ , (iii) generation of the translation field  $l_m$ .

Finite element analyses are developed for each sample of  $l_m$ . Then, mean, coefficient of variation (c.o.v.), skewness and kurtosis of the distribution of displacements, extracted from the population of data arising from finite element simulations, are evaluated.

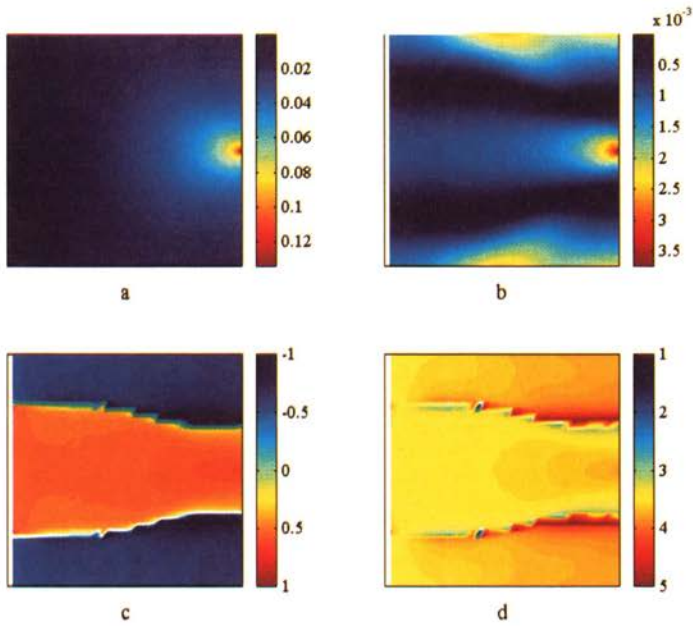


FIGURE 3. Macro-displacement along  $x$ -axis (Case H): (a) mean, (b) c.o.v., (c) skewness coefficient, (d) kurtosis coefficient.

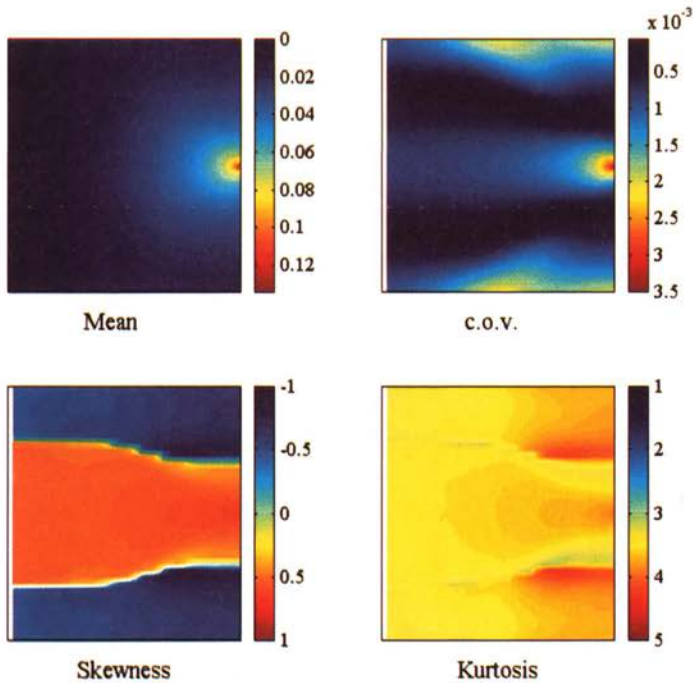


FIGURE 4. Macro-displacement along  $x$ -axis (Case C).

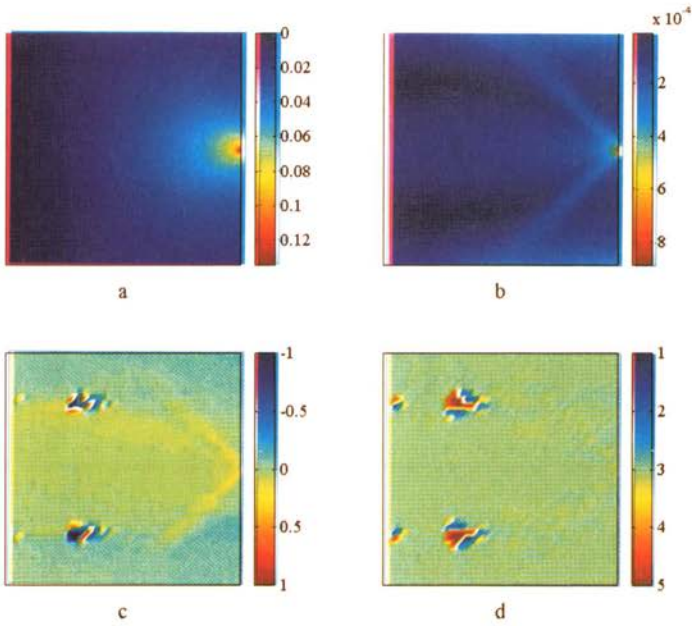


FIGURE 5. Macro-displacement along  $x$ -axis (Case U): (a) mean, (b) c.o.v., (c) skewness coefficient, (d) kurtosis coefficient.

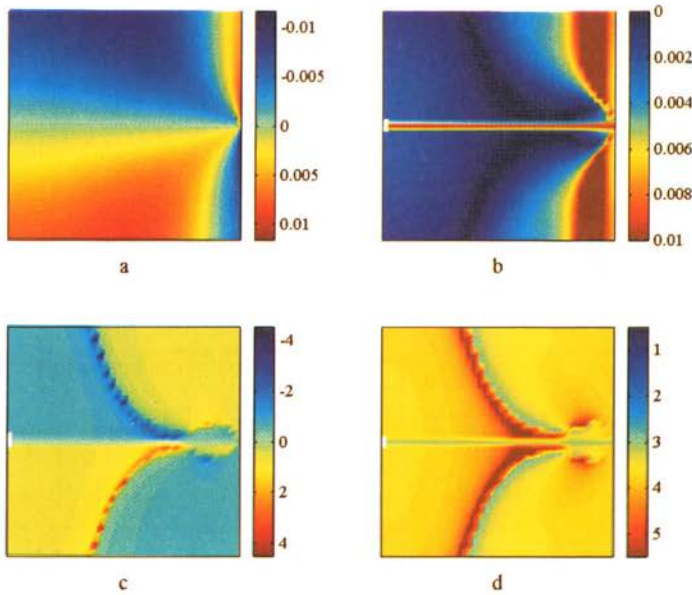
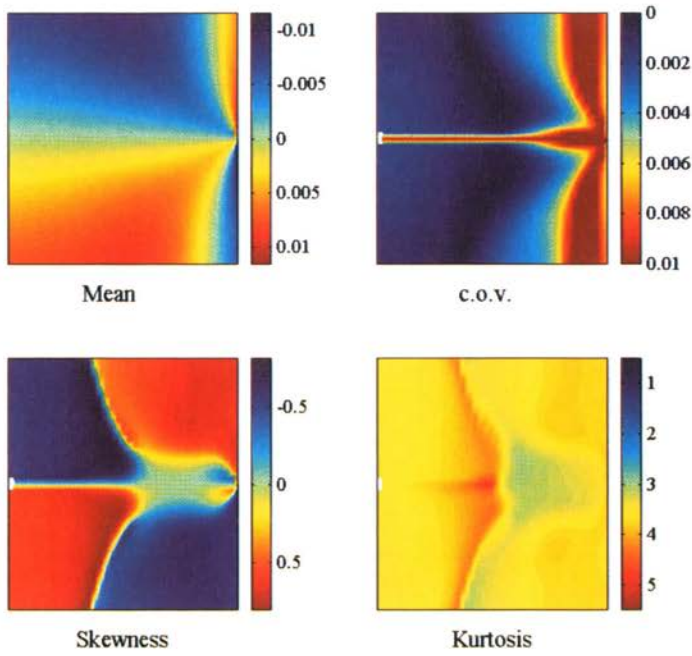
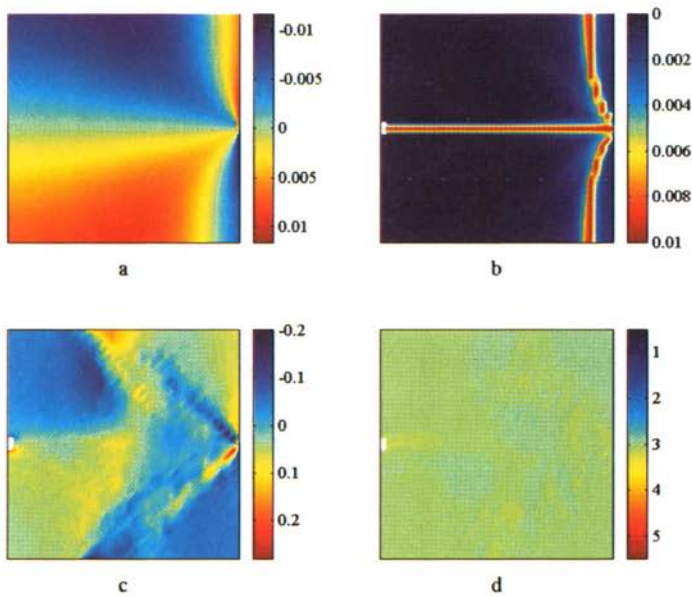


FIGURE 6. Macro-displacement along  $x$ -axis (Case U): (a) mean, (b) c.o.v., (c) skewness coefficient, (d) kurtosis coefficient.

FIGURE 7. Macro-displacement along  $y$ -axis (Case C).FIGURE 8. Macro-displacement along  $y$ -axis (Case U): (a) mean, (b) c.o.v., (c) skewness coefficient, (d) kurtosis coefficient.

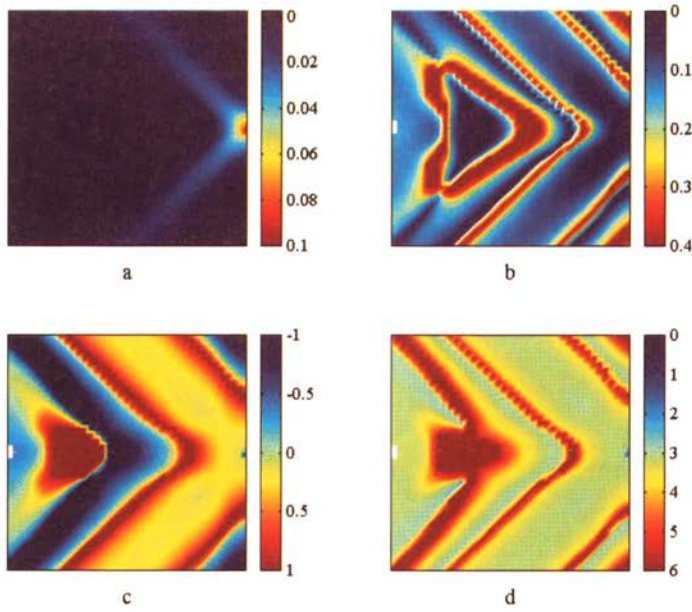


FIGURE 9. Micro-displacement along  $x$ -axis (Case H): (a) mean, (b) c.o.v., (c) skewness coefficient, (d) kurtosis coefficient.

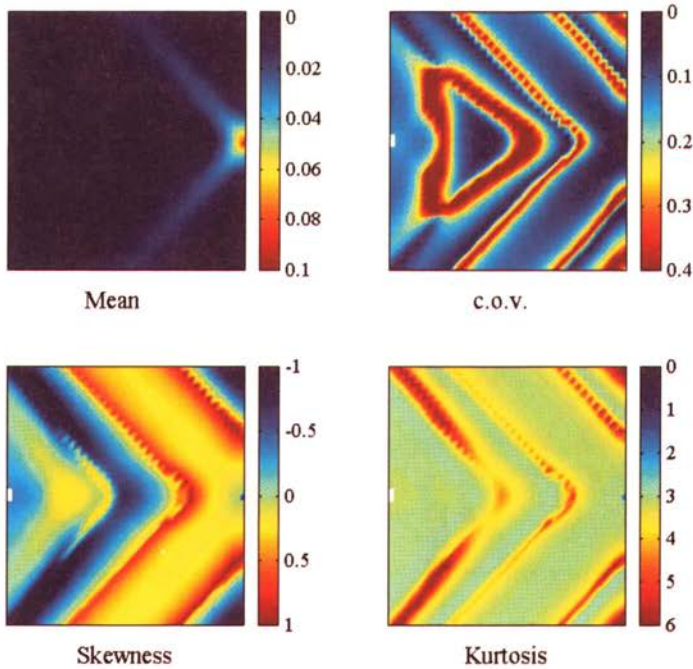


FIGURE 10. Micro-displacement along  $x$ -axis (Case C).

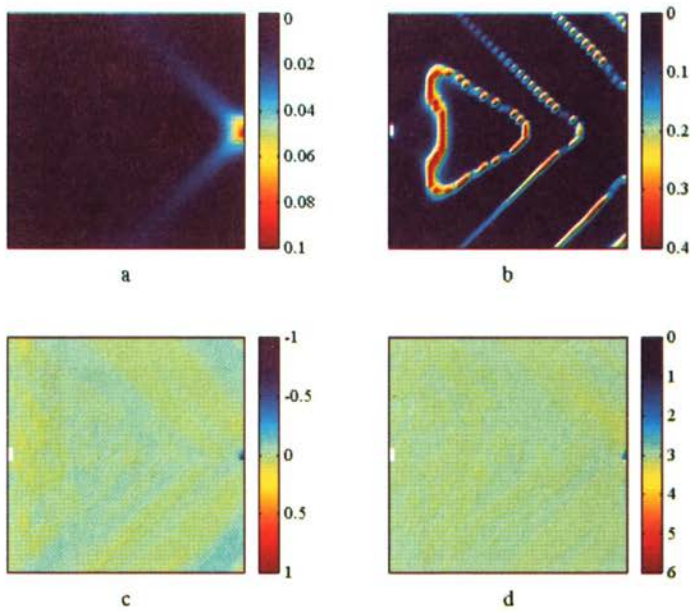


FIGURE 11. Micro-displacement along  $x$ -axis (Case U): (a) mean, (b) c.o.v., (c) skewness coefficient, (d) kurtosis coefficient.

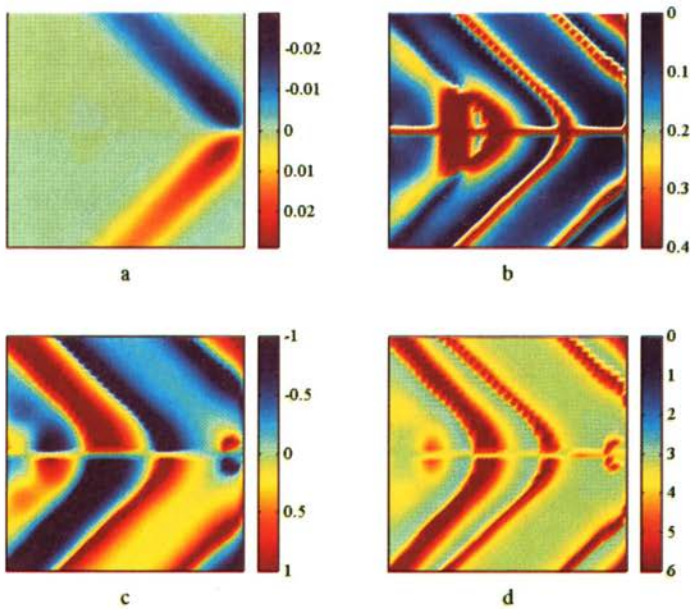


FIGURE 12. Micro-displacement along  $y$ -axis (Case H): (a) mean, (b) c.o.v., (c) skewness coefficient, (d) kurtosis coefficient.

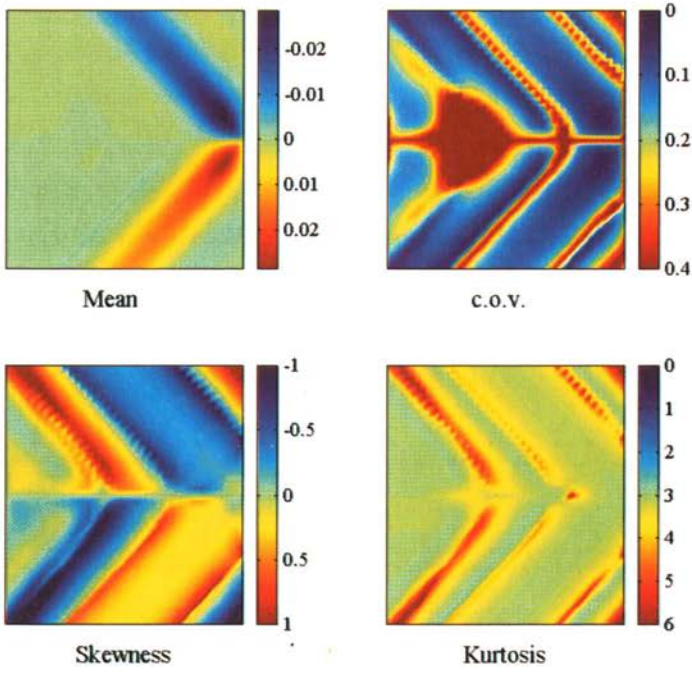


FIGURE 13. Micro-displacement along  $y$ -axis (Case C).

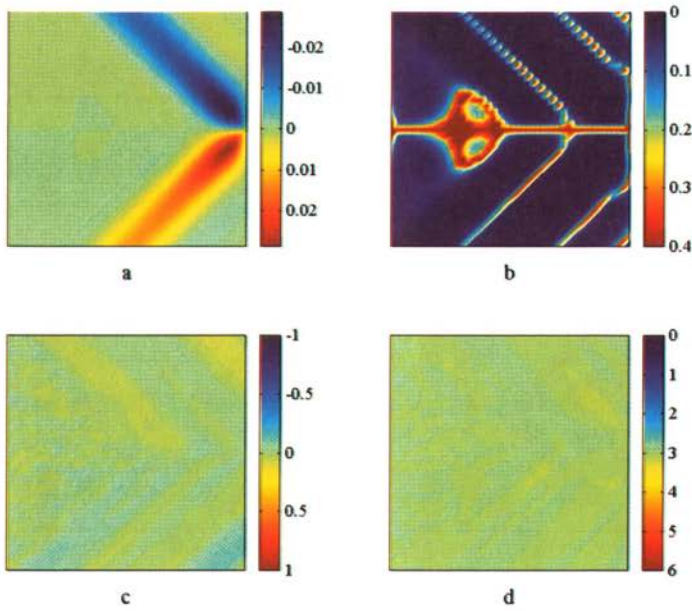


FIGURE 14. Micro-displacement along  $y$ -axis (Case U): (a) mean, (b) c.o.v., (c) skewness coefficient, (d) kurtosis coefficient.

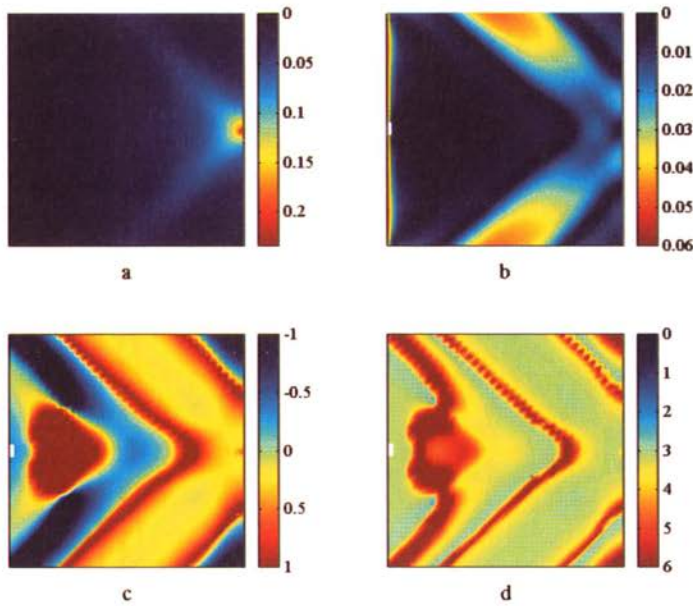


FIGURE 15. Total-displacement along  $x$ -axis (Case H): (a) mean, (b) c.o.v., (c) skewness coefficient, (d) kurtosis coefficient.

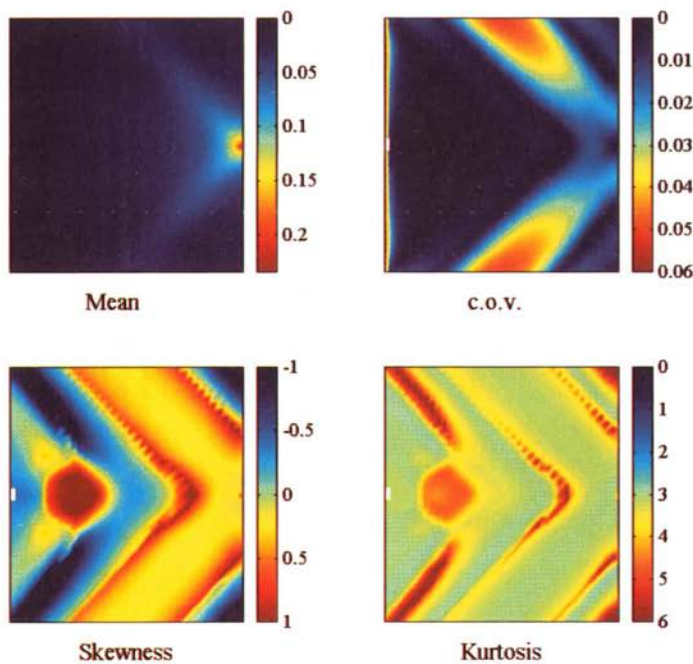


FIGURE 16. Total-displacement along  $x$ -axis (Case C).

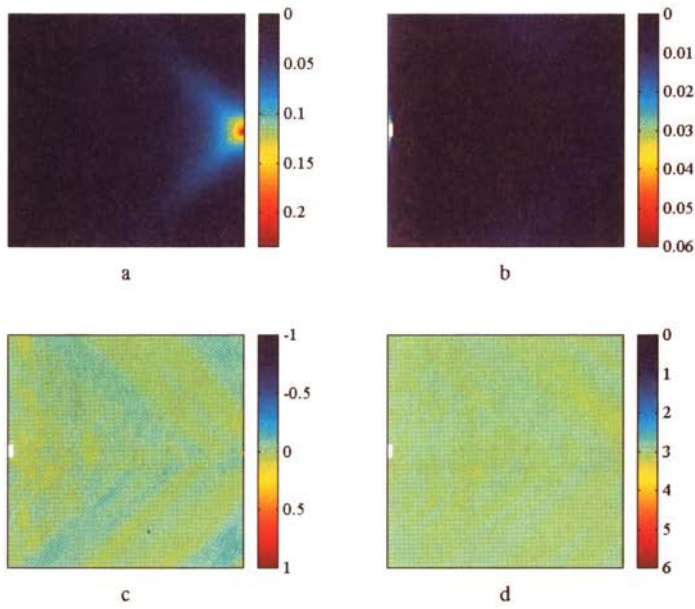


FIGURE 17. Total-displacement along  $x$ -axis (Case U): (a) mean, (b) c.o.v., (c) skewness coefficient, (d) kurtosis coefficient.

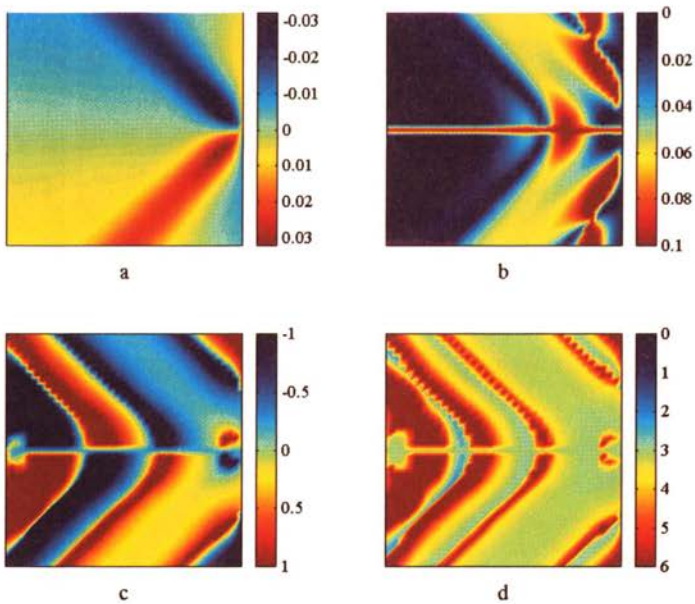
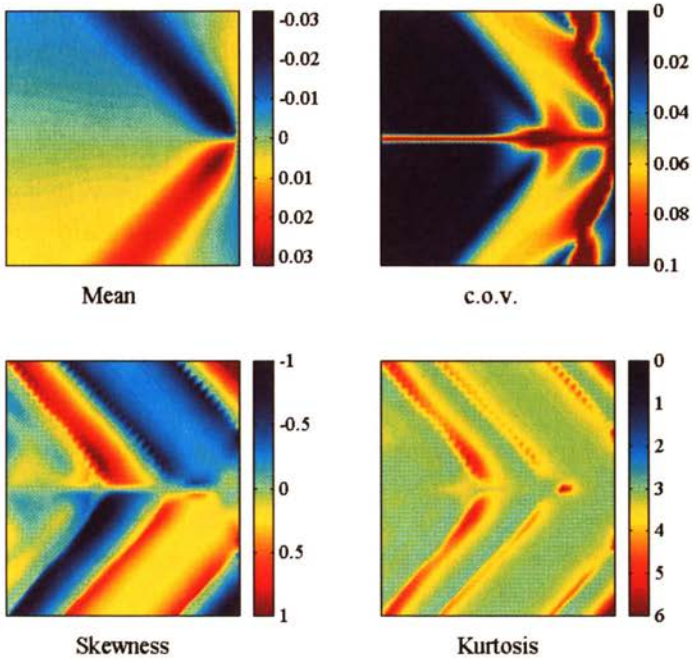
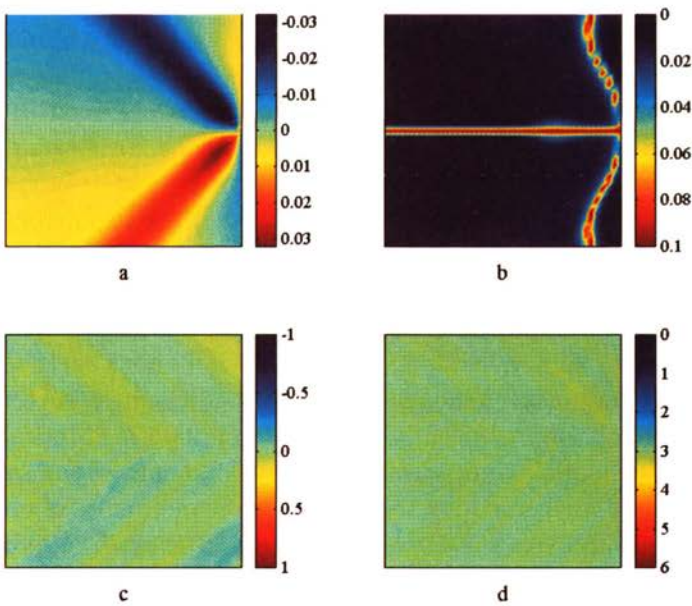


FIGURE 18. Total-displacement along  $y$ -axis (Case H): (a) mean, (b) c.o.v., (c) skewness coefficient, (d) kurtosis coefficient.

FIGURE 19. Total-displacement along  $y$ -axis (Case C).FIGURE 20. Total-displacement along  $y$ -axis (Case U): (a) mean, (b) c.o.v., (c) skewness coefficient, (d) kurtosis coefficient.

Pattern formation occur as evidenced in Figs. 3-20. The random correlation seems to not influence significantly the localization zones of the averaged strain and strain localization phenomena become the more evident as the matter is softer and softer.

Patterns accruing in the diagrams of the moments of the distributions of displacements are strongly influenced by the random correlation of the material properties and depend strictly on the random non-locality of them. Precisely, pattern formation in the portraits of skewness and kurtosis is as stronger as the mesoscale characteristic length is more and more correlated. In case (U), in fact, they are practically absent, while they become more and more evident going from case (U) to case (H).

Localization zones are indicators toward the transition from the elastic to the irreversible behavior. There the distributions are far from Gaussian and we may conjecture that this discrepancy from Gaussian behavior may be due to the presence of a net of strongly interacting microcracks 'oriented' along the localization itself. The presence of such a net, in fact, could break the symmetry of the distribution and its Gaussian properties.

#### 4. Bibliographic remark

The continuum model of elastic microcracked bodies presented here has been formulated and developed in (Mariano, 1999; Mariano and Trovalusci, 1999; Mariano and Stazi, 2001). The contemporary validity of multiplicative and additive decompositions of the gradient of deformation for continua with smeared discontinuities (like microcracks) has been obtained in a rigorous way in (Del Piero and Owen, 1993, 2000) by using an elegant procedure based on the concept of limit of bodies.

The description of the substructural randomness of microcrack distribution has been presented in (Mariano, Giuffrè, Stazi and Augusti, 2004) together with the numerical results collected here.

As regards standard approaches to the description of the mechanical behavior of elastic microcracked bodies, the self-consistent method has been formulated in (Budiansky, 1965; Budiansky and O'Connell, 1976), the differential scheme in (Hashin, 1988), Mori-Tanaka method in (Mori and Tanaka, 1973). Critical remarks, comparisons and developments of the standard approach based on homogenization techniques to the mechanics of microcracked bodies can be found in various works (see e.g. Kachanov, 1993; Torquato, 2002).

## Lecture II

### Geometry of substructural interactions and time-varying states

In the approach to the mechanics of microcracked bodies discussed in Lecture I, the presence of microcracks is accounted for already at the level of kinematics. Such a point of view can be in general adopted in analyzing the mechanics of complex bodies. The essential point is that one introduces information about the morphology of the material substructure at the level of geometrical description of the body. Such information is carried on by an appropriate coarse grained descriptor  $\nu$  (order parameter) of the substructure of each material element. Of course, for any complex body the choice of the order parameter may be not unique: it characterizes the level of detail of substructural description accounted for in each special model.

Such a point of view is different from standard micromechanics. There, in fact, up to level of constitutive issues, each body is a Cauchy's continuum in which each material element is described just by its place in space. Only standard interactions (tensions) accrue between neighboring material elements as objects developing power in the velocity of material elements. Then, when constitutive equations come into play, one tries to account for the presence of material texture (substructure) through homogenization procedures of various nature. As a result one obtains a stiffness altered to simulate at a macroscopic level the effects of the material texture.

However, not always homogenization can capture prominent aspects of the physical behavior as for example in the case of nematic liquid crystals. Often, the introduction of appropriate kinematical descriptors of the substructure allows one to describe directly interactions due to substructural changes. They are represented by quantities power conjugated with the rate of the order parameter and are appropriately balanced.

Order parameters can be variously chosen. However, it is not necessary to specify the nature of the order parameter to construct the essential structures of the mechanics of complex bodies. To this aim we need just to presume that the order parameter  $\nu$  belongs to an abstract differentiable manifold  $\mathcal{M}$  that we assume here with finite dimension for the sake of simplicity.

Once the formal structure has been constructed, special models describing particular physical behaviors follow from the explicit choice of  $\nu$  and appropriate constitutive equations.

## 5. Elementary notions about manifolds

A topological space  $\mathfrak{M}$  is *Hausdorff* if for any pair of distinct elements  $\nu_1$  and  $\nu_2$  of it one may find neighborhoods  $\mathcal{I}_{\nu_1}$  and  $\mathcal{I}_{\nu_2}$  of  $\nu_1$  and  $\nu_2$  respectively

which do not intersect each other. Here we assume also that each element of  $\mathfrak{M}$  has a topology with countable basis.

$\mathfrak{M}$  is *locally Euclidean* of dimension  $m$  if each point of it has a neighborhood  $\mathcal{U}$  homeomorphic to an open subset  $\mathcal{V}$  of  $\mathbb{R}^m$ . In other words, for any  $\nu \in \mathfrak{M}$ , there is  $\mathcal{U} \subseteq \mathfrak{M}$  containing  $\nu$  and a one-to-one mapping  $\varphi : \mathcal{U} \rightarrow \mathcal{V} \subseteq \mathbb{R}^m$  from  $\mathcal{U}$  onto  $\mathcal{V}$ , with  $\mathcal{V}$  open.  $(\mathcal{U}, \varphi)$  is called *chart* (or *coordinate system*) and  $\nu^\alpha = \varphi^\alpha(\nu)$  is in this sense the  $\alpha$ -th coordinate of  $\nu$  (indeed  $\varphi^\alpha(\nu)$  is the  $\alpha$ -th coordinate of  $\varphi(\nu) \in \mathbb{R}^m$ ).

Let  $\mathfrak{F} = \{(\mathcal{U}_i, \varphi_i)\}$  be a collection of coordinate systems indexed by  $i \in I$  such that  $\bigcup_{i \in I} \mathcal{U}_i = \mathfrak{M}$ . If for all  $i, j \in I$

(i)  $\varphi_i \circ \varphi_j^{-1}$  is of class  $C^k$  with  $1 \leq k \leq +\infty$ , and

(ii) for any coordinate system  $(\mathcal{U}, \varphi)$  such that  $\varphi \circ \varphi_i^{-1}$  and  $\varphi_i \circ \varphi^{-1}$  are of class  $C^k$  for all  $i \in I$ , one finds  $(\mathcal{U}, \varphi) \in \mathfrak{F}$ ,

then  $\mathfrak{F}$  is called *differentiable structure* of class  $C^k$  over  $\mathfrak{A}$ .

**Definition 1:** A  $C^k$  differentiable manifold  $\mathcal{M}$  of finite dimension  $m$  is a locally Euclidean space of dimension  $m$  endowed with a differentiable structure of class  $C^k$  and dimension  $m$ .

When  $C^k$  is not specified, it is intended that  $\mathcal{M}$  is smooth, i.e. of class  $C^\infty$ .

Let  $f : [-\bar{s}, \bar{s}] \rightarrow \mathcal{M}$  be a continuous and differentiable curve over  $\mathcal{M}$ . We indicate with  $\nu$  the value  $f(0)$  and with  $\dot{\nu}$  the value  $\frac{df}{ds} \Big|_{s=0}$ . We say that  $\dot{\nu}$  is tangent to  $\mathcal{M}$  at  $\nu$ . It can be considered as defined by an equivalence class of curves if one considers  $f$  and  $f_1 : [-\bar{s}, \bar{s}] \rightarrow \mathcal{M}$  equivalent when  $f(0) = f_1(0)$  and  $\lim_{s \rightarrow 0} \frac{1}{s} (f(s) - f_1(s)) = 0$ .

With the notation  $T_\nu \mathcal{M}$ , the space of all  $\dot{\nu}$  determined by all possible equivalence classes of curves at  $\nu$  is indicated. It is called *tangent space* of  $\mathcal{M}$  at  $\nu$ , is a linear space and has the same dimension  $m$  of  $\mathcal{M}$ . The union  $T\mathcal{M} = \bigcup_{\nu \in \mathcal{M}} T_\nu \mathcal{M}$  of all tangent spaces of  $\mathcal{M}$  (called *tangent bundle*) has the natural structure of differentiable manifold and its dimension is equal to  $2m$ . A generic element of  $T\mathcal{M}$  is then the pair  $(\nu, \dot{\nu})$ . Each  $\dot{\nu}$  cannot be separated by its pertinent  $\nu$  unless a remote parallelism is defined on  $\mathcal{M}$  (see for details any textbook on differential geometry). Notice that  $T\mathcal{M}$  is not a linear space although each  $T_\nu \mathcal{M}$  be.

For each  $T_\nu \mathcal{M}$ , the space of linear functions over it is indicated with  $T_\nu^* \mathcal{M}$  and called *cotangent space* of  $\mathcal{M}$  at  $\nu$ . It is a linear space with dimension equal to  $m$ . The union  $T^* \mathcal{M} = \bigcup_{\nu \in \mathcal{M}} T_\nu^* \mathcal{M}$  of all cotangent spaces of  $\mathcal{M}$  (called *cotangent bundle*) has the natural structure of differentiable manifold and its dimension is still equal to  $2m$ . Notice that if  $\mathbf{z} \in T_\nu^* \mathcal{M}$  and  $\dot{\nu} \in T_\nu \mathcal{M}$ , the product  $\mathbf{z} \cdot \dot{\nu}$  is well defined and is the value of  $\mathbf{z}$  at  $\dot{\nu}$ .

Let  $\mathcal{M}$  and  $\mathcal{N}$  be two manifolds. We may imagine to decorate  $\mathcal{M}$  by attaching at each  $\nu \in \mathcal{M}$  a copy of  $\mathcal{N}$  (a comb is an intuitive representation of what we are describing). The resulting structure, say  $\mathcal{Y}$ , is called *fiber bundle* and is endowed with a natural projection  $\pi : \mathcal{Y} \rightarrow \mathcal{M}$  such that for each  $\nu \in \mathcal{M}$  one gets  $\pi^{-1}(\nu) = \mathcal{N}$ .

Given  $\mathcal{M}$ , a differentiable k-form  $\omega^k(\nu)$  at  $\nu \in \mathcal{M}$  is a k-linear skew-symmetric function  $\omega^k(\nu) : T_\nu \mathcal{M} \rightarrow \mathbb{R}$ .

For example, in the three-dimensional Euclidean space  $\mathcal{E}^3$ , the infinitesimal volume element  $d(vol)$  is a 3-form that we may indicate with  $dx_1 \wedge dx_2 \wedge dx_3$  (where  $\wedge$  denotes the external product involving the one forms  $dx_i$  - see any textbook on differential geometry). In particular, below we indicate with  $d^3\mathbf{X} \wedge dt$  the volume form in the four-dimensional space-time tube  $\mathcal{B}_0 \times [0, \bar{t}]$ , where  $[0, \bar{t}]$  is a given interval of time.

### 6. Lagrangian structures in the conservative setting

To portray some general aspects of the mechanics of complex bodies, we follow here the pattern of Lecture I at least up to a certain extent, generalizing it. So, once more,  $\mathcal{B}_0$  is the regular region of the three-dimensional Euclidean point space  $\mathcal{E}^3$  occupied by a body in its reference place. A standard deformation is a sufficiently smooth injective mapping

$$\mathcal{B}_0 \ni \mathbf{X} \xrightarrow{\tilde{\mathbf{x}}} \mathbf{x} = \tilde{\mathbf{x}}(\mathbf{X}) \in \mathcal{E}^3. \tag{6.1}$$

It transfers the material element ‘collapsed’ at  $\mathbf{X} \in \mathcal{B}_0$  in the new (current) place  $\mathbf{x}$ , is orientation preserving (in the sense that  $\det \mathbf{F} > 0$ , at each  $\mathbf{X}$ , with  $\mathbf{F}$  the gradient  $\nabla \mathbf{x}(\mathbf{X})$ ) and the region  $\mathcal{B} = \tilde{\mathbf{x}}(\mathcal{B}_0)$  is regular.

To represent the substructure of each material element we introduce a coarse grained morphological descriptor  $\nu$ . As remarked above, we do not specify here the nature of  $\nu$ , requiring only that  $\nu$  belongs to an abstract finite dimensional differentiable manifold  $\mathcal{M}$ . Each special model needs the selection of specific features of  $\mathcal{M}$ . We have then a sufficiently smooth mapping

$$\mathcal{B}_0 \ni \mathbf{X} \xrightarrow{\tilde{\nu}} \nu = \tilde{\nu}(\mathbf{X}) \in \mathcal{M}. \tag{6.2}$$

For subsequent developments we need just to assume that  $\tilde{\nu}$  be continuous and piecewise continuously differentiable.

Let  $\mathcal{C}_{\mathbf{x}}$  be the space of  $\tilde{\mathbf{x}}$  and  $\mathcal{C}_\nu$  the space of  $\tilde{\nu}$ . *Motions* are curves in  $\mathcal{C}$  represented by  $[0, \bar{t}] \ni t \mapsto (\tilde{\mathbf{x}}_t, \tilde{\nu}_t) \in \mathcal{C} \equiv \mathcal{C}_{\mathbf{x}} \times \mathcal{C}_\nu$ , with  $t$  the time, and we denote with  $\dot{\mathbf{x}} = \frac{d\tilde{\mathbf{x}}(\mathbf{X}, t)}{dt}$  and  $\dot{\nu} = \frac{d\tilde{\nu}(\mathbf{X}, t)}{dt}$  the relevant rates.

Let us consider a fiber bundle

$$\pi : \mathcal{Y} \rightarrow \mathcal{B}_0 \times [0, \bar{t}] \tag{6.3}$$

such that  $\pi^{-1}(\mathbf{X}, t) = \mathcal{E}^3 \times \mathcal{M}$ . A generic section  $\eta \in \Gamma(\mathcal{Y})$  is then  $\eta(\mathbf{X}, t) = (\mathbf{X}, t, \mathbf{x}, \nu)$ . If one requires sufficient smoothness for sections, the first jet bundle  $J^1\mathcal{Y}$  over  $\mathcal{Y}$  is such that

$$J^1\mathcal{Y} \ni j^1(\eta)(\mathbf{X}, t) = (\mathbf{X}, t, \mathbf{x}, \dot{\mathbf{x}}, \mathbf{F}, \nu, \dot{\nu}, \nabla\nu). \quad (6.4)$$

Just geometry is involved in the representation of the morphology of a complex body. In constructing a mechanical model, at this point one introduces usually physical issues. Precisely, one discusses the representation of interactions and their balance first, then the explicit representation of constitutive relations. The two issues are essentially separated. The representation of interactions by means of appropriate vectors or higher order tensors is a consequence of the essential geometrical description of the body (interactions are in fact entities power conjugated with the rates of morphological descriptors) and the balance is independent of the constitutive nature of the material.

Below, in the conservative case we develop appropriate Lagrangian and Hamiltonian formalism for complex bodies. In making this, precisely in introducing the Lagrangian density just after geometrical issues, we put on the same ground the representation of interactions and constitutive issues because they are mixed in the variational description.

If the body is made of a non-linear elastic material, we may associate with it the canonical Lagrangian 3 + 1 form

$$L : J^1\mathcal{Y} \rightarrow \wedge^{3+1}(\mathcal{B}_0 \times [0, \bar{t}]) \quad (6.5)$$

that we presume to admit sufficiently smooth density such that

$$L(j^1(\eta)(\mathbf{X}, t)) = \mathcal{L}(\mathbf{X}, \mathbf{x}, \dot{\mathbf{x}}, \mathbf{F}, \nu, \dot{\nu}, \nabla\nu) d^3\mathbf{X} \wedge dt. \quad (6.6)$$

We assume the following typical general Lagrangian density:

$$\begin{aligned} \mathcal{L}(\mathbf{X}, \mathbf{x}, \dot{\mathbf{x}}, \mathbf{F}, \nu, \dot{\nu}, \nabla\nu) = & \frac{1}{2}\rho_0 |\dot{\mathbf{x}}|^2 + \rho_0\chi(\nu, \dot{\nu}) - \\ & - \rho_0 e(\mathbf{X}, \mathbf{F}, \nu, \nabla\nu) - \rho_0 w(\mathbf{x}, \nu), \end{aligned} \quad (6.7)$$

where  $\rho_0$  is the referential mass density (conserved during the motion),  $\chi$  is the *kinetic co-energy* pertaining possibly to the substructure<sup>2)</sup>,  $e$  is the elastic energy density, and  $w$  is the density of the potential of external actions, all per unit mass.

<sup>2)</sup> The kinetic energy  $k(\nu, \dot{\nu})$  pertaining possibly to the substructure is given by  $k = \partial_{\dot{\nu}}\chi \cdot \dot{\nu} - \chi$ .

In principle, since  $\mathcal{B}_0 \times [0, \bar{t}]$  is a manifold with boundary (constituted by  $\mathcal{B}_0 \times \{0\}$  and  $\mathcal{B}_0 \times \{\bar{t}\}$ ) we should take care in defining each element of the space of 3 + 1 forms  $\Lambda^{3+1}(\mathcal{B}_0 \times [0, \bar{t}])$ . However, our main interest in elasticity is to evaluate the variation of the total Lagrangian  $\bar{L}(\mathcal{B}_0) = \int_{\mathcal{B}_0 \times [0, \bar{t}]} \mathcal{L} d^3\mathbf{X} \wedge dt$ ; so that, in defining  $L(j^1(\eta))$ , possible problems related with boundary do not play any rôle and we may find at least one section (with the properties of  $\tilde{\mathbf{x}}$  and  $\tilde{\nu}$ ) satisfying Euler-Lagrange equations for  $\bar{L}(\mathcal{B}_0)$ , namely

$$\overline{\partial_{\tilde{\mathbf{x}}}\mathcal{L}} = \partial_{\tilde{\mathbf{x}}}\mathcal{L} - \text{Div } \partial_{\mathbf{F}}\mathcal{L}, \tag{6.8}$$

$$\overline{\partial_{\tilde{\nu}}\mathcal{L}} = \partial_{\tilde{\nu}}\mathcal{L} - \text{Div } \partial_{\nabla_{\nu}}\mathcal{L}. \tag{6.9}$$

### 6.1. Changes of observers and relabeling

As anticipated in discussing the mechanics of microcracked bodies, in dealing with complex materials we need to include in the definition of observer all the geometrical environments necessary to the description of the morphology of the body. In fact, to describe a complex body we call upon the time interval  $[0, \bar{t}]$ , the reference place  $\mathcal{B}_0$ , the ambient space  $\mathcal{E}^3$  and the manifold of substructural states  $\mathcal{M}$ . We deal with changes in observers characterized by the same measure of time, so that our attention is focused on different representations of  $\mathcal{E}^3$  and  $\mathcal{M}$ . Moreover we consider also relabeling of material elements in  $\mathcal{B}_0$ , simulating a redistribution of possible defects. We then consider smooth one-parameter families of transformations defined below.

**Changes of observers.** For complex bodies a generic change of observer involves a couple of transformations: one of the ambient space, the other of the manifold of substructural states  $\mathcal{M}$ . They are described below.

- $\mathbb{R}^+ \ni s_1 \mapsto \mathbf{f}_{s_2}^2 \in \text{Aut}(\mathcal{E}^3)$ , with  $\mathbf{f}_0^2$  the identity<sup>3)</sup>. We put  $\mathbf{f}_0^2(\mathbf{X}) = \mathbf{v}$ .
- A Lie group  $G$ , with Lie algebra  $\mathfrak{g}$ , acts over  $\mathcal{M}$ . If  $\xi \in \mathfrak{g}$ , its action over  $\nu \in \mathcal{M}$  is indicated with  $\xi_{\mathcal{M}}(\nu)$ . By indicating with  $\nu_g$  the value of  $\nu$  after the action of  $g \in G$  (the way is not essential), if we consider a one-parameter smooth curve  $\mathbb{R}^+ \ni s_1 \mapsto g_{s_3} \in G$  over  $G$  and its corresponding curve  $s_1 \mapsto \nu_{g_{s_3}}$  over  $\mathcal{M}$ , starting from a given  $\nu$ , we have  $\xi_{\mathcal{M}}(\nu) = \left. \frac{d}{ds_3} \nu_{g_{s_3}} \right|_{s_3=0}$ .

---

<sup>3)</sup>  $\text{Aut}(\mathcal{E}^3)$  is the group of automorphisms of  $\mathcal{E}^3$ .

**Relabeling.** It is in certain sense a ‘permutation of inhomogeneities’. Formally it is described by the action of the special group of isocoric diffeomorphisms  $SDiff$  on  $\mathcal{B}_0$ .

- $\mathbb{R}^+ \ni s_1 \mapsto \mathbf{f}_{s_1}^1 \in SDiff(\mathcal{B}_0, \mathcal{E}^3)$ , with  $\mathbf{f}_0^1$  the identity; i.e. at each  $s_1$  we get  $\mathbf{X} \mapsto \mathbf{f}_{s_1}^1(\mathbf{X})$ , with  $\text{Div } \mathbf{f}_{s_1}^{1'}(\mathbf{X}) = 0$ , where the prime denotes differentiation with respect to the parameter (here  $s_1$ ). We put  $\mathbf{f}_0^{1'}(\mathbf{X}) = \mathbf{w}$ .

**Definition 2 (Invariance of  $\mathcal{L}$ ):** A Lagrangian density  $\mathcal{L}$  is invariant with respect to the action of  $\mathbf{f}_{s_1}^1$ ,  $\mathbf{f}_{s_2}^2$  and  $G$  if

$$\begin{aligned} \mathcal{L}(\mathbf{X}, \mathbf{x}, \dot{\mathbf{x}}, \mathbf{F}, \nu, \dot{\nu}, \nabla \nu) \\ = \mathcal{L}\left(\mathbf{f}^1, \mathbf{f}^2, (\text{grad } \mathbf{f}^2) \dot{\mathbf{x}}, (\text{grad } \mathbf{f}^2) \mathbf{F} (\nabla \mathbf{f}^1)^{-1}, \nu_g, \dot{\nu}_g, (\nabla \nu_g) (\nabla \mathbf{f}^1)^{-1}\right). \end{aligned} \quad (6.10)$$

where we indicate with  $\mathbf{f}^1$ ,  $\mathbf{f}^2$  and  $\nu_g$  the values  $\mathbf{f}_{s_1}^1(\mathbf{X})$ ,  $\mathbf{f}_{s_2}^2(\mathbf{x})$ ,  $\nu_{g_{s_3}}(\mathbf{X})$ .

Let  $\mathcal{Q}$  and  $\mathfrak{F}$  be scalar and vector densities given respectively by

$$\mathcal{Q} = \partial_{\dot{\mathbf{x}}} \mathcal{L} \cdot (\mathbf{v} - \mathbf{F}\mathbf{w}) + \partial_{\dot{\nu}} \mathcal{L} \cdot (\xi_{\mathcal{M}}(\nu) - (\nabla \nu) \mathbf{w}), \quad (6.11)$$

$$\mathfrak{F} = \mathcal{L}\mathbf{w} + (\partial_{\mathbf{F}} \mathcal{L})^T (\mathbf{v} - \mathbf{F}\mathbf{w}) + (\partial_{\nabla \nu} \mathcal{L})^T (\xi_{\mathcal{M}}(\nu) - (\nabla \nu) \mathbf{w}). \quad (6.12)$$

**Theorem 1:** If the Lagrangian density  $\mathcal{L}$  is invariant under  $\mathbf{f}_{s_1}^1$ ,  $\mathbf{f}_{s_2}^2$  and  $G$ , then

$$\dot{\mathcal{Q}} + \text{Div } \mathfrak{F} = 0. \quad (6.13)$$

The proof follows by direct calculation.

The key usefulness of the theorem above (a multifield generalization of Noether theorem for classical elasticity) is clear in the corollaries below.

**Corollary 1.** If  $\mathbf{f}_{s_2}^2$  alone acts on  $\mathcal{L}$  leaving  $\mathbf{v}$  arbitrary, from (6.13) we get Cauchy’s balance of momentum

$$\rho_0 \ddot{\mathbf{x}} = \rho_0 \mathbf{b} + \text{Div } \mathbf{P}, \quad (6.14)$$

where  $\mathbf{P} = -\partial_{\mathbf{F}} \mathcal{L}$  is the first Piola–Kirchhoff stress and  $\mathbf{b} = \partial_{\mathbf{x}} \mathcal{L}$  the vector of body forces.

At each  $\mathbf{X}$ ,  $\mathbf{P}(\mathbf{X}) \in \text{Hom}(T_{\mathbf{X}}^* \mathcal{B}_0, T_{\mathbf{X}}^* \mathcal{B})$ . In other words, it maps linearly normals to surfaces in  $\mathcal{B}_0$  into tensions in  $\mathcal{B}_0$ .

**Corollary 2.** If  $G$  arbitrary acts alone on  $\mathcal{L}$ , from (6.13) we get Capriz’s balance of substructural interactions

$$\rho_0 \left( \overline{\partial_{\dot{\nu}} \chi} - \partial_{\nu} \chi \right) = -\mathbf{z} + \rho_0 \beta^{ni} + \text{Div } \mathcal{S}, \quad (6.15)$$

in covariant way, where  $\beta^{ni} = -\rho_0 \partial_\nu w$  represents bulk non-inertial external interactions acting on the substructure,  $\mathcal{S} = -\partial_{\nabla\nu} \mathcal{L}$  contact substructural interactions between neighboring material elements (and is called *microstress*),  $\mathbf{z} = -\rho_0 \partial_\nu e$  self-interactions of the substructure in each material element (and is called *self-force*).

At each  $\mathbf{X}$ ,  $\mathcal{S}(\mathbf{X}) \in Hom(T_{\mathbf{X}}^* \mathcal{B}_0, T_{\nu}^* \mathcal{M})$  and  $\mathbf{z}(\mathbf{X}) \in T_{\nu}^* \mathcal{M}$ . In other words, at each  $\mathbf{X}$  in  $\mathcal{B}_0$ ,  $\mathbf{z}$  is an element of the cotangent space of the manifold  $\mathcal{M}$  of substructural states at  $\nu = \tilde{\nu}(\mathbf{X})$  and the microstress  $\mathcal{S}$  maps linearly normals to surfaces in  $\mathcal{B}_0$  into elements of  $T_{\nu}^* \mathcal{M}$  which play the rôle of generalized tensions.

**Corollary 3.** Let  $G = SO(3)$  and, for any element  $\dot{\mathbf{q}} \times$  of its Lie algebra,  $\mathbf{f}_{s_3}^2$  be such that  $\mathbf{v} = \dot{\mathbf{q}} \times (\mathbf{x} - \mathbf{x}_0)$  with  $\mathbf{x}_0$  a fixed point in space. If  $w$  is independent of  $\mathbf{x}$ ,  $\chi$  on  $\nu$ , and only the special choices of  $\mathbf{f}_{s_2}^2$  and  $G$  just defined act on  $\mathcal{L}$ , one gets from (6.13)

$$\text{skw}(\partial_{\mathbf{F}} e \mathbf{F}^T) = \mathbf{e} \left( \mathcal{A}^T \partial_\nu e + (\nabla \mathcal{A}^T)^t \partial_{\nabla\nu} e \right), \tag{6.16}$$

where  $\mathbf{e}$  is Ricci's alternating tensor and  $\text{skw}(\cdot)$  extracts the skew-symmetric part of its argument.

**Corollary 4.** If  $\mathbf{f}_{s_1}^1$  alone acts on  $\mathcal{L}$ , with  $\mathbf{w}$  arbitrary, from (6.13) one gets

$$\overline{(\mathbf{F}^T \partial_{\dot{\mathbf{x}}} \mathcal{L} + \nabla \nu^T \partial_{\dot{\nu}} \mathcal{L})} - \text{Div} \left( \mathbb{P} - \left( \frac{1}{2} \rho_0 |\dot{\mathbf{x}}|^2 + \rho_0 \chi(\nu, \dot{\nu}) \right) \mathbf{I} \right) - \partial_{\mathbf{X}} \mathcal{L} = \mathbf{0} \tag{6.17}$$

where  $\mathbb{P} = \rho_0 e \mathbf{I} - \mathbf{F}^T \mathbf{P} - \nabla \nu^T \mathcal{S}$ , with  $\mathbf{I}$  the second order unit tensor, is the generalized Eshelby tensor for complex bodies.

**Corollary 5.** Let  $G = SO(3)$  and, for any element  $\dot{\mathbf{q}} \times$  of its Lie algebra,  $\mathbf{f}_{s_1}^1$  is such that  $\mathbf{w} = \dot{\mathbf{q}} \times (\mathbf{X} - \mathbf{X}_0)$  with  $\mathbf{X}_0$  a fixed point in  $\mathcal{B}_0$ . If the material is homogeneous, and only the special choices of  $\mathbf{f}_{s_2}^2$  and  $G$  just defined act on  $\mathcal{L}$ ,  $\mathbb{P}$  is symmetric.

### 7. Elementary Hamiltonian structures

From the Lagrangian description of the mechanics of complex bodies, Hamiltonian structures follow in a natural way. Let  $\mathbf{p}$  and  $\mu$  be respectively the *canonical momentum* and the *canonical substructural momentum* defined by  $\mathbf{p} = \partial_{\dot{\mathbf{x}}} \mathcal{L}$  and  $\mu = \partial_{\dot{\nu}} \mathcal{L}$ .

The *Hamiltonian density*  $\mathcal{H}$  can be then introduced. It is given by

$$\mathcal{H}(\mathbf{X}, \mathbf{x}, \mathbf{p}, \mathbf{F}, \nu, \mu, \nabla \nu) = \mathbf{p} \cdot \dot{\mathbf{x}} + \mu \cdot \dot{\nu} - \mathcal{L}(\mathbf{X}, \mathbf{x}, \dot{\mathbf{x}}, \mathbf{F}, \nu, \dot{\nu}, \nabla \nu). \tag{7.1}$$

In terms of partial derivatives of  $\mathcal{H}$ , the balances (6.8) and (6.9) can be written as

$$\dot{\mathbf{p}} = -\partial_{\mathbf{x}}\mathcal{H} + \text{Div } \partial_{\mathbf{F}}\mathcal{H}, \tag{7.2}$$

$$\dot{\mathbf{x}} = \partial_{\mathbf{p}}\mathcal{H},$$

$$\dot{\mu} = -\partial_{\nu}\mathcal{H} + \text{Div } \partial_{\nabla\nu}\mathcal{H}, \tag{7.3}$$

$$\dot{\nu} = \partial_{\mu}\mathcal{H},$$

which are Hamilton equations for complex bodies. They are associated with general boundary conditions of the type

$$\mathbf{x}(\mathbf{X}) = \bar{\mathbf{x}} \quad \text{on } \partial^{(\mathbf{x})}\mathcal{B}_0, \tag{7.4}$$

$$\partial_{\mathbf{F}}\mathcal{H}\mathbf{n} = \mathbf{t} \quad \text{on } \partial^{(\mathbf{t})}\mathcal{B}_0, \tag{7.5}$$

$$\nu(\mathbf{X}) = \bar{\nu} \quad \text{on } \partial^{(\nu)}\mathcal{B}_0, \tag{7.6}$$

$$\partial_{\nabla\nu}\mathcal{H}\mathbf{n} = \mathbf{t} \quad \text{on } \partial^{(\mathbf{t})}\mathcal{B}_0; \tag{7.7}$$

where  $\bar{\mathbf{x}}$ ,  $\mathbf{t}$ ,  $\bar{\nu}$  and  $\mathbf{t}$  are prescribed on the relevant parts  $\partial^{(\cdot)}\mathcal{B}_0$  of the boundary,  $Cl(\partial\mathcal{B}_0) = Cl(\partial^{(\mathbf{x})}\mathcal{B}_0 \cup \partial^{(\mathbf{t})}\mathcal{B}_0)$ , with  $\partial^{(\mathbf{x})}\mathcal{B}_0 \cap \partial^{(\mathbf{t})}\mathcal{B}_0 = \emptyset$ , and  $Cl(\partial\mathcal{B}_0) = Cl(\partial^{(\nu)}\mathcal{B}_0 \cup \partial^{(\mathbf{t})}\mathcal{B}_0)$ , with  $\partial^{(\nu)}\mathcal{B}_0 \cap \partial^{(\mathbf{t})}\mathcal{B}_0 = \emptyset$ , where  $Cl$  indicates closure and  $\mathbf{n}$  is the outward unit normal to  $\partial\mathcal{B}_0$  at all points in which it is well defined.

For some special cases (like microcracked bodies or liquids with bubbles) one may not find even in principle a loading device able to prescribe  $\mathbf{t}$  in (7.7). In this case the boundary of the body can be considered as a structured interface between the body itself and the rest of the environment. So that one may assume that there exist two surface densities  $\bar{U}(\mathbf{x})$  and  $U(\nu)$  such that  $\mathbf{t} = \rho_0\partial_{\mathbf{x}}\bar{U}$  and  $\mathbf{t} = \rho_0\partial_{\nu}U$ .

The Hamiltonian  $H$  of the whole body is then given by

$$H(\mathbf{x}, \mathbf{p}, \nu, \mu) = \int_{\mathcal{B}_0} \mathcal{H}(\mathbf{X}, \mathbf{x}, \mathbf{p}, \nu, \mu) d(vol) - \int_{\partial^{(2)}\mathcal{B}_0} (\bar{U}(\mathbf{x}) - U(\nu)) d(area). \tag{7.8}$$

Notice that we write  $\mathcal{H}(\mathbf{X}, \mathbf{x}, \mathbf{p}, \nu, \mu)$  instead of  $\mathcal{H}(\mathbf{X}, \mathbf{x}, \mathbf{p}, \mathbf{F}, \nu, \mu, \nabla\nu)$  because below we consider directly variational derivatives.

**Theorem 2:** *The canonical Hamilton equation*

$$\dot{F} = \{F, H\} \tag{7.9}$$

is equivalent to the Hamiltonian system of balance equations (7.2)-(7.3) for a continuum with substructure where  $F$  is any functional of the type  $\int_{B_0} f(\mathbf{X}, \mathbf{x}, \mathbf{p}, \nu, \mu)$ , with  $f$  a sufficiently smooth scalar density, and the Poisson bracket  $\{\cdot, \cdot\}$  for a complex material is given by

$$\begin{aligned} \{F, H\} = & \int_{B_0} \left( \frac{\delta f}{\delta \mathbf{x}} \cdot \frac{\delta \mathcal{H}}{\delta \mathbf{p}} - \frac{\delta \mathcal{H}}{\delta \mathbf{x}} \cdot \frac{\delta f}{\delta \mathbf{p}} \right) d(vol) \\ & + \int_{\partial^{(t)}B_0} \left( \frac{\delta f}{\delta \mathbf{x}} \cdot \frac{\delta \mathcal{H}}{\delta \mathbf{p}} \Big|_{\partial^{(t)}B_0} - \frac{\delta \mathcal{H}}{\delta \mathbf{x}} \cdot \frac{\delta f}{\delta \mathbf{p}} \Big|_{\partial^{(t)}B_0} \right) d(area) \\ & + \int_{\partial^{(t)}B_0} \left( \frac{\delta f}{\delta \nu} \cdot \frac{\delta \mathcal{H}}{\delta \mu} \Big|_{\partial^{(t)}B_0} - \frac{\delta \mathcal{H}}{\delta \nu} \cdot \frac{\delta f}{\delta \mu} \Big|_{\partial^{(t)}B_0} \right) d(area) \\ & + \int_{B_0} \left( \frac{\delta f}{\delta \nu} \cdot \frac{\delta \mathcal{H}}{\delta \mu} - \frac{\delta \mathcal{H}}{\delta \mu} \cdot \frac{\delta f}{\delta \nu} \right) d(vol), \end{aligned} \tag{7.10}$$

where the variational derivative  $\frac{\delta \mathcal{H}}{\delta \mathbf{x}}$  is obtained fixing  $\mathbf{p}$  and allowing  $\mathbf{x}$  to vary; an analogous meaning is valid for the variational derivative with respect to the order parameter.

The bracket  $\{\cdot, \cdot\}$  is bilinear, skew symmetric and satisfies Jacobi identity. The proof of Theorem 2 can be obtained by direct calculation.

**Corollary 6.** When one selects  $F = H$ , (7.9) coincides with the equation of conservation of energy.

The formulation in terms of Poisson brackets in Theorem 2 may be helpful in constructing numerical algorithms while Hamilton equations are essential in constructing a possible statistical mechanics over manifolds to account in a general manner substructural events occurring within the material element.

### 8. Time-dependent states

The balance equations of standard (6.14) and substructural (6.15) interactions remain still formally valid in non-conservative setting. However, at thermodynamic equilibrium, the measures of interaction coincide with the partial derivatives of the free energy density  $\psi$  that has a general structure of the type  $\psi = \hat{\psi}(\mathbf{F}, \nu, \nabla \nu)$ . One then gets  $\mathbf{P}^{eq} = \partial_{\mathbf{F}} \psi$ ,  $\mathcal{S}^{eq} = \partial_{\nabla \nu} \psi$ ,  $\mathbf{z}^{eq} = \partial_{\nu} \psi$ , where the superscript *eq* means that the interactions are at thermodynamic equilibrium.

When non-equilibrium dissipative phenomena occur, we may imagine to proceed like in the theory of viscous processes in simple bodies and to

decompose the measures of interaction in their equilibrium (eq) and non-equilibrium (ne) part in additive way. So that we get

$$\mathbf{P} = \mathbf{P}^{\text{eq}} + \mathbf{P}^{\text{ne}}, \quad \mathcal{S} = \mathcal{S}^{\text{eq}} + \mathcal{S}^{\text{ne}}, \quad \mathbf{z} = \mathbf{z}^{\text{eq}} + \mathbf{z}^{\text{ne}}, \quad (8.1)$$

where the equilibrium parts are given by the partial derivatives of the free energy density as above. Notice that the second law of thermodynamics excludes strictly the possibility that  $\psi$  could depend on rates of its entries at the equilibrium. However, the non-equilibrium parts of stress measures may depend on such rates and one may have constitutive equations of the form

$$\mathbf{P}^{\text{ne}} = \hat{\mathbf{P}}^{\text{ne}}(\mathbf{F}, \nu, \nabla \nu; \dot{\mathbf{F}}, \dot{\nu}, \nabla \dot{\nu}), \quad (8.2)$$

$$\mathcal{S}^{\text{ne}} = \hat{\mathcal{S}}^{\text{ne}}(\mathbf{F}, \nu, \nabla \nu; \dot{\mathbf{F}}, \dot{\nu}, \nabla \dot{\nu}), \quad (8.3)$$

$$\mathbf{z}^{\text{ne}} = \hat{\mathbf{z}}^{\text{ne}}(\mathbf{F}, \nu, \nabla \nu; \dot{\mathbf{F}}, \dot{\nu}, \nabla \dot{\nu}). \quad (8.4)$$

The non-equilibrium parts of stress measures are also intrinsically dissipative in the sense that they satisfy a reduced dissipation inequality of the form

$$\mathbf{P}^{\text{ne}} \cdot \dot{\mathbf{F}} + \mathcal{S}^{\text{ne}} \cdot \nabla \dot{\nu} + \mathbf{z}^{\text{ne}} \cdot \dot{\nu} \geq 0. \quad (8.5)$$

Let us consider the special prominent case in which

$$\mathbf{P}^{\text{ne}} = \mathbf{0}, \quad \mathcal{S}^{\text{ne}} = \mathbf{0}, \quad \mathbf{z}^{\text{ne}} = \hat{\mathbf{z}}^{\text{ne}}(\mathbf{F}, \nu, \nabla \nu; \dot{\mathbf{F}}, \dot{\nu}, \nabla \dot{\nu}), \quad (8.6)$$

with

$$\mathbf{z}^{\text{ne}} \cdot \dot{\nu} \geq 0. \quad (8.7)$$

A solution of (8.7) is

$$\mathbf{z}^{\text{ne}} = a(\mathbf{F}, \nu, \nabla \nu) \dot{\nu}, \quad (8.8)$$

with  $a(\cdot)$  a positive definite scalar function.

In this case the balance of substructural interactions (6.15) becomes

$$\begin{aligned} a(\mathbf{F}, \nu, \nabla \nu) \dot{\nu} &= \text{Div } \mathcal{S}^{\text{eq}} - \mathbf{z}^{\text{eq}} \\ &= \text{Div } \partial_{\nabla \nu} \psi - \partial_{\nu} \psi. \end{aligned} \quad (8.9)$$

It includes as special cases many models of condensed matter physics. Examples are the time-dependent Ginzburg–Landau and sin-Gordon equations. Gilbert equation accrues in presence of gyroscopic inertia as well as Landau Lifschitz continuum approximation of ferromagnetic Heisenberg spin chains.

In presence of internal constraints one may obtain Kuramoto–Sivashinsky equation for pattern formation as well as strain gradient viscoelasticity. When Eq. (8.9) is coupled with a transport equation one may get extended forms of Cahn–Hilliard equation and so on.

The list of possible interesting special cases is very rich and techniques of disparate nature can be used. To add another simple example, let us consider in one-dimensional setting a problem in which bulk deformations are absent, the order parameter is scalar and the free energy is quadratic with coefficients varying randomly, ruled by a Brownian motion (accounting for substructural randomness). In this case, remarkably the balance of substructural interactions (8.9) reduces to an equations admitting solutions in terms of Feynman–Kac and Girsanov formula.

## 9. Bibliographic remark

The notes about Lagrangian and Hamiltonian formulation of the mechanics of complex bodies are based on (Capriz and Mariano, 2004) where, in addition, appropriate Hamilton–Jacobi equations are developed together with a pure spatial formulation. It involves in the list of entries of the Lagrangian density just the spatial metric instead of the gradient of deformation and allows one to get a generalized Doyle–Ericksen formula.

A general treatment of Lagrangian and Hamiltonian mechanics of simple bodies can be found in (Marsden and Hughes, 1983). The special case of the Hamiltonian structures for Cosserat materials is fully developed in (Simo, Marsden and Krishnaprasad, 1988).

Time dependent states in multifield theories of complex bodies are discussed in (Mariano, 2001). For an extensive treatment of them in simple bodies see (Šilhavý, 1997).

## Lecture III

### Suggestions for researches

In the present lecture, possible research themes are discussed. We describe the mechanical models of some physical circumstances and suggest possible stochastic analyses to be developed. Fields covered are:

- the interaction of a macrocrack with a population of microcracks,
- the elastic behavior of quasicrystals,
- the modeling of fullerene-based composites.

## 10. Interaction of a macrocrack with a population of microcracks

If a macrocrack is present and grow eventually in a microcracked body, it interacts with the population of microcracks. Substructural interactions due to the presence of microcracks alter the force driving the crack tip with respect to the values predicted by classical Griffith's theory.

In the multifield setting for microcracked bodies we discussed in the first lecture, the description of the interactions between a macrocrack and a population of microcracks is rather natural and we develop it here in a two-dimensional setting for the sake of simplicity.  $\mathcal{B}_0$  is then a regular region in the *two-dimensional point space* and we assume that it is free of any macrocrack. A macrocrack occurs in the current placement  $\mathcal{B}$  of the body, so that the deformation map  $\hat{\mathbf{x}}(\cdot)$  is no more bijective everywhere. In fact it is one-to-one everywhere except a curve  $\Gamma$  each point of which has two different images on the two margins of the real crack. We assume that in  $\mathcal{B}$  the crack starts from the boundary, is regular so that  $\Gamma$  is smooth and does not cut completely the body in two different pieces. Consequently, the first end point of  $\Gamma$  is placed on the boundary of  $\mathcal{B}_0$ , while the rest of  $\Gamma$  is inside  $\mathcal{B}_0$ .  $\Gamma$  is represented by means of a smooth function  $\mathbf{r}(s)$  parametrized by arc-length  $s \in [0, \bar{s}]$ . The end point of  $\Gamma$  on  $\partial\mathcal{B}_0$  is indicated with  $\mathbf{r}(0)$ , the point occupied by the crack tip is  $\mathbf{r}(\bar{s})$  and is denoted with  $\mathbf{X}_z$ . We indicate with  $\mathbf{m}$  the unit normal of  $\Gamma$  at  $\mathbf{X} \in \Gamma$  and with  $\mathbf{t} = \partial_s \mathbf{r}$  the tangent there.

When the macrocrack grows in  $\mathcal{B}$ , its evolution may be described by a time-parametrized monotonically increasing family of curves, namely  $\Gamma(t)$ , with  $t \in [0, \bar{t}]$ , such that  $\Gamma(t_1) \subseteq \Gamma(t_2)$ , for  $t_2 \geq t_1$ . The image  $\mathbf{X}_z$  in  $\mathcal{B}_0$  of the real crack tip in  $\mathcal{B}$  depends then on time so that its velocity is defined in  $\mathcal{B}_0$  by

$$\mathbf{v}_{\text{tip}} = \frac{d\mathbf{X}_z(t)}{dt} = V\mathbf{t}_z, \quad (10.1)$$

where  $\mathbf{t}_z$  is the direction of propagation of the crack. As a consequence there is in  $\mathcal{B}_0$  an independent 'fictitious' kinematics. On the contrary,  $\mathcal{B}_0$  would remain fixed once and for all. Velocities relative to the motion of the crack tip can be defined by

$$\mathbf{x}^\diamond = \hat{\mathbf{x}} + \mathbf{F}\mathbf{v}_{\text{tip}}, \quad \mathbf{d}^\diamond = \dot{\mathbf{d}} + (\nabla\mathbf{d})\mathbf{v}_{\text{tip}}. \quad (10.2)$$

For later use, we now need to define velocities with respect to the boundary of a part  $b$  varying virtually in time away from the tip. The boundary of  $b$  is a closed smooth curve  $\partial b$  parametrized by the parameter  $p$ . The velocity of a generic point of  $\partial b$  is

$$\mathbf{v}_b = \frac{\partial \mathbf{X}(p, t)}{\partial t}. \quad (10.3)$$

Velocity fields relative to the motion of  $\partial b$  are given by

$$\mathbf{x}^o = \dot{\mathbf{x}} + \mathbf{F}\mathbf{v}_b, \quad \mathbf{d}^o = \dot{\mathbf{d}} + (\nabla\mathbf{d})\mathbf{v}_b. \tag{10.4}$$

Let  $\zeta$  be any field smooth on  $\mathcal{B}_0$  except  $\Gamma$ , where it may suffer finite jumps. The limits  $\zeta^\pm(\mathbf{X}) = \lim_{\varepsilon \rightarrow 0; \mathbf{X} \in \Gamma} \zeta(\mathbf{X} \pm \varepsilon \mathbf{m})$ , with  $\varepsilon$  a real parameter, allow us to define the jump  $[\zeta]$  of  $\zeta$  and the mean value  $\langle \zeta \rangle$  respectively by  $[\zeta] = \zeta^+ - \zeta^-$ ,  $\langle \zeta \rangle = \frac{1}{2}(\zeta^+ + \zeta^-)$  when the difference and the sum make sense, i.e. when  $\zeta$  takes values in a linear space.

When the crack remains closed during the deformation, we must have  $[\mathbf{x}] \cdot \mathbf{m} = 0$ ,  $[\mathbf{d}] \cdot \mathbf{m} = 0$ .

Gauss and transport theorems hold in appropriate form for fields suffering bounded jumps across  $\Gamma$ . Consider a disc  $D_R$  of radius  $R$  centered at the crack tip. Its boundary  $\partial D_R$  is endowed with outward unit normal  $\mathbf{n}$ . If for a field  $\phi$ , as defined above, the limit  $\lim_{r \rightarrow 0} \int_{\partial D_r} (\zeta \mathbf{n}) d(\text{length})$  (denoted with  $\int_{\text{tip}} \zeta \mathbf{n}$ ) exists, by indicating with  $D_r$  a disc centered at  $\mathbf{X}_z$  with radius  $r < R$ , the Gauss theorem over  $D_R$  can be written as

$$\int_{D_R} (\nabla\zeta) d(\text{area}) = \int_{\partial D_R} (\zeta \mathbf{n}) d(\text{length}) - \int_{\partial D_R \cap \Gamma} ([\zeta] \mathbf{m}) d(\text{length}) - \int_{\text{tip}} \zeta \mathbf{n}. \tag{10.5}$$

On a region  $b_\Gamma$  crossed by  $\Gamma$ , the last integral in (10.5) disappears because the tip is not contained in  $b_\Gamma$ . Basically, to obtain (10.5) one writes the Gauss theorem over  $D_R \setminus D_r$ , then evaluate the limit as  $r \rightarrow 0$ .

Moreover, if we imagine to vary  $D_R$  ‘virtually’ in time to follow the evolution of the tip, and denote with  $\mathbf{u}_D$  the velocity of its boundary, we get

$$\frac{d}{dt} \int_{D_R(t)} \zeta d(\text{area}) = \int_{\partial D_R(t)} \dot{\zeta} d(\text{length}) - \int_{\partial D_R(t) \cap \Gamma} (\zeta U) d(\text{length}) - \int_{\text{tip}} \zeta V. \tag{10.6}$$

where  $U = \mathbf{u}_D \cdot \mathbf{n}$  and  $V$  is the amplitude of the velocity of the tip as defined in (10.1).

If we consider an arbitrary part  $b_\Gamma$  crossed by  $\Gamma$  and far from the tip, write the integral balances of forces and moments (1.15) and (1.16) on it and shrink  $b_\Gamma$  to  $\partial b \cap \Gamma$ , we obtain

$$\int_{\partial b \cap \Gamma} [\mathbf{P}] \mathbf{m} d(\text{length}) = 0, \quad \int_{\partial b \cap \Gamma} \mathbf{d} \times [\mathbf{S}] \mathbf{m} d(\text{length}) = 0. \tag{10.7}$$

The arbitrariness of  $b$  implies

$$[\mathbf{P}] \mathbf{m} = 0, \quad \mathbf{d} \times [\mathcal{S}] \mathbf{m} = 0, \quad \text{along } \Gamma, \quad (10.8)$$

which are the *pointwise balances* of interactions along the crack.

Equation (10.8)<sub>1</sub> prescribes that the tractions on both sides of  $\Gamma$  are such that  $\mathbf{P}^+ \mathbf{m} = \mathbf{P}^- \mathbf{m}$ . Equation (10.8)<sub>2</sub> implies

$$[\mathcal{S}] \mathbf{m} = \lambda_\Gamma \mathbf{d}. \quad (10.9)$$

We assume that  $\lambda_\Gamma$  be zero. Such an assumption implies that the crack faces are free of microcracks because  $\lambda_\Gamma \mathbf{d}$  plays the rôle of a self-force. In fact, as remarked in Lecture I, microcracks loose significance at boundaries because each single microcrack does not exist *per se* but is determined by the surrounding material. This circumstance implies that surface self-forces are absent along  $\Gamma$ , so  $\lambda_\Gamma$  must be zero.

*Balance equations at the crack tip* are obtained by writing integral balances of forces and moments on a disc centered at the crack tip and shrinking it to the tip itself. At the limit we get

$$\int_{\text{tip}} \mathbf{P} \mathbf{n} = 0, \quad \int_{\text{tip}} \mathcal{S} \mathbf{n} = \lambda_{\text{tip}} \mathbf{d} \quad \text{at the tip}, \quad (10.10)$$

with  $\lambda_{\text{tip}}$  an undetermined scalar.

The real behavior of the body suggests to consider both stress and microstress to be bounded up to the tip. This point of view (which is indirectly an assumption on the behavior of the solution) allows us to assume that

$$\int_{\text{tip}} \mathcal{S} \mathbf{n} = 0, \quad (10.11)$$

as  $r \rightarrow 0$ .

On the contrary, one may conjecture that a priori  $\lambda_{\text{tip}} = 0$  as a consequence of the same reasoning leading to  $\lambda_\Gamma = 0$ .

### 10.1. J integral

When the crack grows in the actual configuration,  $\Gamma$  evolves since it is the 'shadow' in  $\mathcal{B}_0$  of the real crack in  $\mathcal{B}$ . As a consequence, interactions power conjugated with the kinematics of  $\Gamma$  arise. They are defined in  $\mathcal{B}_0$  and disappear when  $\mathcal{B}_0$  is fixed once and for all.

To represent them, by following standard instances we select a second order bulk stress tensor  $\mathbb{P}$ , internal and external bulk forces  $\mathbf{g}$  and  $\mathbf{e}$  respectively, a surface tension  $\sigma \mathbf{t}$  along  $\Gamma$ , with  $\sigma$  a scalar and  $\mathbf{t}$  the tangent

to  $\Gamma$ , an internal force  $\mathbf{g}_\Gamma$  along  $\Gamma$ , internal and external tip forces  $\mathbf{g}_{\text{tip}}$  and  $\mathbf{e}_{\text{tip}}$ , respectively. We assume also that  $\mathbf{e}_{\text{tip}}$  be only of inertial nature. These interactions satisfy the following balances:

$$\text{Div } \mathbb{P} + \mathbf{g} + \mathbf{e} = 0 \quad \text{in } \mathcal{B}_0, \quad (10.12)$$

$$[\mathbb{P}] \mathbf{m} + \mathbf{g}_\Gamma + \sigma \mathbf{h} = 0 \quad \text{along } \Gamma, \quad (10.13)$$

$$\mathbf{g}_{\text{tip}} + \mathbf{e}_{\text{tip}} - \sigma_{\text{tip}} \mathbf{t}_Z + \int_{\text{tip}} \mathbb{P} \mathbf{n} = 0 \quad \text{at the tip}, \quad (10.14)$$

where  $\mathbf{h}$  is the curvature vector of  $\Gamma$ , i.e.  $\mathbf{h} = \mathbf{t}_{,s}$ .

Since we are not considering inertial effects, for us  $\mathbf{e}_{\text{tip}} = 0$ . Balance equations (10.12)-(10.14) can be obtained from requirements of invariance of the power of all interactions acting on all kinematic mechanisms represented in  $\mathcal{B}_0$ , including the evolution of  $\Gamma$ . References are listed in the bibliographic remark.

Since the kinematics of  $\Gamma$  is only apparent, fictitious, all interactions work-conjugated with it must be expressed in terms of the referential counterparts of the real interactions acting in the current configuration and determining the evolution of the crack. To render explicit these relations, we make use of a mechanical dissipation inequality (an isothermal version of the second law of thermodynamics).

On any time-dependent part  $b$  away from the crack tip, such an inequality prescribes that the rate of the free energy on the same part minus the power of all interactions acting on  $b$  must be lesser or equal to zero for any choice of the rates involved.

In rendering explicit it we should consider the power of the interactions work-conjugated with the kinematics due to the time variation of  $b$ . We write such a power with respect to a fixed referential observer. Consequently, the bulk traction  $\mathbb{P} \mathbf{n}$  at the boundary  $\partial b$  expends power on the intrinsic velocity  $\mathbf{v}_b$  of  $b$  in  $\mathcal{B}_0$  and the bulk interactions  $\mathbf{g}$  and  $\mathbf{e}$  do not perform work because the particles inside  $b$  are not dragged materially during the 'fictitious' (just geometrical) motion of  $b$ .

The standard and substructural interactions ( $\mathbb{P} \mathbf{n}$  and  $\mathcal{S} \mathbf{n}$ ) develop power on the rates  $\mathbf{x}^\circ$  and  $\mathbf{d}^\circ$  calculated following the 'fictitious' motion of  $\partial b$ .

The mechanical dissipation inequality on a time-varying part  $b(t)$  far from the crack is then

$$\begin{aligned} \frac{d}{dt} \int_{b(t)} \psi d(\text{area}) - \int_{\partial b(t)} (\mathbf{b} \cdot \dot{\mathbf{x}}) d(\text{area}) \\ - \int_{\partial b(t)} (\mathbf{P}\mathbf{n} \cdot \mathbf{x}^\circ + \mathbf{S}\mathbf{n} \cdot \mathbf{d}^\circ + \mathbb{P}\mathbf{n} \cdot \mathbf{v}_b) d(\text{length}) \leq 0, \end{aligned} \quad (10.15)$$

where  $\psi$  is the bulk free energy density. By using (10.2), (10.15) becomes

$$\begin{aligned} \int_{b(t)} \dot{\psi} d(\text{area}) + \int_{\partial b(t)} \psi U d(\text{length}) - \int_{b(t)} (\mathbf{b} \cdot \dot{\mathbf{x}}) d(\text{area}) \\ - \int_{\partial b(t)} \left( \mathbf{P}\mathbf{n} \cdot \dot{\mathbf{x}} + \mathbf{S}\mathbf{n} \cdot \dot{\mathbf{d}} + \left( \mathbb{P} + \mathbf{F}^T \mathbf{T} + (\nabla \mathbf{d})^T \mathcal{S} \right) \mathbf{n} \cdot \mathbf{v}_b \right) d(\text{length}) \leq 0. \end{aligned} \quad (10.16)$$

Here, only the normal component of the velocity field  $\mathbf{v}_b$  is independent of the parametrization on  $\partial b$ . As a consequence, since the inequality (10.16) must be independent of that parametrization (which is unphysical and suggested only by some special convenience), the vector  $\left( \mathbb{P} + \mathbf{F}^T \mathbf{T} + (\nabla \mathbf{d})^T \mathcal{S} \right) \mathbf{n}$  must be purely normal to  $\partial b$ , then  $\left( \mathbb{P} + \mathbf{F}^T \mathbf{T} + (\nabla \mathbf{d})^T \mathcal{S} \right) \mathbf{n} = \omega \mathbf{n}$ , with  $\omega$  some not specified (at the moment) scalar density.

If we insert  $\omega \mathbf{n}$  in (10.16), since  $\omega \mathbf{n} \cdot \mathbf{v}_b = \omega U$ , and (10.16) must hold for any choice of the velocity fields, then for any  $U$ , the density  $\omega$  must coincide with the free energy  $\psi$ , i.e.  $\omega = \psi$ , because an integrand of the form  $(\psi - \omega) U$  appears, so that we have

$$\mathbb{P} = \psi \mathbf{I} - \mathbf{F}^T \mathbf{P} - (\nabla \mathbf{d})^T \mathcal{S}. \quad (10.17)$$

In the elastic case the free energy is substituted by the elastic energy.

If the body is not homogeneous and  $\psi = \hat{\psi}(\mathbf{X}, \mathbf{F}, \mathbf{d}, \nabla \mathbf{d})$ , by using the constitutive restrictions (1.27) and the balance (10.12), we obtain the standard identifications  $\mathbf{g} = -\partial_{\mathbf{X}} \psi$ ,  $\mathbf{e} = \mathbf{F}^T \mathbf{b}$ . When the body is homogeneous  $\mathbf{g}$  vanishes identically.

The surface stress  $\sigma \mathbf{t}$  can be identified by considering a part  $b_\Gamma$  crossed by the crack away from the tip and writing once again the mechanical dissipation inequality on such a part. In this case the intersection of  $\Gamma$  with  $\partial b$  is made of

two points, say  $A$  and  $B$ , and we denote by  $\int_{b_{\Gamma}(t) \cap \Gamma} f d(\text{length})$  the difference  $f(B) - f(A)$ . We then have

$$\begin{aligned} \frac{d}{dt} \left( \int_{b_{\Gamma}(t)} \psi d(\text{area}) + \int_{b_{\Gamma}(t) \cap \Gamma} \phi d(\text{length}) \right) \\ - \int_{b_{\Gamma}(t)} (\mathbf{b} \cdot \dot{\mathbf{x}}) d(\text{area}) - \int_{b_{\Gamma}(t) \cap \Gamma} \sigma \mathbf{t} \cdot \mathbf{v} d(\text{length}) \\ - \int_{\partial b_{\Gamma}(t)} (\mathbf{Pn} \cdot \mathbf{x}^\circ + \mathcal{S} \mathbf{n} \cdot \mathbf{d}^\circ + \mathbb{P} \mathbf{n} \cdot \mathbf{v}_b) d(\text{length}) \leq 0, \end{aligned} \quad (10.18)$$

where  $\phi$  is the surface free energy along the margins of the crack. It renders stable the margins themselves.

By shrinking  $b_{\Gamma}$  to  $\Gamma$ , taking into account the assumed continuity for bulk densities and that the mechanical dissipation inequality must hold for any choice of the velocity fields, we get

$$\phi = \sigma. \quad (10.19)$$

When we apply the same procedure on a part  $b_{\text{tip}}$  around the crack tip, we should consider into the expression of the power the *tip* force  $\mathbf{g}_{\text{tip}}$  developing power in the *tip* velocity. If we shrink  $b_{\text{tip}}$  up to the tip, we obtain  $(\mathbf{g}_{\text{tip}} \cdot \mathbf{t}_{\mathbf{z}}) V \leq 0$ .

By using previous relations, the balance at the crack tip can be rewritten as

$$-\phi_{\text{tip}} \mathbf{t}_{\mathbf{z}} + \int_{\text{tip}} (\psi \mathbf{I} - \mathbf{F}^T \mathbf{P} - \nabla d^T \mathcal{S}) \mathbf{n} = -\mathbf{g}_{\text{tip}}, \quad (10.20)$$

where  $\phi_{\text{tip}}$  is the tip value of the surface free energy density.

The term

$$\mathbf{j} = \int_{\text{tip}} (\psi \mathbf{I} - \mathbf{F}^T \mathbf{P} - \nabla d^T \mathcal{S}) \mathbf{n} = \int_{\text{tip}} \mathbb{P} \mathbf{n} = \lim_{\text{diam}(b_{\text{tip}}) \rightarrow 0} \int_{\partial b_{\text{tip}}} \mathbb{P} \mathbf{n} d(\text{length}) \quad (10.21)$$

represents the traction at the crack tip. Its component along the direction of propagation of the crack is the so called *J-integral* for quasi-static crack growth conditions, namely

$$\mathbf{J} = \mathbf{t}_{\mathbf{z}} \cdot \mathbf{j} = \phi_{\text{tip}} - \mathbf{t}_{\mathbf{z}} \cdot \mathbf{g}_{\text{tip}} = \mathbf{t}_{\mathbf{z}} \cdot \int_{\text{tip}} \mathbb{P} \mathbf{n}. \quad (10.22)$$

**Theorem 3:** *In absence of inertial effects, when the material is homogeneous, the faces of the crack are traction free, i.e.,  $\mathbf{P}^\pm \mathbf{m} = 0$  and  $\mathbf{S}^\pm \mathbf{m} = 0$ , and the crack is straight  $J$ , is path independent.*

## 10.2. Weak form of balance equations

Previous theoretical results, in particular the explicit expression of the traction  $\mathbf{j}$  at the tip, show the influence of populations of microcracks on the behavior of a macrocrack. To obtain quantitative results we may make use of numerical methods. Among the ones available, we choose to use the extended finite element method (X-FEM). It is characterized by two essential features:

1. The crack is not considered as a part of the boundary, rather it is a level set of a certain function defined over  $\mathcal{B}_0$ .
2. The approximation space at the nodes around the crack is enlarged with respect to the one of the nodes far from the crack.

The boundary value problem that we put in the setting of X-FEM in a two-dimensional environment is

$$\text{Div } \mathbf{P} + \mathbf{b} = 0 \quad \text{on } \mathcal{B}_0, \quad (10.23)$$

$$\text{Div } \mathbf{S} - \mathbf{z} = 0 \quad \text{on } \mathcal{B}_0, \quad (10.24)$$

$$\mathbf{u} = \bar{\mathbf{u}} \quad \text{on } \partial\mathcal{B}_{0u}, \quad (10.25)$$

$$\mathbf{d} = \bar{\mathbf{d}} \quad \text{on } \partial\mathcal{B}_{0d}, \quad (10.26)$$

$$\mathbf{P}\mathbf{n} = \mathbf{t} \quad \text{on } \partial\mathcal{B}_{0t}, \quad (10.27)$$

$$\mathbf{S}\mathbf{n} = \boldsymbol{\tau} \quad \text{on } \partial\mathcal{B}_{0p}, \quad (10.28)$$

$$\mathbf{P}^\pm \mathbf{m} = 0 \quad \text{along } \Gamma, \quad (10.29)$$

$$\mathbf{S}^\pm \mathbf{m} = 0 \quad \text{along } \Gamma, \quad (10.30)$$

where  $\partial\mathcal{B}_{0u}$  is the portion of  $\partial\mathcal{B}_0$  where  $\mathbf{u}$  is prescribed,  $\partial\mathcal{B}_{0d}$  the analogous part where  $\mathbf{d}$  is prescribed,  $\partial\mathcal{B}_{0t}$  the part where standard traction  $\mathbf{t}$  are applied and  $\partial\mathcal{B}_{0p}$  where  $\mathbf{S}\mathbf{n}$  is prescribed constitutively. We have

$$\partial\mathcal{B}_0 = \partial\mathcal{B}_{0u} \cup \partial\mathcal{B}_{0t} = \partial\mathcal{B}_{0d} \cup \partial\mathcal{B}_{0p}, \quad (10.31)$$

$$\partial\mathcal{B}_{0u} \cap \partial\mathcal{B}_{0t} = \emptyset \quad \text{and} \quad \partial\mathcal{B}_{0d} \cap \partial\mathcal{B}_{0p} = \emptyset. \quad (10.32)$$

Let  $\mathcal{C}_u$  and  $\mathcal{C}_d$  be sets of *continuous and piecewise continuously differentiable vector valued fields defined on  $\mathcal{B}_0$* . We define two sets of trial functions,

namely  $\mathcal{U}$  and  $\mathcal{V}$ , by

$$\mathcal{U} = \{\mathbf{u} \in \mathcal{C}_u \mid \mathbf{u} = \bar{\mathbf{u}} \text{ on } \partial\mathfrak{B}_{0u}\}, \tag{10.33}$$

$$\mathcal{V} = \{\tilde{\mathbf{d}} \in \mathcal{C}_d \mid \tilde{\mathbf{d}} = \bar{\mathbf{d}} \text{ on } \partial\mathfrak{B}_{0d}\}, \tag{10.34}$$

and two sets of test functions

$$\mathcal{U}_0 = \{\delta\mathbf{v} \in \mathcal{C}_u \mid \delta\mathbf{v} = 0 \text{ on } \partial\mathfrak{B}_{0u}\}, \tag{10.35}$$

$$\mathcal{V}_0 = \{\delta\mathbf{h} \in \mathcal{C}_d \mid \delta\mathbf{h} = 0 \text{ on } \partial\mathfrak{B}_{0d}\}. \tag{10.36}$$

Then, by multiplying pointwise balances by  $\delta\mathbf{v}$  and  $\delta\mathbf{h}$ , summing the results and integrating over  $\mathfrak{B}_0$ , we get

$$\int_{\mathfrak{B}_0} (\delta\mathbf{v} \cdot (\text{Div } \mathbf{P} + \mathbf{b}) + \delta\mathbf{h} \cdot (\text{Div } \mathcal{S} - \mathbf{z})) d(\text{area}) = 0, \quad \forall \delta\mathbf{v} \in \mathcal{U}_0, \quad \delta\mathbf{h} \in \mathcal{V}_0. \tag{10.37}$$

From (10.37), by using the Gauss theorem and the boundary conditions (10.27), (10.28), we get

$$\begin{aligned} & \int_{\mathfrak{B}_0} (\nabla(\delta\mathbf{v}) \cdot \mathbf{P} - \delta\mathbf{v} \cdot \mathbf{b} + \nabla(\delta\mathbf{h}) \cdot \mathcal{S} + \delta\mathbf{h} \cdot \mathbf{z}) d(\text{area}) \\ & + \int_{\partial\mathfrak{B}_{0t}} (\delta\mathbf{v} \cdot \bar{\mathbf{t}}) d(\text{length}) + \int_{\partial\mathfrak{B}_{0p}} (\delta\mathbf{h} \cdot \tau) d(\text{length}) = 0, \\ & \forall \delta\mathbf{v} \in \mathcal{U}_0, \quad \delta\mathbf{h} \in \mathcal{V}_0. \end{aligned} \tag{10.38}$$

Without loss of generality, we can assume  $\delta\mathbf{v} = \mathbf{u}$  and  $\delta\mathbf{h} = \mathbf{d}$ , so that (10.38) becomes

$$\begin{aligned} & \int_{\mathfrak{B}_0} (\nabla\mathbf{u} \cdot \mathbf{P} + \nabla\mathbf{d} \cdot \mathcal{S} + \mathbf{d} \cdot \mathbf{z}) d(\text{area}) - \int_{\mathfrak{B}_0} (\mathbf{u} \cdot \mathbf{b}) d(\text{area}) \\ & + \int_{\partial\mathfrak{B}_{0t}} (\mathbf{u} \cdot \bar{\mathbf{t}}) d(\text{length}) + \int_{\partial\mathfrak{B}_{0p}} (\mathbf{d} \cdot \tau) d(\text{length}) = 0, \end{aligned} \tag{10.39}$$

where the constitutive relations must be inserted.

### 10.3. Level set description of the crack

We consider  $\Gamma$  as represented by means of a signed distance scalar function  $g$  defined by

$$\mathfrak{B}_0 \ni \mathbf{X} \longmapsto g(\mathbf{X}) = \text{sign} [\mathbf{m} \cdot (\mathbf{X} - \bar{\mathbf{X}})] \min_{\bar{\mathbf{x}} \in \Gamma_{cr}} \|\mathbf{X} - \bar{\mathbf{x}}\|, \tag{10.40}$$

where  $\bar{\mathbf{X}}$  is the closest point projection of  $\mathbf{X}$  on the crack  $\Gamma$ .

Let us consider a finite tessellation  $\{b^e\}$  of  $\mathcal{B}_0$  of finite elements. Arbitrary elements  $b_1^e$  and  $b_2^e$  of  $\{b^e\}$  are such that  $b_1^e \cap b_2^e = \emptyset$ ; moreover  $\bigcup_{i=1}^N b_i^e = \mathcal{B}_0$ , with  $N$  the number of elements of  $\{b^e\}$ . The signed distance function is approximated in the point of view of X-FEM by the same shape functions used to approximate the displacement field, namely we write

$$g(\mathbf{X}) = \sum_{I=1}^6 N_I g(\mathbf{X}_I), \quad (10.41)$$

where  $N_I$  denotes the  $I$ -th shape function within a given finite element  $b^e$ .

We also need another function  $\bar{g}$  given by  $\bar{g} = \|\mathbf{X} - \mathbf{X}^{\text{tip}}\|$  locating the crack tip.

#### 10.4. X-FEM approximation

Three sets of nodes are selected within the tessellation:

- $\mathcal{N}^{\text{Tip}}$ , the set of nodes for which the closure of the support of nodal shape functions contains the crack tip;
- $\mathcal{N}^{\text{Cr}}$ , the set of nodes for which the nodal shape function support intersects the crack front and do not belong to  $\mathcal{N}^{\text{Tip}}$ ;
- $\mathcal{N}$ , the set of all nodes of the mesh.

The X-FEM approximation is obtained by enriching the standard finite element expression of the displacements with a set of functions that enlarge the functional basis approximating the finite element solution. When some discontinuous functions are used among enrichment functions, the approximate fields can be properly represented even if they are discontinuous.

Comparison between the construction of a standard finite element mesh and a X-FEM mesh is shown in Fig. 21. In the former case the crack is part of the boundary while in the latter it is not so.

The jump along the crack is here described by using a modified Heaviside function

$$H(g(\mathbf{X})) = \begin{cases} -1 & \text{if } g(\mathbf{X}) < 0, \\ +1 & \text{if } g(\mathbf{X}) > 0. \end{cases} \quad (10.42)$$

It is symmetric across  $\Gamma$  and is used to enrich those nodes that belong to  $\mathcal{N}^{\text{Cr}}$ .

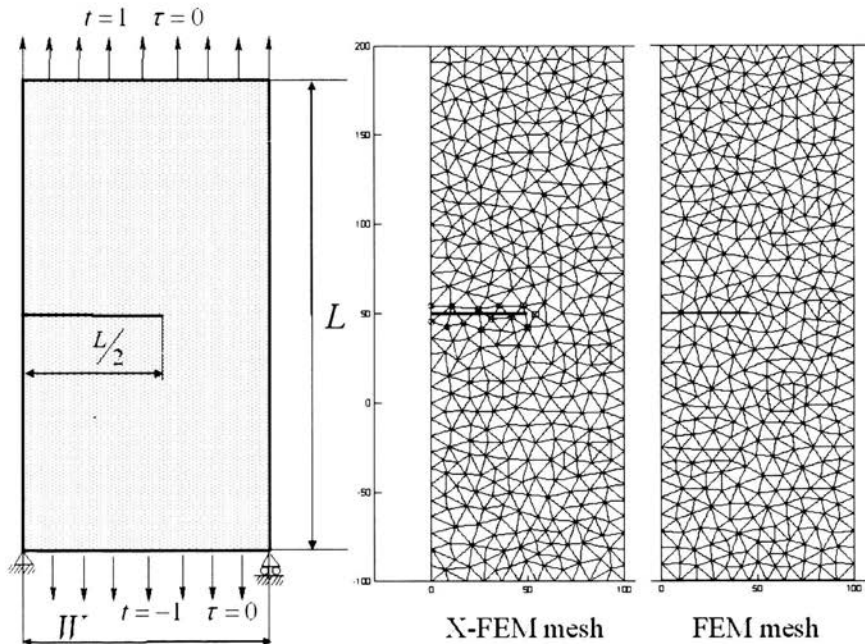


FIGURE 21. Rectangular microcracked membrane endowed with a macrocrack. Comparison between the construction of a X-FEM mesh and a FEM mesh.

In order to represent the displacement fields near the tip, the nodes that belong to  $\mathcal{N}^{\text{Tip}}$  are enriched with four branch functions, namely

$$B^{(1)}(r, \theta) = \sqrt{r} \sin \frac{\theta}{2}, \tag{10.43}$$

$$B^{(2)}(r, \theta) = \sqrt{r} \cos \frac{\theta}{2}, \tag{10.44}$$

$$B^{(3)}(r, \theta) = \sqrt{r} \sin \frac{\theta}{2} \sin \theta, \tag{10.45}$$

$$B^{(4)}(r, \theta) = \sqrt{r} \cos \frac{\theta}{2} \sin \theta. \tag{10.46}$$

In the expression of the branch functions,  $(r, \theta)$  represents a polar coordinate system centered at the crack tip and oriented along the crack. Moreover, only the first branch function is discontinuous along the crack faces while the other branch functions are continuous in the whole domain.

Consequently, the X-FEM approximation for the displacement field  $\mathbf{u}$  is given by

$$\mathbf{u}^h(\mathbf{x}) = \sum_{I \in N} N_I(\mathbf{x}) u_I + \sum_{J \in N^{Cr}} N_J(\mathbf{x}) H(g(\mathbf{x})) a_J^u + \sum_{\alpha=1}^4 \sum_{K \in N^{Tip}} N_K(\mathbf{x}) \left( B^{(\alpha)}(r, \theta) \right) b_J^u, \quad (10.47)$$

while the one for  $\mathbf{d}$  has the following form

$$\mathbf{d}^h(\mathbf{x}) = \sum_{I \in N} N_I(\mathbf{x}) \mathbf{d}_I + \sum_{J \in N^{Cr}} N_J(\mathbf{x}) (H(g(\mathbf{x}))) a_J^d + \sum_{\alpha=1}^4 \sum_{K \in N^{Tip}} N_K(\mathbf{x}) \left( B^{(\alpha)}(r, \theta) \right) b_J^d. \quad (10.48)$$

It is worth noting that both  $\mathbf{u}$  and  $\mathbf{d}$  are enriched with the same functions: the choice seems to be reasonable because both  $\mathbf{u}$  and  $\mathbf{d}$  represent displacements.

Note also that when a node falls on  $\Gamma$ , it is not enriched.

## 10.5. Research themes

**Theme 1:** *Find pattern formation in the diagrams of the moments of the distributions of displacements  $\mathbf{u}$  and  $\mathbf{d}$  around the tip of the crack.*

**Remark 1.** Strain localization phenomena occur around the tip of the crack in linear elastic regime as a consequence of the influence of the presence of microcracks. Let us consider as an example the rectangular membrane in Fig. 21 loaded with a boundary distributed traction  $\mathbf{t}$  along sides where we prescribe also  $\tau = \mathcal{S}\mathbf{n} = 0$ . No boundary conditions are prescribed on the microdisplacement field. In Fig. 22, strain localization phenomena are evident. Then, it could be natural to develop the same type of stochastic analyses as in Lecture I.

**Theme 2:** *Find appropriate criteria for crack evolution that account for the influence of microcracks.*

**Theme 3:** *Evaluate the influence of microcrack randomness on the evolution of the macrocrack.*

## 10.6. Bibliographic remark

Section 4.1 collects results presented in (Mariano and Stazi, 2004) where the first application of X-FEM to multifield problems is shown. The liter-

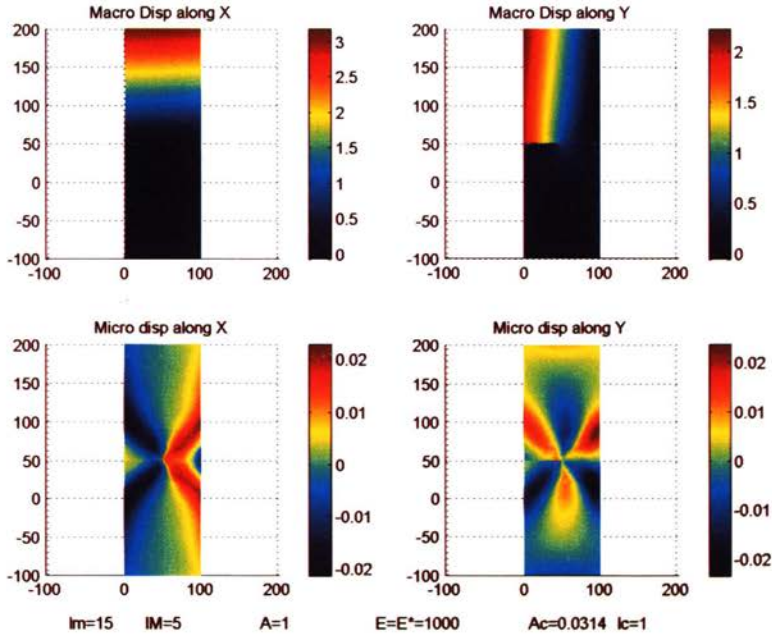


FIGURE 22. Displacement fields for the sample case in Fig. 21.

ature about X-FEM is very rich. Here we mention for further reading just (Moës, Dolbow and Belytschko, 1999; Gravouil, Moës and Belytschko, 2002; Stazi, Budin, Chessa and Belytschko, 2003) and references therein. The origin of balances of interactions generated by the evolution of the crack has been variously discussed in scientific literature. Here we refer just to (Gurtin, 2000).

## 11. Phason activity in icosahedral quasicrystals

In analyzing the behavior of rapidly cooled Al-Mn based alloys, in 1984 Shechtman and co-workers obtained diffraction patterns displaying the characteristic axes of icosahedral symmetry, namely six fivefold, ten threefold and fifteen twofold. In this way they showed the existence of metallic phases with long-range orientational order and absence of the translational one. Such alloys are called *quasicrystals* because they are intrinsically quasiperiodic.

A quasicrystalline structure displaying icosahedral symmetry in the three-dimensional Euclidean point space  $\mathcal{E}^3$  can be obtained by selected projection in 3D of a six-dimensional periodic lattice. So, a quasicrystal appears as the three-dimensional shadow of a six-dimensional structure: the degrees of freedom are decomposed in the standard displacement field,  $\tilde{\mathbf{u}}$ , describing

the propagation of ordinary elastic waves (*phonon* degrees of freedom) and another vector field,  $\tilde{\mathbf{w}}$ , (*phason* degrees of freedom) representing local rearrangements of atoms determining the quasiperiodic structure. Such rearrangements are: (i) collective atomic modes and (ii) tunneling of atoms below energetic barriers separating places at a distance lesser than the atomic diameter. The material element is then no more as an indistinct sphere: it is a crystalline cell undergoing internal changes. So that the mechanics of quasicrystalline structures falls naturally within the general setting of multifield theories describing complex bodies. The phason displacement  $\mathbf{w}$  plays the rôle of order parameter.

### 11.1. Continuum model

As mentioned above, for quasicrystals the material element is a crystalline cell that we imagine *collapsed* at the point  $\mathbf{X} \in \mathcal{B}_0$ . If we consider the material element as a perfect crystalline cell, during a motion  $[0, \tilde{t}] \ni t \mapsto \tilde{\mathbf{x}}(\mathbf{X}, t) \in \mathcal{E}^3$ , the standard displacement field  $\mathbf{u} = \tilde{\mathbf{u}}(\mathbf{X}, t) = \tilde{\mathbf{x}}(\mathbf{X}, t) - \mathbf{X}$  is the descriptor of the phonon degrees of freedom. At each  $\mathbf{X}$  and  $t$ ,  $\mathbf{u}$  is an element of the translation space *Vec* over  $\mathcal{E}^3$ . In presence of substructural changes as collective atomic modes and/or tunneling of atoms below energetic barriers, a sort of internal shift occurs and is represented by a sufficiently smooth vector field  $\mathcal{B}_0 \ni \mathbf{X} \mapsto \tilde{\mathbf{w}} = \tilde{\mathbf{w}}(\mathbf{X}) \in \text{Vec}$ . During a motion, we then have  $[0, \tilde{t}] \ni t \mapsto \mathbf{w} = \tilde{\mathbf{w}}(\mathbf{X}, t) \in \text{Vec}$ , with a slight abuse of notation because  $\mathbf{u}$  and  $\mathbf{w}$  belong strictly to different copies of *Vec*. In other words, from the point of view of the general setting of multifield theories, the copy of *Vec* containing  $\mathbf{w}$  plays the rôle of the manifold  $\mathcal{M}$  of substructural states. Here, the order parameter has the geometrical nature of a microdisplacement, exactly like in the case of microcracked bodies described in Lecture I and above in the present lecture. However, the type of physical phenomena described is different.

Measures of interactions power conjugated with the rates  $\dot{\mathbf{x}}$  and  $\dot{\mathbf{w}}$  at  $\mathbf{X}$  and  $t$ , have then the same geometrical nature of the ones in Lecture I. Precisely, we introduce the following densities:

- the density of bulk forces:

$$\mathcal{B}_0 \ni \mathbf{X} \mapsto \mathbf{b} = \tilde{\mathbf{b}}(\mathbf{X}) \in T_{\mathbf{x}}^* \mathcal{B},$$

- the first Piola–Kirchhoff stress:

$$\mathcal{B}_0 \ni \mathbf{X} \mapsto \mathbf{P} = \tilde{\mathbf{P}}(\mathbf{X}) \in \text{Hom}(\text{Vec}, T_{\mathbf{x}}^* \mathcal{B}),$$

- the phason stress:

$$\mathcal{B}_0 \ni \mathbf{X} \mapsto \mathcal{S} = \tilde{\mathcal{S}}(\mathbf{X}) \in \text{Hom}(\text{Vec}, T_{\mathbf{w}}^* \text{Vec}).$$

We consider the bulk interactions continuous over  $\mathcal{B}_0$ , and assume that the first Piola–Kirchhoff stress and the phason stress are continuous and piecewise continuously differentiable over  $\mathcal{B}_0$ .

The phason stress indicates contact interactions between neighboring material elements as a consequence of phason changes within at least one of them. External bulk interactions associated with phason activity are absent. They appear in other circumstances in which phason activity occur with sound-like modes as in the case of incommensurate intergrowth compounds.

The above listed measures of interaction satisfy balance equations (1.17), (1.20) and (1.19) provided that in (1.19)  $\mathbf{d}$  is substituted by  $\mathbf{w}$ .

In the pure elastic range, the energetic landscape of icosahedral quasicrystals may be described just by the gradient  $\nabla\mathbf{u}$  of phonon displacement and the gradient  $\nabla\mathbf{w}$  of phason displacement, so that the density of internal energy  $e$  displays a constitutive structure of the form

$$e = \hat{e}(\nabla\mathbf{u}, \nabla\mathbf{w}), \tag{11.1}$$

and is such that its rate equals the power of phonon (standard) and phason (substructural) interactions in a way formally analogous to (1.23). With the same procedure used in Lecture I, we then obtain the constitutive restrictions

$$\mathbf{P} = \partial_{\nabla\mathbf{u}}\psi, \quad \mathbf{z} = \mathbf{0}, \quad \mathcal{S} = \partial_{\nabla\mathbf{w}}\psi. \tag{11.2}$$

The self-force appears only when ‘viscous’ irreversible phenomena occur.

By restricting the treatment to the infinitesimal deformation regime in which  $\mathbf{P} \approx \sigma$  and  $\mathcal{S} \approx \mathcal{S}_a$ , where  $\sigma$  is Cauchy’s stress and  $\mathcal{S}_a$  the phason stress in the current place, and considering a linear constitutive behavior, we may prescribe

$$\mathbf{P} \approx \sigma = \mathbb{C}\nabla\mathbf{u} + \mathbb{K}'\nabla\mathbf{w}, \tag{11.3}$$

$$\mathcal{S} \approx \mathcal{S}_a = \mathbb{K}'^T\nabla\mathbf{u} + \mathbb{K}\nabla\mathbf{w}. \tag{11.4}$$

In this case the elastic energy is decomposed in three contributions:

1. a pure phonon part equal to  $\frac{1}{2}\mathbb{C}\nabla\mathbf{u} \cdot \nabla\mathbf{u}$ ,
2. a pure phason part equal to  $\frac{1}{2}\mathbb{K}\nabla\mathbf{w} \cdot \nabla\mathbf{w}$ , and
3. an interaction energy given by  $\mathbb{K}'\nabla\mathbf{w} \cdot \nabla\mathbf{u}$ .

In the case of *planar quasicrystals with fivefold symmetry*,  $\mathbb{C}_{ijhk}$  has the standard expression for simple isotropic elastic bodies with Lamé constants  $\lambda$  and  $\mu$ , namely

$$\mathbb{C}_{ijhk} = \lambda\delta_{ij}\delta_{kl} + \mu(\delta_{ik}\delta_{jl} + \delta_{il}\delta_{jk}), \tag{11.5}$$

and

$$\mathbb{K}_{ijkl} = K_1 \delta_{ik} \delta_{jl} + K_2 (\delta_{ij} \delta_{kl} - \delta_{il} \delta_{jk}), \quad (11.6)$$

$$\mathbb{K}'_{ijkl} = R (\delta_{i1} - \delta_{i2}) (\delta_{ij} \delta_{kl} - \delta_{ik} \delta_{jl} + \delta_{il} \delta_{jk}). \quad (11.7)$$

## 11.2. Stochastic aspects of phonon-phason coupling

The estimation of the phonon-phason coupling coefficient  $R$  is controversial. Theoretical models suggest that  $R$  be of at least one order of magnitude smaller than  $K_1$  and  $K_2$ . On the other hand, experiments based on X-ray diffuse scattering in a grain of Al-Pb-Mn quasicrystals indicate a value of  $R$  greater than  $K_1$  and  $K_2$ , at least for a sample in which off-stoichiometry defects are included in a single phase. Moreover, some X-ray diffuse scattering data may be also interpreted by assuming  $R = 0$ .

Really, the discrepancy of data arising from the same class of experiments could be partially associated with the difficulty to eliminate circumstantial effects influencing the resolution of measure instruments during X-ray based experiments. In a realistic picture, the phonon-phason coupling could be then considered as a stochastic field over  $\mathcal{B}_0$ . At a first glance one could think to represent it as a Gaussian process, but in this case one would imply the possibility of values of  $R$  excluded by experimental data. We propose to adopt for  $R$  a lognormal model with cut-off, as it occurs for  $l_m$  in randomly microcracked elastic bodies.

As cut-off one could imagine to select  $R = 0$  by assuming in this way as lower bound the ideal situation in which the elastic distortion does not influence the substructural phason changes. However, the elastic distortion of each crystalline cell alters the energetic landscape of the cell itself, favouring shifts in atomic places with transition from a quasiperiodic structure to another. So that, more reasonably, one may propose to put the lower cut-off at  $R \approx 0.01K_1$ , a value at which it is nearly impossible to evaluate experimentally the velocity anisotropy between modes propagating along fivefold axis and modes along twofold axis.

Quasicrystals display also topological randomness. They may be described by appropriate random tiling. A *tiling* of  $\mathcal{B}_0$  is a countable covering obtained through bounded closed sets with pairwise disjoint interiors, and non vanishing intersection with  $\mathcal{B}_0$ , such that each of them is homeomorphic to a ball.

In constructing the cover, one should satisfy the requirements of quasiperiodicity and of a given symmetry, so that the tiling may be constructed with the repetition of at least two prototiles, one of them forming the main part of the tiling (say, e.g., hexagons or pentagons in the plane), the other(s) gener-

ating the so-called ‘worms’, i.e. topological alterations that assure quasiperiodicity and allow the tiling to fit the space. In other words, each random tile is a representation of a (quasi)crystalline cell, a region of space in which there is a cluster of potential atomic sites that we decorate with real atoms in each realization of the quasiperiodic material substructure. When one selects a material symmetry (say, e.g., fivefold) then, though the tiling is random, one should have deterministic rules to decorate each tile with real atoms in order to maintain the selected material symmetry.

When the quasicrystalline structure is excited by means of a X-ray beam, the resulting diffraction scenario contains Bragg peaks as ideal crystals but also diffuse scattering due to phason activity.

### 11.3. Research themes

**Theme 4:** *Prove or disprove the possible presence of pattern formation (for quasicrystalline bodies with some special geometry) when one consider  $R$  as a shifted lognomal random field over the body.*

**Theme 5:** *Investigate the influence of the randomness of  $R$  (still considered as a random field over  $B_0$ ) on the force driving the tip of a macrocrack in a quasicrystalline body.*

**Remark 2.** Since the substructural phason activity is described by a vector order parameter, its influence on the force driving the tip of a crack can be formally described with the same procedure adopted for elastic microcracked bodies. In particular, one obtains an evolution law in the direction of propagation of the crack given by the relation

$$a_{\text{tip}}V = J - \phi_{\text{tip}}, \quad (11.8)$$

where  $a_{\text{tip}}$  is a positive kinetic material coefficient,  $\phi_{\text{tip}}$  is as above the tip value of the surface energy,

$$J = \mathbf{t}_Z \cdot \int_{\text{tip}} \left( \psi \mathbf{I} - \mathbf{F}^T \partial_{\nabla \mathbf{u}} \psi - (\nabla \mathbf{w})^T \partial_{\nabla \mathbf{w}} \psi \right) \mathbf{n}. \quad (11.9)$$

The difference  $J - \phi_{\text{tip}}$  is the force driving the crack tip. The velocity of the crack is different from zero when  $J - \phi_{\text{tip}}$  overcomes some material threshold. Since  $a_{\text{tip}}$  is positive, as a consequence of the second law, the power developed by the driving force is always positive when the crack evolves, and we get  $(J - \phi_{\text{tip}})V \geq 0$ , where the equality sign holds when  $V = 0$  if  $J \neq \phi_{\text{tip}}$ . If, just to make an example, we analyze a four point bending test on a quasicrystalline sample, as shown in Fig. 23, we obtain the portraits of

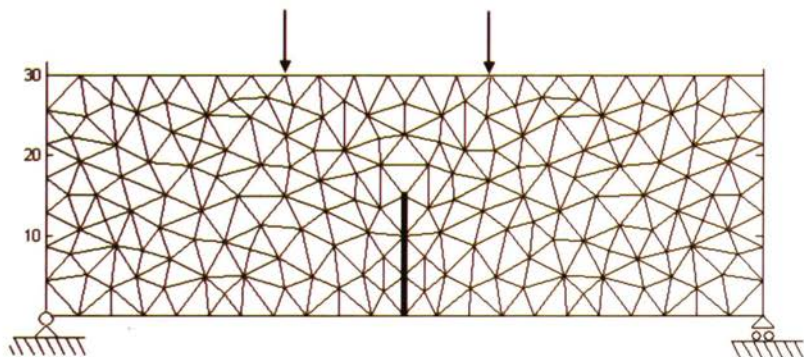


FIGURE 23. Four point bending test on a sample of quasicrystalline alloy.

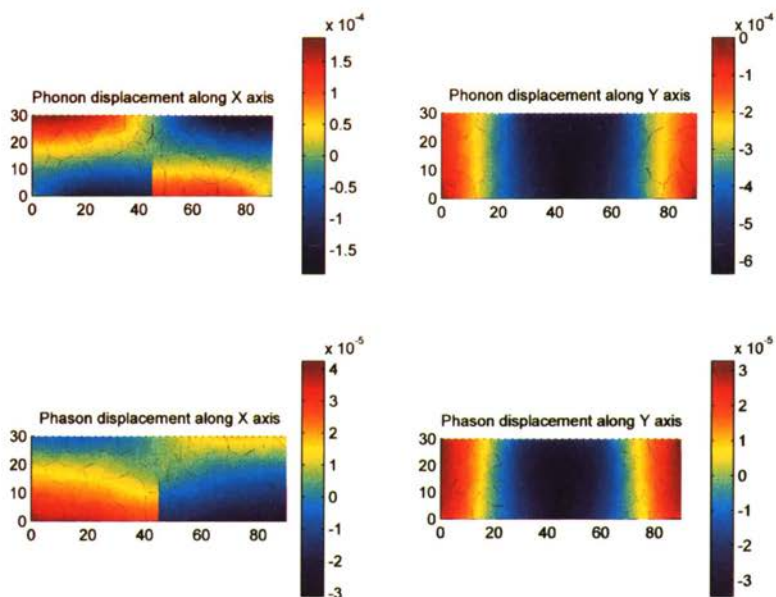


FIGURE 24. Phonon and phason displacement fields for the sample in Fig. 23.

phonon and phason displacements in Fig. 24. To obtain them, in addition to the standard boundary conditions associated with the applied forces of density  $10 \text{ N}$  and the geometric constraints in Fig. 22, only the value  $\mathbf{w} = \mathbf{0}$  is prescribed where  $\mathbf{u}$  vanishes in the two points of the lowest side of the sample. Values of the material parameters chosen in fivefold symmetry are the following:  $\lambda = 0.75 \times 10^{11} \text{ N/m}^2$ ,  $\mu = 0.65 \times 10^{11} \text{ N/m}^2$ ,  $K_1 = 0.81 \times 10^{11} \text{ N/m}^2$ ,  $K_2 = -0.42 \times 10^{11} \text{ N/m}^2$  and  $R \approx 0.1K_1$ .

**Remark 3.** Preliminary results that show the possible influence of the randomness of phonon-phason coupling can be obtained by considering simply  $R$  just as a random variable, rather than as a random field. In this case one realizes that the components of phonon and phason tip displacements along  $x$ -axis are not influenced by the variation of  $R$  up to  $R \approx 8 \cdot 10^4$ , while the one along  $y$ -axis is weakly influenced by the variation of  $R$ . Finally, phason tip displacement is influenced strongly by the variation of  $R$  in a non-linear way. Figure 25 displays the behavior of the components of phonon and phason displacements at the tip of the crack for 50 samples of  $R$  randomly selected in the ideal interval  $[0, K_1]$ .

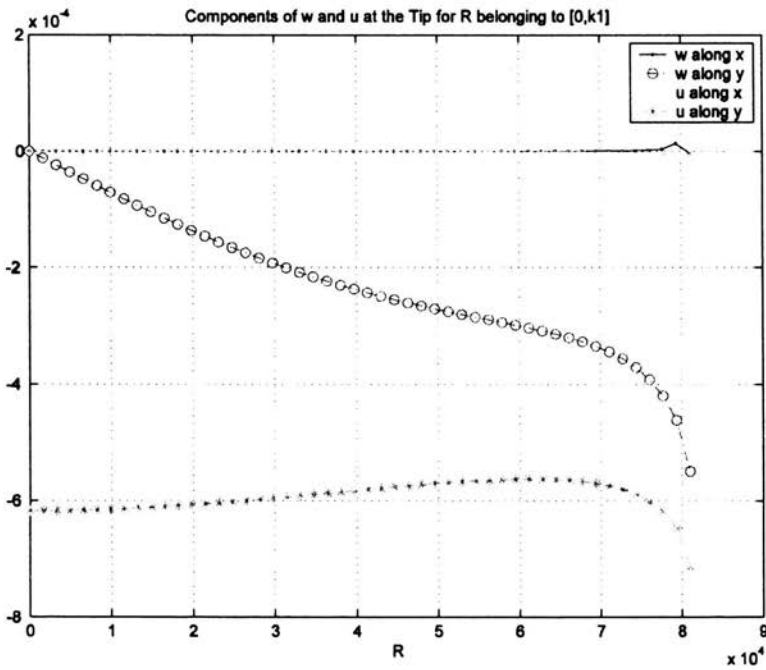


FIGURE 25. Tip components of phonon and phason displacement fields varying the phonon-phason coupling coefficient.

**Theme 6:** *Prove or disprove the presence of patterns when a 'viscous' self-force of the type  $\alpha \dot{w}$  (with  $\alpha$  a constants with values reported in literature) when  $R$  behaves as a random field.*

#### 11.4. Bibliographic remark

Section 4.2 is based on (Mariano, Stazi and Augusti, 2004). The discovery of quasicrystals has been presented in (Shechtman, Blech, Gratias and

Cahn, 1984). Physical remarks of basic nature can be found in (Lifshitz, 2003; Rochal and Lorman, 2001; Baake and Höffe, 2000).

## 12. Fullerene based composites

Fullerenes are carbon-based macromolecules with closed-cage structure made of pentagons or hexagons. The investigation of their properties and the construction of appropriate predictive models of their behavior is a challenging topic.

Here we analyze composites made of a matrix in which fullerenes are finely and randomly dispersed. Typically they are sol-gel structures that combine the optical and electronic properties of semiconductors with the mechanical features of polymers.

### 12.1. Continuum model

The material element may be represented as a 'box' collapsed at  $\mathbf{X} \in \mathcal{B}_0$  and containing a family of fullerene molecules dispersed within a gel. Each molecule is characterized by a positive definite symmetric second-order tensor  $\mathfrak{A}^* \in Sym^+$  representing its independent deformation with respect to the surrounding matrix. A distribution function  $f : Sym^+ \rightarrow \mathbb{R}^+$  assigns to each  $\mathfrak{A}^*$  the number of molecules described by  $\mathfrak{A}^*$  in the material element, should depend on  $\mathfrak{A}^*$  through its invariants (a consequence of a requirement of objectivity) and is also such that  $\int_{Sym^+} f(\mathfrak{A}^*) d\mu = 1$  with  $\mu$  an appropriate probability measure. With these premises, we select as coarse grained descriptor of the material element the average  $\mathfrak{A}$  of  $\mathfrak{A}^*$  over the family characterizing the element under consideration, then we put

$$\mathfrak{A} = \int_{Sym^+} \mathfrak{A}^* f(\mathfrak{A}^*) d\mu. \quad (12.1)$$

Two sufficiently smooth mappings are defined over  $\mathcal{B}_0$ : the placement  $\hat{\mathbf{x}} : \mathcal{B}_0 \rightarrow \mathcal{E}^3$  and the order parameter  $\mathfrak{A}^\sim : \mathcal{B}_0 \rightarrow Sym^+$ . As usual, motions are then defined by time-parametrized families  $\hat{\mathbf{x}}_t$  and  $\mathfrak{A}^\sim$  and we write  $\hat{\mathbf{x}}(\mathbf{X}, t)$  and  $\mathfrak{A}^\sim(\mathbf{X}, t)$  to indicate the current place  $\mathbf{x}$  and the current value  $\mathfrak{A}$  of the order parameter at the time  $t$ . Rates (velocities) as fields over  $\mathcal{B}_0$  are indicated at  $\mathbf{X}$  and  $t$  with  $\dot{\hat{\mathbf{x}}}$  and  $\dot{\mathfrak{A}}$ . In this case, two different observers  $\mathcal{O}$  and  $\mathcal{O}^\#$ , agreeing about the measure of time, are two different representations of the ambient space and  $Sym^+$ . If they are related isometrically, the rates  $\dot{\hat{\mathbf{x}}}$  and  $\dot{\hat{\mathbf{x}}}^*$  evaluated before and after the change of observer are linked by (1.11) while  $\dot{\mathfrak{A}}$  and  $\dot{\mathfrak{A}}^*$ , still measured before and after the change of observer, are

connected by

$$\dot{\mathfrak{A}}^* = \dot{\mathfrak{A}} + (\mathbf{e}\mathfrak{A} - \mathfrak{A}\mathbf{e}) \dot{\mathfrak{q}}, \tag{12.2}$$

with  $\mathbf{e}$  Ricci's permutation index and  $\dot{\mathfrak{q}}$  the vector of rotational velocity as in (1.11). The third-order tensor  $\mathbf{e}\mathfrak{A} - \mathfrak{A}\mathbf{e}$ , in components  $\mathbf{e}_{ijk}\mathfrak{A}_{kl} - \mathfrak{A}_{ij}\mathbf{e}_{jkl}$  (where summation over repeated indices is understood), is the infinitesimal generator of the action of the special orthogonal group  $SO(3)$  over  $Sym^+$ .

For any arbitrary part  $b \subseteq \mathcal{B}_0$  we then write the external power  $\mathcal{P}_b^{\text{ext}}(\dot{\mathfrak{x}}, \dot{\mathfrak{A}})$  of all interactions acting over  $b$ :

$$\mathcal{P}_b^{\text{ext}}(\dot{\mathfrak{x}}, \dot{\mathfrak{A}}) = \int_b (\mathbf{b} \cdot \dot{\mathfrak{x}}) d(vol) + \int_{\partial b} (\mathbf{P}\mathbf{n} \cdot \dot{\mathfrak{x}} + \mathcal{S}\mathbf{n} \cdot \dot{\mathfrak{A}}) d(area) \tag{12.3}$$

where  $\mathbf{b}$  is the vector density of bulk forces, including inertia,  $\mathbf{P}$  the Piola-Kirchhoff stress tensor and  $\mathcal{S}$  the microstress tensor measuring the interactions associated with the rate of  $\dot{\mathfrak{A}}$ . Note that inertial contributions due to the vibrations of fullerene molecules are assumed to be negligible together with the effects due to the presence of external fields like electric ones. If we use as in Lecture I the invariance of the external power under isometric changes of observed ruled by  $SO(3)$ , we get the pointwise balances of standard interactions

$$\mathbf{b} + \text{Div } \mathbf{P} = 0, \tag{12.4}$$

and the existence of a self-force  $\mathbf{z}$  (now a second order symmetric tensor) satisfying the balance of substructural interactions, namely

$$\text{Div } \mathcal{S} - \mathbf{z} = 0, \tag{12.5}$$

with

$$\mathbf{e}\mathbf{P}\mathbf{F}^T = (\mathbf{e}\mathfrak{A} - \mathfrak{A}\mathbf{e})^T \mathbf{z} + (\nabla(\mathbf{e}\mathfrak{A} - \mathfrak{A}\mathbf{e}))^T \mathcal{S}. \tag{12.6}$$

Constitutive restrictions clarify the nature of the balances of substructural interactions. In fact, if we consider the mechanical dissipation inequality

$$\frac{d}{dt} \int_b (\psi) d(vol) - \mathcal{P}_b^{\text{ext}}(\dot{\mathfrak{x}}, \dot{\mathfrak{A}}) \leq 0, \tag{12.7}$$

where now  $\psi$  is the free energy density, and assume for it a constitutive structure of the form

$$\psi = \hat{\psi}(\mathbf{F}, \mathfrak{A}, \nabla \mathfrak{A}), \tag{12.8}$$

we get

$$\mathbf{P} = \partial_{\mathbf{F}}\psi, \quad \mathcal{S} = \partial_{\nabla \mathfrak{A}}\psi, \quad \mathbf{z} = \partial_{\mathfrak{A}}\psi. \tag{12.9}$$

Once the expression of the free energy is chosen, the constitutive structure of the measures of interactions follow. In the following we restrict our attention to the elastic behavior, then substitute the free energy with the elastic energy  $e = \hat{e}(\mathbf{F}, \mathfrak{A}, \nabla \mathfrak{A})$ . If we consider a linear elastic behavior in the range of infinitesimal deformations, by substituting  $\mathbf{F}$  with the gradient  $\nabla \mathbf{u}$  of the displacement, the simplest expression of  $e$  is given by

$$e = \frac{1}{2} (\mathbb{C}(\nabla \mathbf{u})) \cdot \nabla \mathbf{u} + (\mathbb{D}_1 \mathfrak{A}) \cdot \nabla \mathbf{u} + \frac{1}{2} (\mathbb{D}_2 \mathfrak{A}) \cdot \mathfrak{A} + \frac{1}{2} (\mathfrak{D}_3(\nabla \mathfrak{A})) \cdot \nabla \mathfrak{A}, \quad (12.10)$$

where  $\mathbb{C}$ ,  $\mathbb{D}_1$  and  $\mathbb{D}_2$  are fourth-order tensors displaying major symmetries and  $\mathfrak{D}_3$  is a sixth-order tensor with major symmetries.

## 12.2. Deriving constitutive equations from complex lattices

We identify the explicit expression of the constitutive tensors in (12.10) from a complex lattice by means of the same identification procedure used for microcracked bodies in Lecture I. We consider a complex two-level periodic lattice whose characteristic cell is shown in Fig. 23. The cell is the ‘model’ of the material element and through the identification procedure we attribute all the properties of the cell to each point in  $\mathcal{B}_0$ . The complex lattice is made of two superposed lattices connected by elastic links: the former made of material points (the black spheres in Fig. 26) the latter by four sub-lattices. In the lattice the links can carry only axial forces and we write  $\mathbf{t}$  for the interactions in the first lattice (links between black spheres),  $\mathbf{t}^\circ$  for the interactions between the two lattices (diagonal links),  $\mathbf{t}^*$  for the interactions between sub-lattices,  $\mathbf{t}^\#$  for interactions in each sub-lattice. We also indicate with  $\mathbf{i}, \mathbf{j}, \dots$

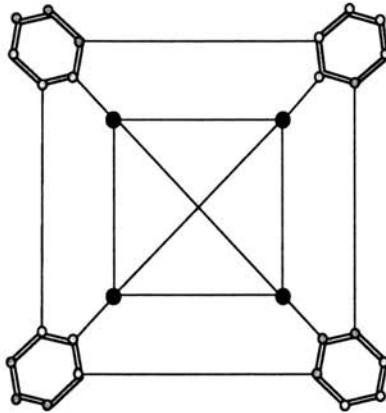


FIGURE 26. Characteristic cell of the two-level lattice representing fullerene-based composites.

the placements of the black spheres, with  $\mathbf{r}, \mathbf{s}, \dots$  the end points of each link between sub-lattices and with  $\mathbf{h}, \mathbf{k}, \dots$  the placements of the spheres in the sub-lattices, and with  $\mathbf{u}^i$  the displacement of the point at  $\mathbf{X}^i$  in the lattice.

Some vectors are appropriate measures of deformation in the lattice if rigid displacements are avoided as we assume here. They are

$$\delta = \frac{\mathbf{u}^i - \mathbf{u}^j}{l}, \tag{12.11}$$

$$\delta^{in} = \frac{\mathbf{u}^s - \mathbf{u}^j}{l^{in}}, \tag{12.12}$$

$$\delta^{ful} = \frac{\mathbf{u}^h - \mathbf{u}^k}{l^{ful}}, \tag{12.13}$$

$$\delta^{if} = \frac{\mathbf{u}^s - \mathbf{u}^r}{l^{if}}, \tag{12.14}$$

where  $\delta$  is the elongation of the generic rod of initial length  $l$  between black spheres in the first lattice,  $\delta^{in}$  is the elongation of interlattice links,  $\delta^{ful}$  the one of the links in the sub-lattice and  $\delta^{if}$  is related to the links between sub-lattices;  $l^{in}, l^{ful}, l^{if}$  are the relevant lengths of the links.

The power  $\pi$  of interactions in the cell is thus

$$\pi = \sum_{L=1}^N (\mathbf{t} \cdot \delta)_L + \sum_{L^i=1}^{N^i} (\mathbf{t}^\circ \cdot \delta^{in})_{L^i} + \sum_{L^f=1}^{N^f} (\mathbf{t}^* \cdot \delta^{ful})_{L^f} + \sum_{L^{if}=1}^{N^{if}} (\mathbf{t}^\# \cdot \delta^{if})_{L^{if}}, \tag{12.15}$$

where  $N$  is the number of links connecting black spheres,  $N^i, N^f, N^{if}$  are respectively the numbers of interlattice links, the ones in the sublattices and the ones between sub-lattices.

To obtain the constitutive expressions of the measures of interactions in the continuum, namely  $\mathbf{P}, \mathcal{S}$  and  $\mathbf{z}$  in terms of the geometry and the constitutive properties of the lattice system we need to follow three steps (the ones used in Lecture I):

1. We identify the work of interactions in the lattice cell with the density of work in the continuum in infinitesimal deformation regime, namely

$$\pi = V_{RVE} (\mathbf{P} \cdot \nabla \mathbf{u} + \mathbf{z} \cdot \mathcal{A} + \mathcal{S} \cdot \nabla \mathcal{A}). \tag{12.16}$$

2. We assume that the first lattice (the one made of black spheres in Fig. 26) undergoes only homogeneous deformations and that the sub-lattices undergo also homogeneous deformations but the deformation of one sub-lattice is different (in principle) from the deformation of the neighboring ones. The links between  $\delta$ 's,  $\mathcal{A}$  and  $\nabla \mathcal{A}$  follows immediately in the infinitesimal deformation regime.

3. We also assume that the interactions in the lattice have the following constitutive structure:

$$\mathbf{t} = \mathbf{K}\delta, \quad \mathbf{t}^\circ = \mathbf{K}\delta^{in}, \quad \mathbf{t}^* = \mathbf{K}^*\delta^{ful}, \quad \mathbf{t}^\# = \mathbf{K}^\#\delta^{if}. \quad (12.17)$$

where  $\mathbf{K}'$ 's are second-order tensors.

We then find

$$\begin{aligned} \mathbb{C} = & \frac{1}{V_{RVE}} \sum_{L=1}^N \left( (\mathbf{X}^i - \mathbf{X}^j) \otimes \mathbf{K} \otimes (\mathbf{X}^i - \mathbf{X}^j) \right) \\ & + \frac{1}{V_{RVE}} \sum_{L^i=1}^{N^i} \left( (\mathbf{X}^i - \mathbf{X}^0) \otimes \mathbf{K}^\circ \otimes (\mathbf{X}^i - \mathbf{X}^0) \right), \quad (12.18) \end{aligned}$$

$$\begin{aligned} \mathbb{D}_1 = & \frac{1}{V_{RVE}} \sum_{L^i=1}^{N^i} \left( (\mathbf{X}^s - \mathbf{X}^0) \otimes \mathbf{K}^\circ \otimes (\mathbf{X}^i - \mathbf{X}^0) \right) \\ & + \frac{1}{V_{RVE}} \sum_{L^i=1}^{N^i} \left( (\mathbf{X}^i - \mathbf{X}^0) \otimes \mathbf{K}^\circ \otimes (\mathbf{X}^s - \mathbf{X}^0) \right) \quad (12.19) \end{aligned}$$

$$\begin{aligned} \mathbb{D}_2 = & \frac{1}{V_{RVE}} \sum_{L^f=1}^{N^f} \left( (\mathbf{X}^h - \mathbf{X}^k) \otimes \mathbf{K} \otimes (\mathbf{X}^h - \mathbf{X}^k) \right) \\ & + \frac{1}{V_{RVE}} \sum_{L^i=1}^{N^i} \left( (\mathbf{X}^s - \mathbf{X}^0) \otimes \mathbf{K}^\circ \otimes (\mathbf{X}^s - \mathbf{X}^0) \right) \quad (12.20) \end{aligned}$$

$$\begin{aligned} \mathbb{D}_3 = & \frac{1}{V_{RVE}} \sum_{L^{if}=1}^{N^{if}} \left( (\mathbf{X}^s - \mathbf{X}^0) \otimes (\mathbf{X}^s - \mathbf{X}^r) \otimes \mathbf{K}^\# \right. \\ & \left. \otimes (\mathbf{X}^s - \mathbf{X}^r) \otimes (\mathbf{X}^s - \mathbf{X}^0) \right), \quad (12.21) \end{aligned}$$

where  $\mathbf{X}^0$  is an arbitrary point chosen in the lattice cell.

### 12.3. Research themes

**Theme 7:** *Prove or disprove the existence of possible pattern formation in the distribution of microdeformation due to fullerene molecules when the distance between them (i.e. the length of the link between fullerene structures in the lattice) varies as a random field. Construct also the appropriate structure of such a field.*

**Theme 8:** *Analyze the influence of the presence of fullerene molecules on the force driving a tip of a macrocrack.*

## 12.4. Bibliographic remarks

For an extensive description of the physical properties of fullerenes, one may refer to (Kadish and Ruoff, 2000).

## Acknowledgements

Numerical calculations in Lecture I should be attributed to Massimiliano Giofrè and Furio Lorenzo Stazi, while the ones in Lecture III are of Furio Lorenzo Stazi. My gratitude goes to them for their essential effort and for having interpreted the theoretical things I try to imagine. I thank also Giuliano Augusti, Gianfranco Capriz, Carlotta Costa, Chiara de Fabritiis, Thomas J. Pence, Luciano Rosati, Reuven Segev, Miroslav Šilhavý, Peter Ván and Paolo Vannucci for direct and indirect comments and suggestions. Above all, discussions with Gianfranco Capriz about his last basic work on granular gases (in particular on distributions of energies within material elements) were essential for me to address my thoughts toward some general aspects of substructural randomness. I thank also Izabela Ślęczkowska and Jerzy Trębicki for their kind and efficient assistance. Last but not least, I thank Kazimierz Sobczyk for the organization of the school at the Centre of Excellence AMAS in Warsaw and above all because he had the fantasy of inviting me as a lecturer amid other possible candidates.

## References

1. M. BAAKE and M. HÖFFE (2000), Diffraction of random tilings: some rigorous results, *J. Stat. Phys.*, Vol.99, pp.219-261.
2. B. BUDIANSKY (1965), On the elastic moduli of some heterogeneous materials, *J. Mech. Phys. Solids*, Vol.13, pp.223-227.
3. B. BUDIANSKY and R.J. O'CONNELL (1976), Elastic moduli of a cracked solids, *Int. J. Solids Structures*, Vol.12, pp.81-97.
4. G. CAPRIZ (1985), Continua with latent microstructure, *Arch. Rational Mech. Anal.*, Vol.90, pp.43-56.
5. G. CAPRIZ, *Continua with Microstructure*, Springer Verlag, Berlin, 1989.
6. G. CAPRIZ (2000), Continua with substructure, *Phys. Mesomech.*, Vol.3, 5-14, pp.37-50.
7. G. CAPRIZ and P.M. MARIANO (2003), Balance at a junction between coherent interfaces in continua with microstructure, in *Advances in Multifield Theories of Continua with Substructure*, G. Capriz and P.M. Mariano (Eds.), Birkhauser Verlag.

8. G. CAPRIZ and P.M. MARIANO (2004), Symmetries and Hamiltonian formalism for complex materials, *J. Elasticity*, Vol.72, arXiv: math-ph/0304046.
9. G. CAPRIZ and E.G. VIRGA (1990), Interactions in general continua with microstructure, *Arch. Rational Mech. Anal.*, Vol.109, pp.323-342.
10. G. DEL PIERO and D.R. OWEN (1993), Structured deformations of continua, *Arch. Rational Mech. Anal.*, Vol.124, pp.99-155.
11. G. DEL PIERO and D.R. OWEN, *Structured Deformations*, Quaderni dell'Istituto di alta Matematica, Florence, 2000.
12. A. GRAVOUIL, N. MOËS, and T. BELYTSCHKO (2002), Non-planar 3D crack growth by the extended finite element and level sets. Part II: Level set update, *Int. J. Num. Meth. Eng.*, Vol.53, pp.2569-2586.
13. M.E. GURTIN, *Configurational Forces as Basic Concept of Continuum Physics*, Springer Verlag, Berlin, 2000.
14. Z. HASHIN (1988), The differential scheme and its applications to cracked materials, *J. Mech. Phys. Solids*, Vol.36, pp.719-734.
15. M. KACHANOV (1993), Elastic solids with many cracks and related problems, *Adv. Appl. Mech.*, Vol.30, pp.259-445.
16. K.M. KADISH and R.S. RUOFF, *Fullerenes*, Wiley Interscience, New York, 2000.
17. R. LIFSHITZ (2003), Quasicrystals: a matter of definition, *Found. Phys.*, Vol.33, pp.1703-1711.
18. P.M. MARIANO (1999), Some remarks on the variational description of microcracked bodies, *Int. J. Non-Linear Mech.*, Vol.34, pp.633-642.
19. P.M. MARIANO (2000), Configurational forces in continua with microstructure, *Z. Angew. Math. Phys. ZAMP*, Vol.51, pp.752-791.
20. P.M. MARIANO (2001), Multifield theories in mechanics of solids, *Adv. Appl. Mech.*, Vol.38, 1-93.
21. P.M. MARIANO (2003), Cancellation of vorticity in steady-state non-isentropic flows of complex fluids, *J. Phys. A: Math. Gen.*, Vol.36, pp.9961-9972.
22. P.M. MARIANO, M. GIOFFRÈ, F.L. STAZI and G. AUGUSTI (2004), Elastic microcracked bodies with random properties, *Prob. Eng. Mech.*, Vol.19, pp.127-143.
23. P.M. MARIANO and F.L. STAZI (2001), Strain localization in elastic microcracked bodies, *Comp. Meth. Appl. Mech. Eng.*, Vol.190, pp.5657-5677.
24. P.M. MARIANO and F.L. STAZI (2004), Strain localization due to crack-microcrack interactions: X-FEM for a multifield approach, *Comp. Meth. Appl. Mech. Eng.*, in press.
25. P.M. MARIANO, F.L. STAZI and G. AUGUSTI (2004), Phason effects around a crack in Al-Pb-Mn quasicrystals: stochastic aspects of the phonon-phonon coupling, *Comp. Str.*, in press.
26. P.M. MARIANO and P. TROVALUSCI (1999), Constitutive relations for elastic microcracked bodies: from a lattice model to a multifield continuum description, *Int. J. of Damage Mech.*, Vol.8, pp.153-173.

27. J.E. MARSDEN and T.J.R. HUGHES, *Mathematical Foundations of Elasticity*, Prentice-Hall, Englewood Cliffs, New Jersey, 1983.
28. N. MOËS, J. DOLBOW, and T. BELYTSCHKO (1999), A finite element method for crack growth without remeshing, *Int. J. Num. Meth. Eng.*, Vol.46, pp.131-150.
29. T. MORI and K. TANAKA (1973), Average stress in matrix and average elastic energy of materials with misfitting inclusions, *Acta Metall.*, Vol.21, pp.571-574.
30. S.B. ROCHAL and V.L. LORMAN (2001), Minimal model of the phonon-phason dynamics in icosahedral quasicrystals and its application to the problem of internal friction in the *i*-AlPdMn alloy, *Phys. Rev. B*, Vol.66, 144204, pp.1-9.
31. R. SEGEV (1994), A geometrical framework for the statics of materials with microstructure, *Math. Mod. Meth. Appl. Sci.*, Vol.4, pp.871-897.
32. D. SHECHTMAN, I. BLECH, D. GRATIAS, J.W. CAHN (1984), Metallic phase with long-range orientational order and no translational symmetry, *Phys. Rev. Letters*, Vol.53, pp.1951-1954.
33. M. ŠILHAVÝ, *The Mechanics and Thermodynamics of Continuous Media*, Springer Verlag, Berlin, 1997.
34. J.C. SIMO, J.E. MARSDEN and P.S. KRISHNAPRASAD (1988), The Hamiltonian structure of nonlinear elasticity: The material and convective representation of solids, rods and plates, *Arch. Rational Mech. Anal.*, Vol.104, pp.125-183.
35. F.L. STAZI, E. BUDYN, J. CHESA and T. BELYTSCHKO (2003), An extended Finite Element Method with higher-order element for crack problems with curvature, *Comp. Mech.*, Vol.31, pp.38-48.
36. S. TORQUATO, *Random Heterogeneous Materials*, Springer Verlag, Berlin, 2002.

